Carderock Division, Naval Surface Warfare Center

West Bethesda, Maryland 20817-5700

NSWCCD-50-TR-2005/063 December 2005
Hydromechanics Department Report

Resistance Tests of a Systematic Series of U.S. Coast Guard Planing Hulls

by
Bryson J. Metcalf
Lisa Faul
Elissa Bumiller
Jonathan Slutsky

APPROVED FOR PUBLIC RELEASE; DISTRIBUTION UNLIMITED

REPORT DOCUMENTATION PAGE

Form Approved
OMB No. 0704-0188

Public reporting burden for this collection of information is estimated to average 1 hour per response, including the time for reviewing instructions, searching existing data sources, gathering and maintaining the data needed, and completing and reviewing the collection of information. Send comments regarding this burden estimate or any other aspect of this collection of information, including suggestions for reducing this burden to Washington Headquarters Services, Directorate for Information, Operations and Reports, 1215 Jefferson Davis Highway, Suite 1204, Arlington, VA 22202-4302, and to the Office of Management and Budget, Paperwork Reduction Project (0704-0188), Washington, DC 20503.

1. AGENCY USE ONLY (Leave blank)	2. REPORT DATE	3. REPORT TYPE AND DATES COVERED
	December 2005	Final

4. TITLE AND SUBTITLE
RESISTANCE TESTS OF A SYSTEMATIC SERIES OF USCG PLANING HULLS

5. FUNDING NUMBERS
04-1-5200-158

6. AUTHOR(S)
Bryson J. Metcalf, Lisa Faul, Elissa Bumiller, Jonathan Slutsky

7. PERFORMING ORGANIZATION NAME(S) AND ADDRESS(ES)
NSWCCD Code 5200
9500 MacArthur Blvd.
West Bethesda, MD 20817-5700

8. PERFORMING ORGANIZATION REPORT NUMBER
NSWCCD-50-TR-2005/063

9. SPONSORING / MONITORING AGENCY NAME(S) AND ADDRESS(ES)
United States Coast Guard Engineering and Logistics Center
Propulsion Systems Acquisition Branch- Code 046, M/S 26, Bldg. 31
2401 Hawkins Point Road
Baltimore, MD 21226-5000

10. SPONSORING / MONITORING AGENCY REPORT NUMBER

11. SUPPLIMENTARY NOTES

12a. DISTRIBUTION / AVAILABILITY STATEMENT
Approved for Public Release; Distribution Unlimited.

12b. DISTRIBUTION CODE

13. ABSTRACT *(Maximum 200 words)*

Resistance experiments were performed on a systematic series of models based on the United States Coast Guard 47-foot Motor Lifeboat (MLB) hull form. The series includes three models with varying length-to-beam ratios and one model with transom dead-rise angle variation. Resistance tests were completed on each model for a range of conditions, with displacements varying from 298 lbs to 680 lbs and longitudinal center of gravity located at 38% and 42% of the length between perpendiculars (measured forward of the aft perpendicular). The results are presented as model scale values in the form of; R_T/Δ, S_{DYN}, C_R, LCG Heave, and Pitch angle. Additionally, EHP was calculated for the 47–foot MLB from 5628 model data and compared with EHP calculations from previous 47-foot MLB model test data.

14. SUBJECT TERMS
Calm water resistance, planing hull

15. NUMBER OF PAGES
59+vi

16. PRICE CODE

17. SECURITY CLASSIFICATION OF REPORT	18. SECURITY CLASSIFICATION OF THIS PAGE	19. SECURITY CLASSIFICATION OF ABSTRACT	20. LIMITATION OF ABSTRACT
Unclassified	Unclassified	Unclassified	Unclassified/Limited

Standard Form 298 (Rev. 2-89)

NSN 7540-01-280-5500

THIS PAGE IS INTENTIONALLY LEFT BLANK

CONTENTS

LIST OF TABLES

LIST OF FIGURES

NOTATION

STANDARD SYMBOLS (ABBREVIATED LIST)

V	Speed (Velocity)	Δ	Displacement
$F_{n\forall}$	Volumetric Froude Number $= \frac{V}{\sqrt{g\nabla^{1/3}}}$	R_n	Reynold's Number
R_T	Total Resistance	C_T	Total Resistance Coefficient
C_F	Frictional Resistance Coefficient	C_R	Residuary Resistance Coefficient
S	Wetted Surface	EHP	Effective Horsepower
λ	[Lambda] Model linear scale ratio	ρ	[Rho] Water Density ($lb*sec^2/ft^4$)
ν	[Nu] Kinematic Viscosity (ft^2/s)	S_{DYN}	Dynamic wetted surface area
LBP	Length between Perpendiculars	LWL	Waterline Length
LCG	Longitudinal center of gravity	ABL	Above Baseline
FP	Forward Perpendicular	AP	Aft Perpendicular
$A_P/\nabla^{2/3}$	Hull loading coefficient	∇	Volume
WP_{AREA}	Water-plane Area		
Ap	Projected area on the free surface from the hull, below and including the chine.		

INTERNATIONAL SYSTEM OF UNITS (SI) CONVERSION FACTORS

U.S. CUSTOMARY	METRIC EQUIVALENT
1 inch	25.4 millimeter (mm), 0.0254 meter (m)
1 foot	0.3048 meter (m)
1 pound of force	0.4536 kilograms (kg)
1 foot-pound (ft-lb)	0.1382 kilogram-meter (kg-m)
1 foot per second (ft/s)	0.3048 meter per second (m/s)
1 knot	0.5144 meter per second (m/s)
1 horsepower	0.7457 kilowatts (kW)
1 long ton	1.016 tonnes, 1.016 metric tons, or 1016.0 kilograms
1 inch water (60 F)	248.8 Pascals (Pa)

ABSTRACT

Resistance experiments were performed on a systematic series of models based on the United States Coast Guard 47-foot Motor Lifeboat (MLB) hull form. The series includes three models with varying length-to-beam ratios and one model with transom deadrise-angle variation. Resistance tests were completed on each model for a range of conditions, with displacements varying from 298 lbs to 680 lbs and longitudinal center of gravity located at 38% and 42% of the length between perpendiculars (measured forward of the aft perpendicular). The results are presented as model scale values in the form of; R_T/Δ, S_{DYN}, C_R, LCG Heave, and Pitch angle. Additionally, EHP was calculated for the 47-foot MLB from 5628 model data and compared with EHP calculations from previous 47-foot MLB model test data.

ADMINISTRATIVE INFORMATION

The test results presented in this report were performed by the Resistance and Powering Division (Code 5200) within the Hydromechanics Department of the Naval Surface Warfare Center, Carderock Division (NSWCCD) at the David Taylor Model Basin, herein referred to as DTMB. Dina Kowalyshyn at the Boat Engineering Branch (ELC-024) of the U.S. Coast Guard's Engineering and Logistics Center sponsored the work, under work unit No. 04-1-5200-158.

INTRODUCTION

This report presents the results of calm water resistance experiments that were conducted at DTMB on a systematic series of models based on the United States Coast Guard 47 foot Motor Life Boat (MLB). The 47 foot MLB is a self-righting planing-hull design utilized by the United States Coast Guard (USCG) for inshore search and rescue missions in all sea states. The 47-foot MLB has proven to be a very successful hull form in terms of both seakeeping and resistance. This experimental program was designed to explore the possibility of adapting this hull form to larger length-beam ratio, higher-displacement, and much higher speed vessels.

The objective was to identify the influence of; length-to-beam ratio, transom deadrise angle, longitudinal center of gravity (LCG), and displacement on the resistance and trim attitude of the planing hullforms within the systematic series. This was achieved by constructing a 1/4.3 scale model of the 47-foot MLB, with a slight transom modification, and three variations of that geometry. They were all tested at three displacements and two longitudinal centers of gravity. The range of test conditions simulated ships ranging from 55-100 feet in length and displacements from 23-221 LT.

DESCRIPTION OF MODELS

Four scale models were constructed and designated by DTMB model numbers: 5628, 5629, 5630, and 5631. All models were constructed to a twelve inch station spacing and a length between perpendiculars (LBP) of 120 inches, corresponding to a scale factor of λ=4.30 for the 43 foot full-scale LBP of the 47 foot MLB. The four scale models were developed from the 47 Foot MLB lines plan by removing the stern wedge and extending the buttocks and waterlines to create a flat transom located at the aft perpendicular (AP). Each of the models have the same projected chine length, L_p=124.8 inches and the projected planing-area centroid, A_{pcent}=52.8 inches forward of the aft perpendicular. Table 1 presents the particulars of all four models determined us-

ing the design waterline from the 47-foot MLB drawings. In Table 1 the beam is listed as the maximum width at the waterline, the deadrise angle is taken at the transom, the volume excludes the spray rails, and the projected planning area includes the surfaces below the outer chine (excluding the spray rail). The hullforms body plans and profiles appear in Figures 1 and 2.

Model 5628 is the parent model of this series, as shown in Figure 3. This model is substantially the same as the full scale 47 foot MLB hull with the following differences: model 5628 has a flat transom rather than the rounded transom of the full scale ship, and it does not have the stern wedge found on the actual 47 foot MLB hull. It has a length-to-beam ratio of 3.24 and a beam-to-draft ratio of 3.67.

Model 5629 is considered Variant #1 of the series, as shown in Figure 4. The model was designed to obtain a length-to-beam ratio of 4.0 by scaling the body plan with a constant (0.810), while maintaining the length between perpendiculars, this will be referred to as a yz-scaling in the remainder of the document.

Model 5630 is considered Variant #2 of the series, as shown in Figure 5. The model was also designed by a direct yz-scaling (0.725) of the parent hull. The scale factor was obtained by the minimum beam corresponding to the limit of intact stability of this geometry, resulting in a length-to-beam ratio of 4.47.

Model 5631 is considered Variant #3 of the series, as shown in Figure 6. The model is a variation of Variant #2 in which the hull below the chine was stretched in the z-direction to obtain a transom deadrise of 20 degrees while maintaining the Variant #2 hull shape above and including the chine. Each station line below the chine was scaled independently (1.1-1.22) to achieve a smooth hull form connecting the chine to the flat keel (lowered 0.07036').

Models 5628-5630 were constructed by MAPC from transverse sections of numerically cut (NC) low-density urethane foam. The sections were assembled on a flat table and covered with fiberglass cloth, painted and marked with stations and waterlines. Internal structural members were constructed from ¼ inch plywood.

Model 5631was constructed by Don Trumpy from model-scale station lines provided by MAPC. This model was strip planked and finished with fiberglass.

EXPERIMENTAL PROCEDURES

All the resistance experiments reported herein were conducted on Carriage 3 in the high-speed basin, which has a cross sectional area of 21 feet wide by 16 feet deep. During these experiments the models were free to pitch, heave, and roll, but were restrained in surge, sway and yaw. The test agenda and the static, at rest conditions of the models are presented in Table 2 and 3 respectively.

The longitudinal position of the tow point was set by experimental design at 38 and 42 percent of the LBP forward of the aft perpendicular. The models were attached to the light heave staff mounted to the east end of carriage III. Two two-inch block gauges were used to measure drag (calibrated to ± 200 lbf) and side force (calibrated to ± 20 lbf). Running trim was measured with string potentiometers at the LCG and the stern of each model. A "grasshopper" was mounted at approximately station 8 in each model to restrain the model in yaw and provide a yaw-zeroing adjustment capability, while two tethers extended from the bow forward and outward for safety purposes to prevent excessive yaw and/or break away from the carriage. The

tethers were ¼ inch nylon rope attached with enough slack such that they would not interfere with the model running trim or influence the drag measurements.

Due to the small size and the internal structure of the models, the existing instrument stack could not be mounted to the hull in its standard configuration. A new mount for the existing two-inch gimbal was designed and built to lower the tow points to the desired levels and allow for easy longitudinal adjustment, Figure 7. The tow point heights, listed in Table 4, were determined from the height (above the keel) of the shaft thrust bearing on the full scale MLB. This height was obtained from the 47-foot MLB lines plans supplied by ELC-024. For each variant hullform the height was scaled according to the appropriate yz-scale ratio.

The ballast conditions of the models were given by model displacement and LCG supplied by the ELC-024. To obtain the proper ballast conditions the longitudinal centers of gravity were first determined for the unballasted, rigged models. This was achieved by hanging each model from the 38% LCG such that it was free to pivot about this transverse axis. Trim weights were added to level the model in pitch, which allowed the model's longitudinal center of gravity to be calculated by a simple balancing of moments. Given each of the model's longitudinal centers of gravity, the desired displacement and center of gravity for each test configuration was obtained through the precise placement of ballast weights. The achieved ballast conditions are listed in Table 3.

The models were tested over a range of model speeds corresponding to ship speeds of 10 through 55 knots. Data were collected at 100 Hz in ten-second spots, with two or more spots taken per speed. The number of spots collected per pass varied with the number and magnitude of speeds being run. Additionally, at each speed, the wave profile was observed at 4 locations on the model and documented. This was documented to determine the dynamic (at speed) wetted surface area of the model. These locations pertained to the keel-water intersection, the foremost location of the intersection between the chine and the spray-sheet, the chine reattachment point (the location where the chine no longer sheds water from the hullform above the chine), and the height of the water on station 10 (side of the model at the transom). Figure 8 shows these measurements for Model 5631 at 10.87 knots and 375 lbs of displacement at the 38% LCG. The solid line represents a generalized wave profile from the four observed locations on the model. The surface of the model was discretized into thousands of triangular panels in order to determine the wetted surface areas. The three colors on figure 8 represent panels, which were fully, partially, and non-wetted. The dynamic wetted surface area is then the total of the fully and ½ the partially wetted panels.

The deep transoms of the models, especially at high displacements and speeds, generated large divergent wave systems. With the removal of the wave-dampening troughs in the high-speed basin, the only dampers in the basin were a single line of swimming lane markers. Under these conditions, coherent packets of waves could be seen moving up and down the basin as much as ten minutes after a run. To damp the waves in the basin more quickly, additional lane markers were placed at the east end of the basin and the large horizontal wave suppressor plate was mounted to the carriage. The plate was lowered to the water surface when backing up between runs. This significantly reduced the persistence of the wave systems resulting in calmer tank conditions at the start of each run.

EXPERIMENTAL RESULTS

All of the data presented in this report, shown in Tables 5-29 and Figures 11-56, are model scale values. Figures 9 and 10 are the 47-foot MLB extrapolation to full scale. The results of the resistance experiments' analysis are presented in the form of; R_T/Δ, S_{DYN}, C_R, LCG Heave, and Pitch angle. Additionally, EHP data were calculated for the 5628 model data to compare with EHP calculations from previous 47-foot MLB model test data published in [1] collected at the United States Naval Academy (USNA), Division of Engineering and Weapons.

The EHP comparison plots with [1] are presented in Figures 9 and 10. The EHP data were calculated identically using a correlation allowance of zero, the ITTC 1957 correlation line and assuming the full scale vessel is operating in smooth, deep salt water with a uniform standard temperature of 59° Fahrenheit (15° Celsius). The only differences between the current model geometry and that in [1] were the scale ratios and that Model 5628 had a flat transom and no stern wedge. The only appendages on both models as tested were simple spray rails. By visual inspection it is evident that the current data fits reasonably well with the USNA data, bearing in mind that the displacement conditions are not identical. This comparison gives good assurance that the current data are reasonable.

The influences of L/B and deadrise angle on R_T/Δ, are presented in Figures 11 through 16. The data is plotted for all of the models at a given displacement and LCG location. Through close inspection of the figures and data, four key points are worth noting. The resistance per pound of displacement is influenced approximately equally by the L/B ratio and LCG location and their influences are more substantial at higher speed. The resistance per pound of displacement is clearly ordered in terms of L/B ratio. At nearly all speeds, higher length-beam ratios result in reduced R_T/Δ. Shifting the LCG forward tends to flatten the curve causing the R_T/Δ to increase in the high-speed region and decrease in the low-speed region thus reducing the benefit of planning. The effect of an increased deadrise angle is noticeable however slight. It tends to reduce the benefit of a slender hull.

Figures 17 through 24 present the R_T/Δ for each model individually at a single LCG, revealing the impact of change in displacement. For a given L/B ratio, the displacement has a large impact on the R_T/Δ. The data exhibit an inflection point where the curves change from concave downward to concave upward for all of the hullforms. At approximately this speed all the curves cross over each other. The inflection point of the curves occurs between 11 and 14 knots model speed. At speeds below the inflection point the R_T/Δ is larger for heavy displacements. Above the inflection point the inverse is true. This means that at speeds higher than the inflection-point the hullforms, with regard to resistance, become more efficient as the displacement increases. Another trend exists in which, for increases in length-beam ratio the point of inflection moves slightly to the right, occurring at higher speed.

The dynamic wetted surface areas from the experimental measurements shown in Figures 25 through 32, exhibit a noticeable trend. Looking at each hullform individually it can be seen that the dynamic wetted surface area for all displacements converge to the same value at higher speeds. It is very clear that for a particular hullform and LCG location the dynamic wetted surface area reaches approximately a constant, once planing. For these hullforms the constant is achieved at approximately Fn_V=3.6. For greater displacements it can be seen that a larger reduction occurs in dynamic wetted surface area as a result of planing.

The residuary drag coefficients (C_R) presented in Figures 33 through 40 follow expected trends with regard to displacement. However, no coherent trends can be established with regard to L/B ratio. There does exist however, noticeable and expected effects due to the change in deadrise angle and the LCG location. The curves have the typical peak occurring at a volumetric Froude number slightly greater than 1.0 and arranged in ascending order according to increasing displacement. The forward LCG location results in a decreased C_R curve while the increased deadrise angle acts to increase the C_R curve.

The curves in Figures 41 through 48 represent the CG heave of the models. The curves are S shaped. The initial response as speed increases from very low speed is to sink slightly, before steadily increasing from low to medium speed, prior to leveling out once planing is achieved. They are in ascending order with regard to increasing displacement. At first thought this may seem incorrect, however the effect of planing is to elevate the hullform out of the water until the hullform above the chines is dry. Interestingly, in order to achieve the planing condition at the same speed noted previously (Fn_V =3.6), the rate of heave gets larger with increased displacement. This results in a greater amount of heave when planing for the heavier displacement condition. The figures also show that the amount of CG heave is relatively insensitive to the L/B ratio variation, although an increase in deadrise angle does indicate a higher amount of CG heave.

The pitch angle measurements are shown in Figures 49 through 56. Two humps appear in the curves, which occur very nearly the same speed as the two humps in the C_R curves, especially with the higher two L/B ratios. The curves of pitch angle are well ordered with regard to the displacements. The largest and smallest maximum-pitch angles occur for high and low displacements, respectively. The maximum-pitch angle can also be seen to occur shortly prior to the maximum CG heave, which becomes approximately constant when the hullform is on plane. The pitch angle is also responsive to the LCG location. A forward LCG location will minimally reduce the amount of pitch for a given displacement. Additionally, the maximum pitch angle occurs at a higher speed when the LCG is forward and also when the L/B ratio is larger.

CONCLUSIONS

Model experiments were performed on a systematic series of models based on the United States Coast Guard 47-foot Motor Lifeboat (MLB) hull form. The series includes four models with varying length-to-beam ratios and transom dead-rise angles. Resistance tests were completed on each model for a range of conditions, with displacements varying from 298 lbs to 680 lbs and longitudinal center of gravity located at 38% and 42% of the length between perpendiculars (measured forward of the aft perpendicular). The EHP data, which were calculated for the full-scale 47' MLB, compared well to existing EHP data from the previously collected USNA model data. However, the data presented herein, is collected from larger models and includes much higher speeds than the USNA model-test data.

The results are all presented as model scale values in the form of: R_T/Δ, S_{DYN}, C_R, LCG Heave, and Pitch angle. The experimental data were discussed in a manner to extract the effects of variation in displacement, L/B ratio, LCG location, and deadrise angle. There exist some strong, expected trends and some not-so-obvious, unanticipated trends with regard to the independently varied parameters. The trend most worth noting is that the resistance per pound of

displacement is more favorable for high displacement at high speed and low displacement at low speed. Likewise, the effect of LCG location on the resistance per pound of displacement also reveals a favorable result with aft LCG location at higher speeds and forward LCG location at lower speeds. There exists a common, small, speed range (11-14 V_{MK}) in which this inflection takes place for all independent variables. This speed is where the aft LCG location and heavier displacements become more favorable considering resistance per pound of displacement. Additionally, the dynamic wetted-surface-area data revealed an interesting trend with regard to high-speed and the variation of displacement. The dynamic wetted surface area of a particular hull-form and LCG location for all of the displacements, converge to the same value once the hull-form is planing. It can also be seen that, for the same hullform, a forward LCG location will increase the dynamic wetted-surface-area to which all the displacements converge.

The results in this report are presented as model scale values due to the conceptual nature of the program. It must be noted that the curves of resistance per pound of displacement will be affected when scaled to some notional full-scale vessel. However, the trends will not vary, but may become less obvious. The effect of expanding to full-scale will result in a flatter curve, where the low speed hump becomes less pronounced and less curvature exists at high speed.

ACKNOWLEDGEMENTS

The United States Coast Guard Technical Point of Contact was Dina Kowalyshyn. The author would like to extend a special thanks to the following NSWCCD employees for their contributions and support towards this project: Dennis Mullinix (5200) for calibration and installation of the Data Acquisition System (DAS) electronics and the staff of the Facilities Engineering Division, Code 5100 for reworking the exterior of all 4 models to provide a consistent surface finish with very short notice. Without all of your efforts the test could not have been successfully completed.

Table 1. Model Form Particulars.

Model	LBP [ft]	B [ft]	T [ft]	L/B	B/T	Deadrise [Deg]	Disp. [ft^3]	Ap [ft^2]
5628	10	3.08	0.608	3.24	5.08	16.61	8.05	25.88
5629	10	2.50	0.492	4.0	5.08	16.61	5.29	20.97
5630	10	2.24	0.441	4.47	5.08	16.61	4.24	18.76
5631	10	2.24	0.510	4.47	4.39	20.00	4.88	18.76

Table 2: Test Agenda for Series.

Model	LCG	Displ	$A_p/\nabla^{2/3}$
	%LWL fwd AP	Lbs	
5628	38%	298	9.13
		375	7.83
		483	6.61
		560	5.99
		680	5.27
	42%	298	9.13
		375	7.83
		483	6.61
5629	38%	298	9.13
		375	7.83
		483	6.61
	42%	298	9.13
		375	7.83
		483	6.61
5630	38%	298	9.13
		375	7.83
		483	6.61
	42%	298	9.13
		375	7.83
		483	6.61
5631	38%	298	9.13
		375	7.83
		483	6.61
	42%	298	9.13
		375	7.83
		483	6.61

Table 3. Experimentally Tested Ballast Conditions

Model	LCG	Displ	$A_P/\nabla^{2/3}$	T_{AP}	T_{FP}	TRIM	WP_{AREA}	S
	[%LWL fwd AP]	[Lbs]		[in]	[in]	[in]	[in^2]	[in^2]
5628	38.08%	297.76	9.13	5.406	5.710	-0.304	2950	3228
	37.97%	375.69	7.83	6.000	6.556	-0.556	3211	3558
	38.00%	483.68	6.62	7.000	7.312	-0.312	3391	3867
	38.00%	560.16	5.99	7.750	7.750	0.000	3475	4052
	37.90%	679.94	5.26	9.000	8.243	0.757	3565	4305
	42.12%	297.76	9.13	4.750	6.742	-1.992	2948	3251
	42.04%	375.69	7.83	5.350	7.553	-2.203	3280	3632
	42.01%	484.19	6.61	6.000	8.767	-2.767	3497	3979
5629	37.99%	298.28	7.40	5.593	5.557	0.035	2700	3022
	37.98%	375.85	6.35	6.400	6.274	0.126	2820	3296
	38.00%	484.18	5.36	7.650	7.301	0.349	2924	3583
	41.98%	298.24	7.40	4.905	6.577	-1.672	2777	3131
	42.03%	376.16	6.34	6.030	6.812	-0.782	2855	3334
	42.06%	484.18	5.36	7.030	7.883	-0.853	2969	3638
5630	38.03%	297.77	6.62	5.750	5.518	0.232	2515	2935
	38.01%	375.46	5.68	6.900	5.888	1.012	2590	3153
	38.01%	483.78	4.79	8.250	6.696	1.554	2682	3455
	42.00%	297.77	6.62	5.000	6.587	-1.587	2584	3010
	42.02%	375.46	5.68	5.750	7.489	-1.739	2674	3253
	42.00%	483.78	4.79	7.000	8.410	-1.410	2764	3556
5631	38.01%	298.92	6.62	6.438	5.478	0.960	2439	2870
	38.01%	375.34	5.68	7.500	6.011	1.489	2537	3108
	38.00%	483.59	4.79	8.750	7.006	1.744	2645	3427
	42.00%	298.88	6.62	5.519	6.831	-1.313	2526	2964
	42.00%	375.27	5.68	6.206	7.855	-1.649	2634	3222
	42.01%	483.59	4.79	8.000	8.069	-0.069	2692	3486

Table 4. Tow Point Heights

Model Number	**5628**	**5629**	**5630**	**5631**
Tow Point ABL [in]	6.06	4.91	4.39	5.05

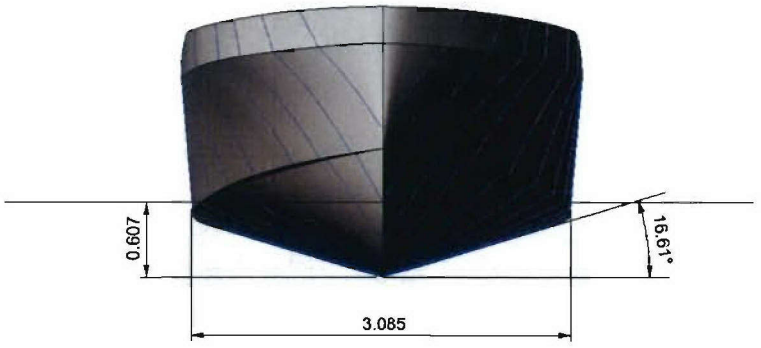

5628, 47' MLB Hull (L/B=3.24, B/T=5.08)

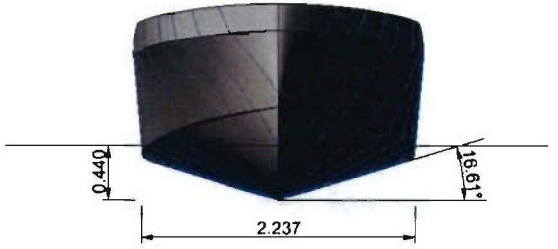

5630, Variant #2 (L/B=4.47, B/T=5.08)

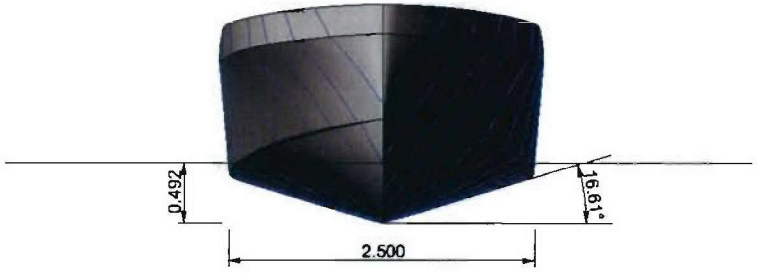

5629, Variant #1 (L/B=4.0, B/T=5.08)

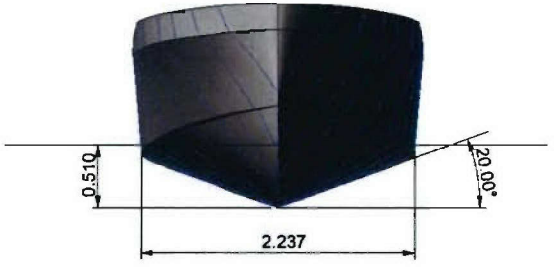

5631, Variant #3 (L/B=4.47, B/T=4.39)

Figure 1. Series Hullforms Body-Plan Views

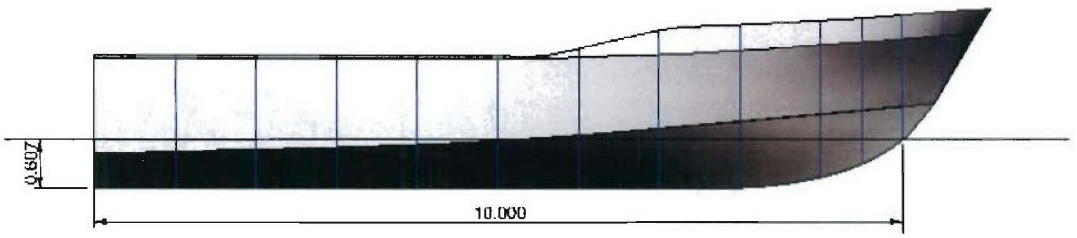

47' MLB Hull Profile

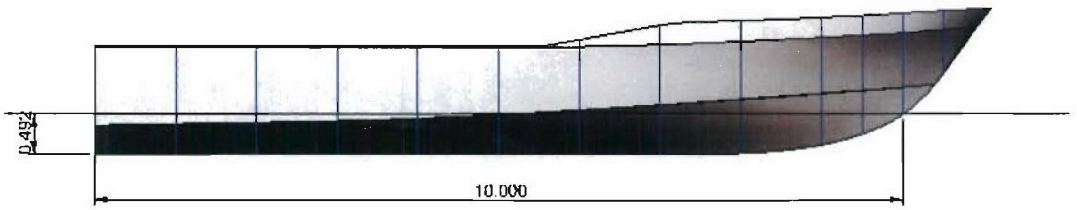

Variant #1 Hull Profile

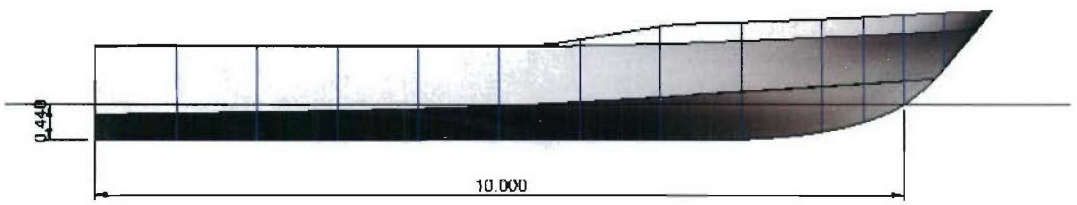

Variant #2 Hull Profile

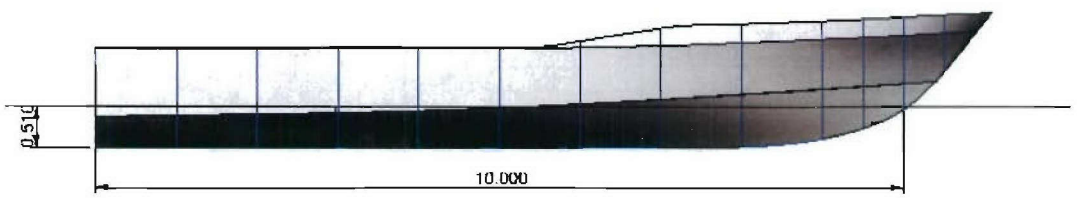

Variant #3 Hull Profile

Figure 2. Series Hullforms Profile-Views

Figure 3. Model 5628 Dry and at 298lbs, 43%, 25.47 Knots

Figure 5. Model 5630 Dry and at 298lbs, 43%, 25.47 Knots

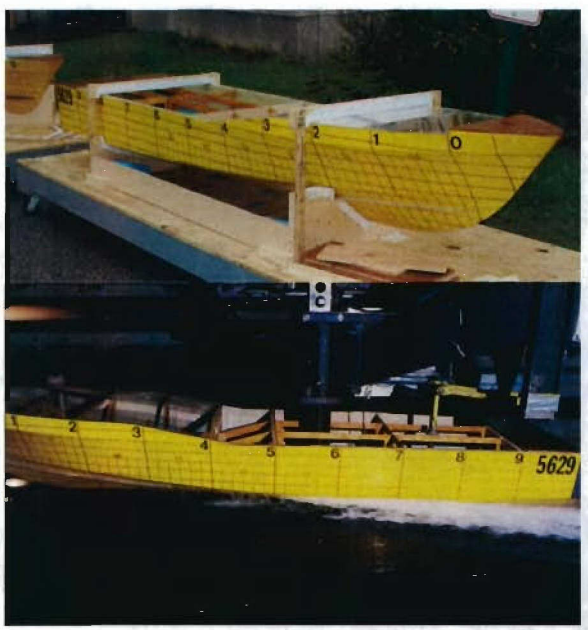

Figure 4. Model 5629 Dry and at 298lbs, 43%, 25.47 Knots

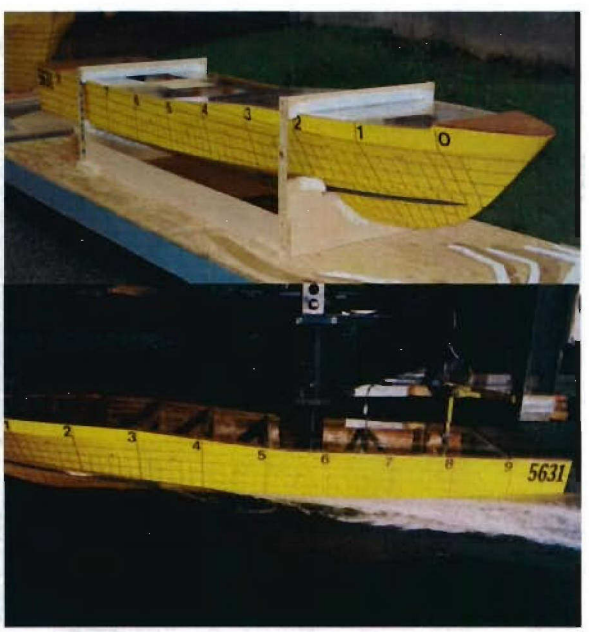

Figure 6. Model 5631 Dry and at 298lbs, 43%, 25.47 Knots

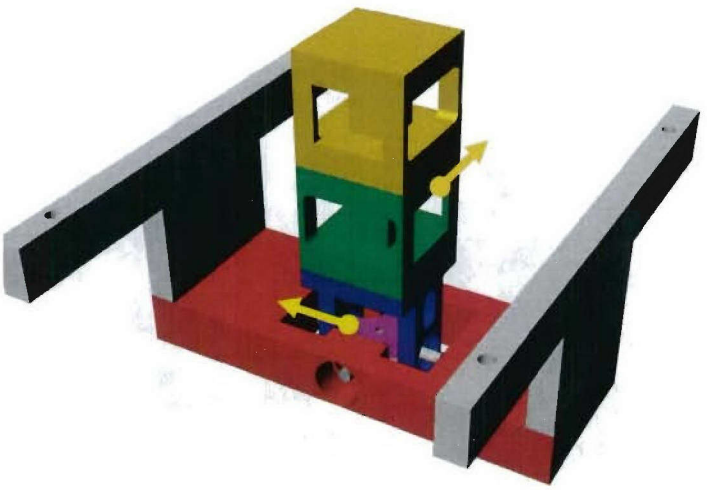

Figure 7. Block Gauge and Gymbal Assembly.

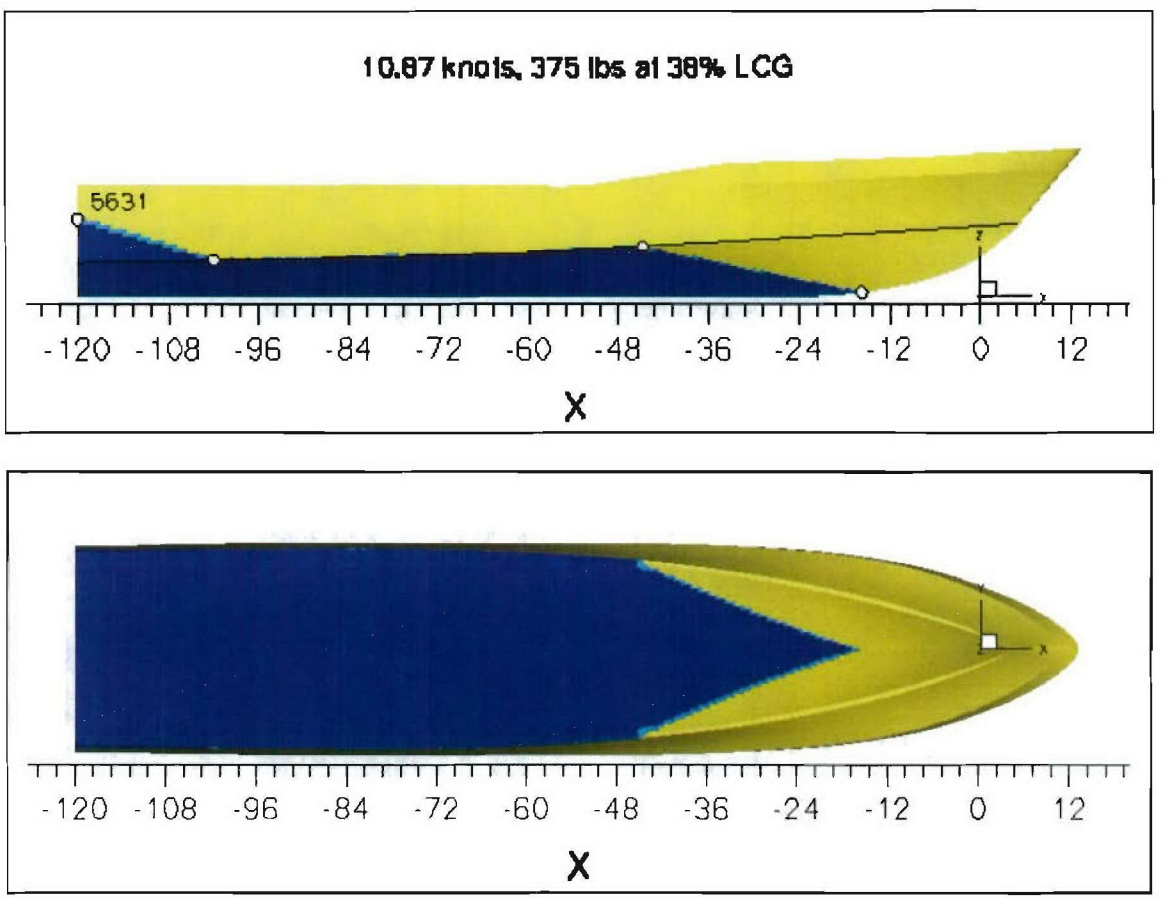

Figure 8. Dynamic Wetted Surface Area of Model 5631

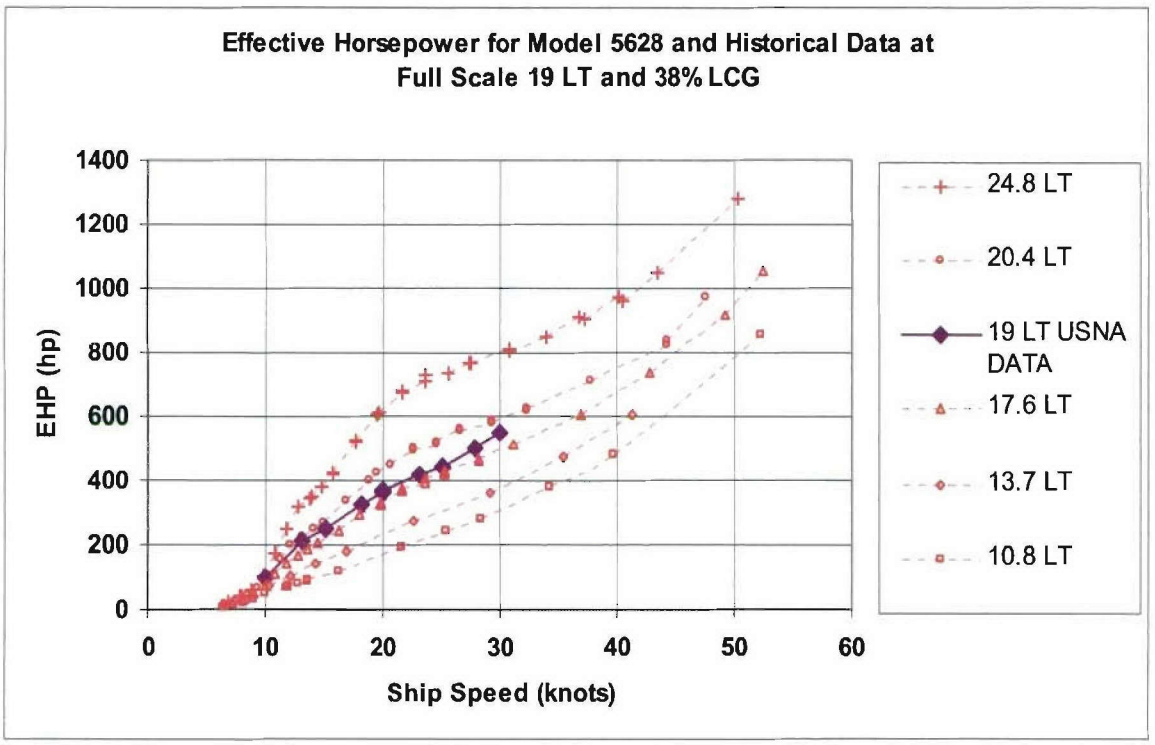

Figure 9. EHP for Full Scale 47 ft MLB at 38% LCG

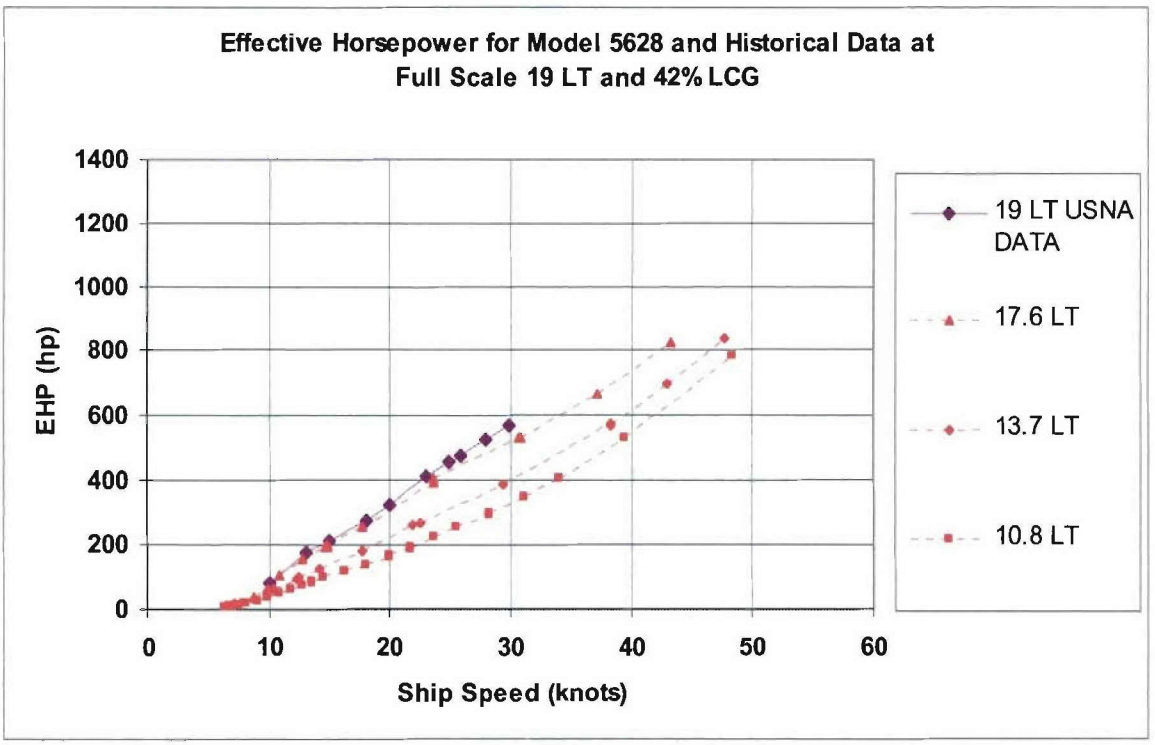

Figure 10. EHP for Full Scale 47 ft MLB at 42% LCG

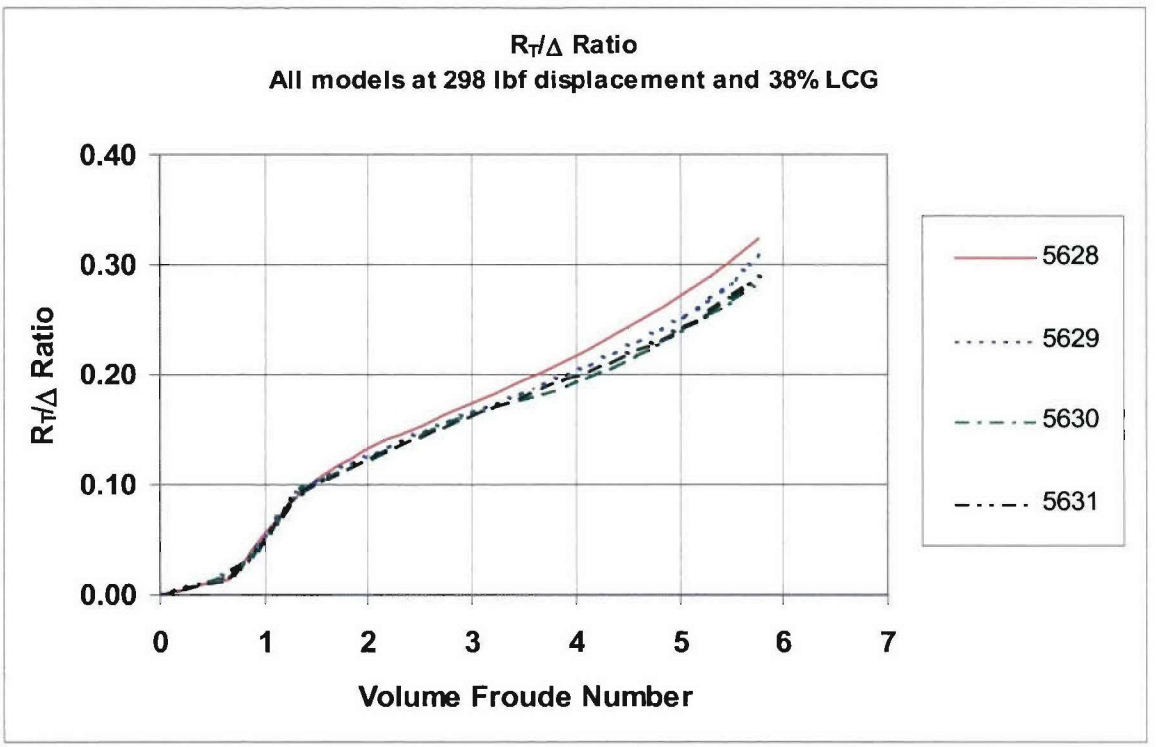

Figure 11. L/B & on Resistance for 298Lbs at 38% LCG

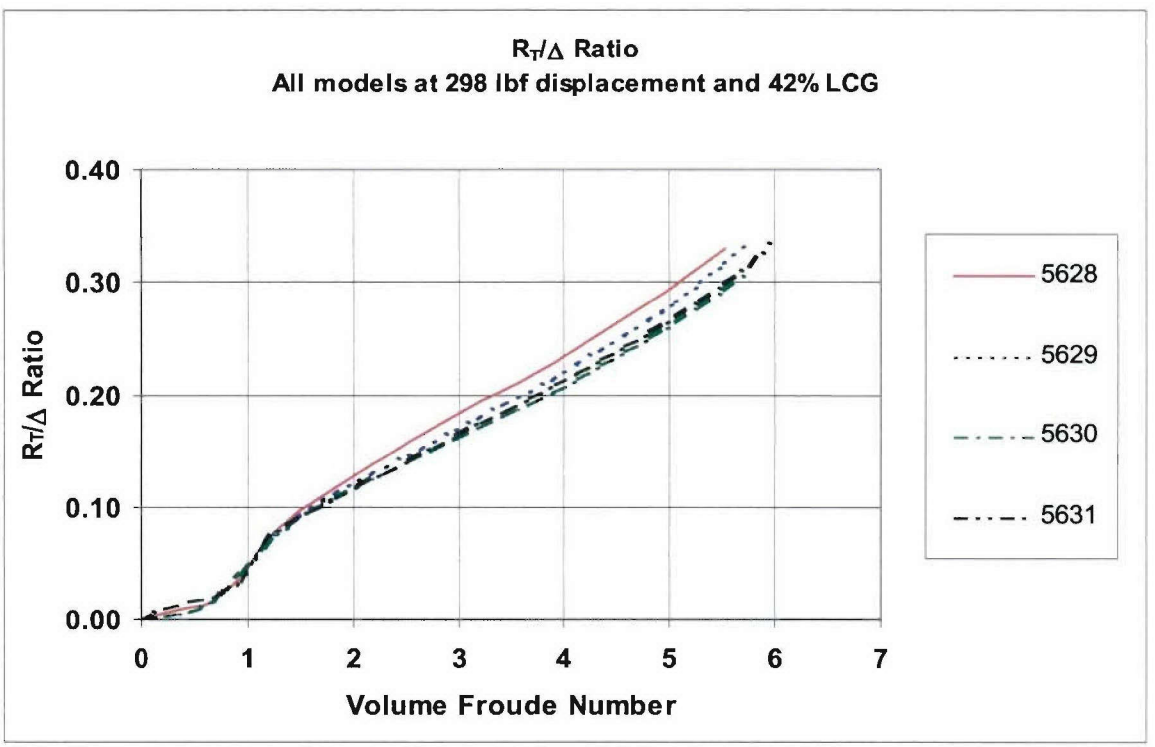

Figure 12. L/B & Deadrise Influence on Resistance for 298Lbs at 42% LCG

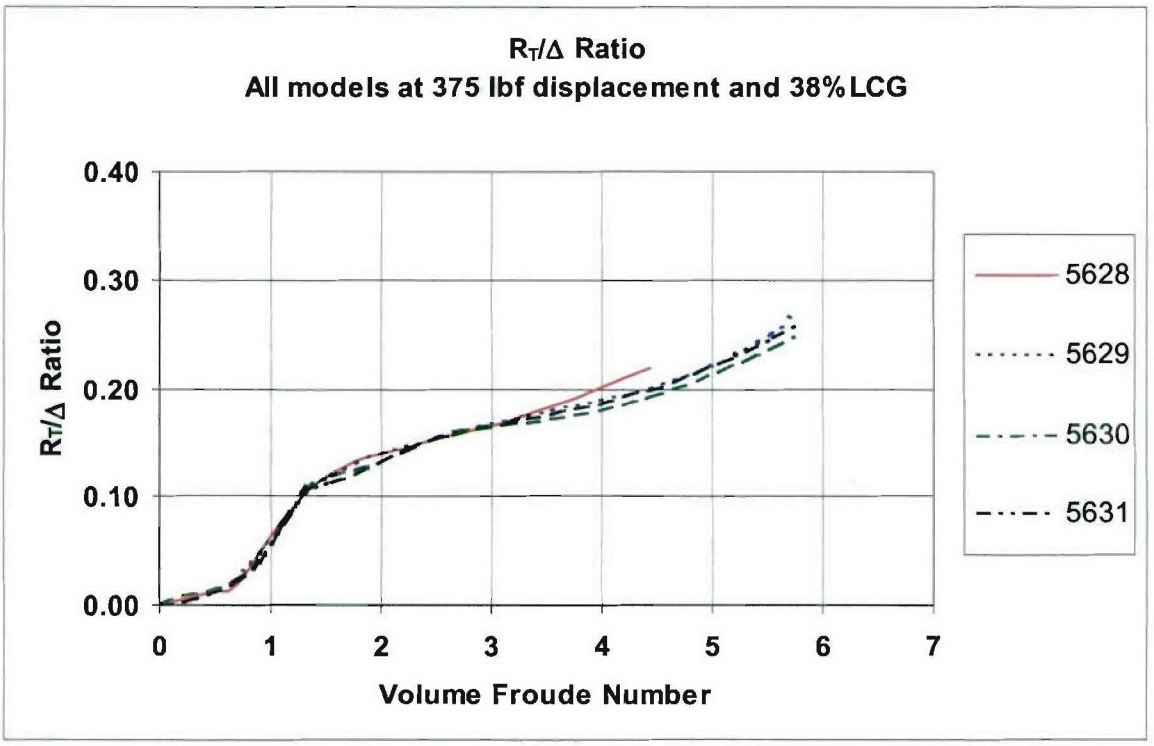

Figure 13. L/B & Deadrise Influence on Resistance for 375Lbs at 38% LCG

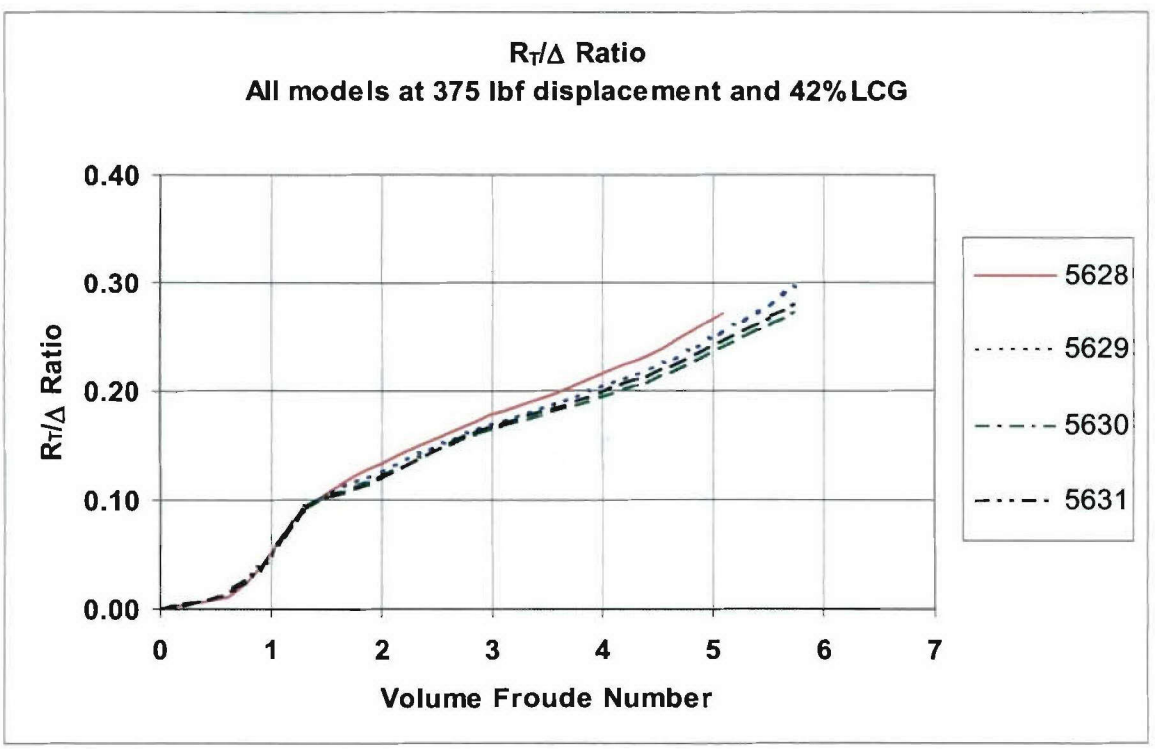

Figure 14. L/B & Deadrise Influence on Resistance for 375Lbs at 42% LCG

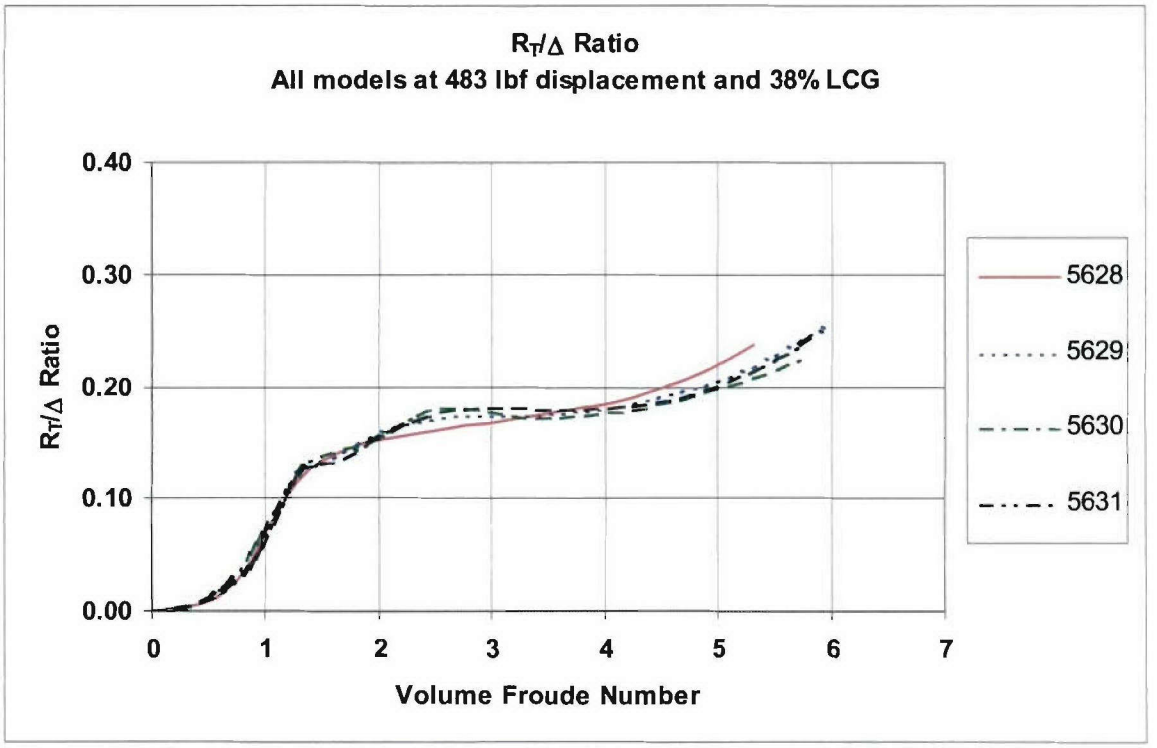

Figure 15. L/B & Deadrise Influence on Resistance for 483Lbs at 38% LCG

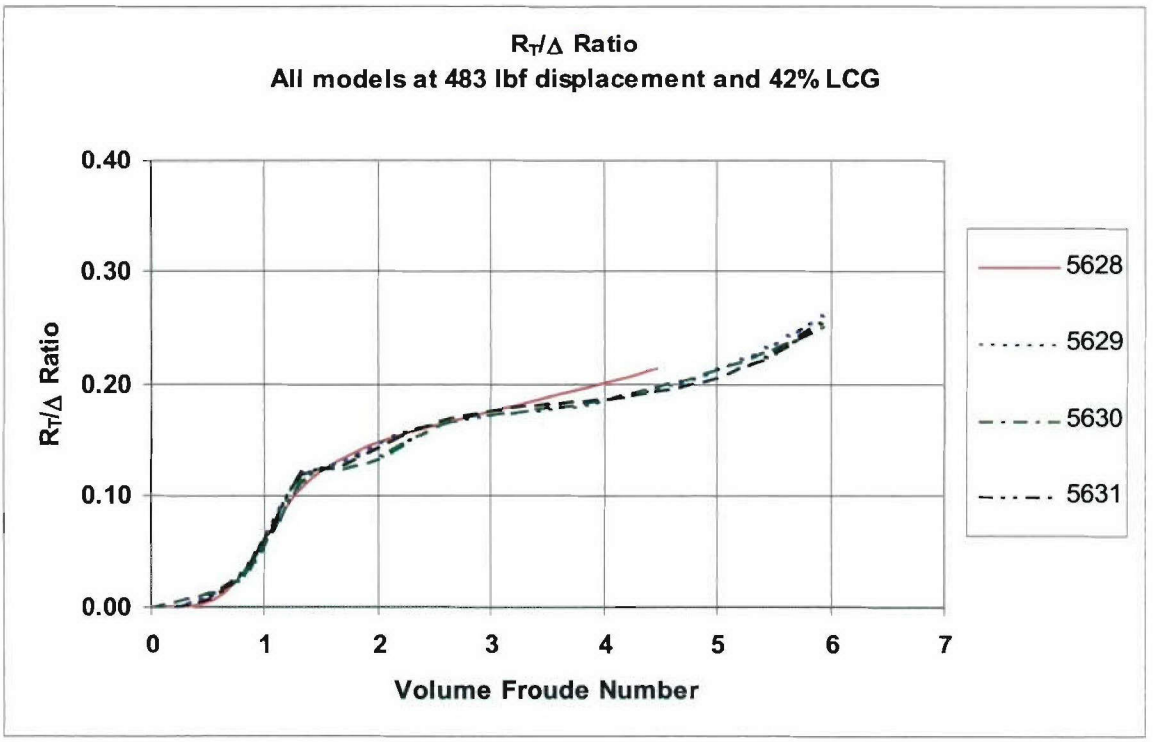

Figure 16. L/B & Deadrise Influence on Resistance for 483Lbs at 42% LCG

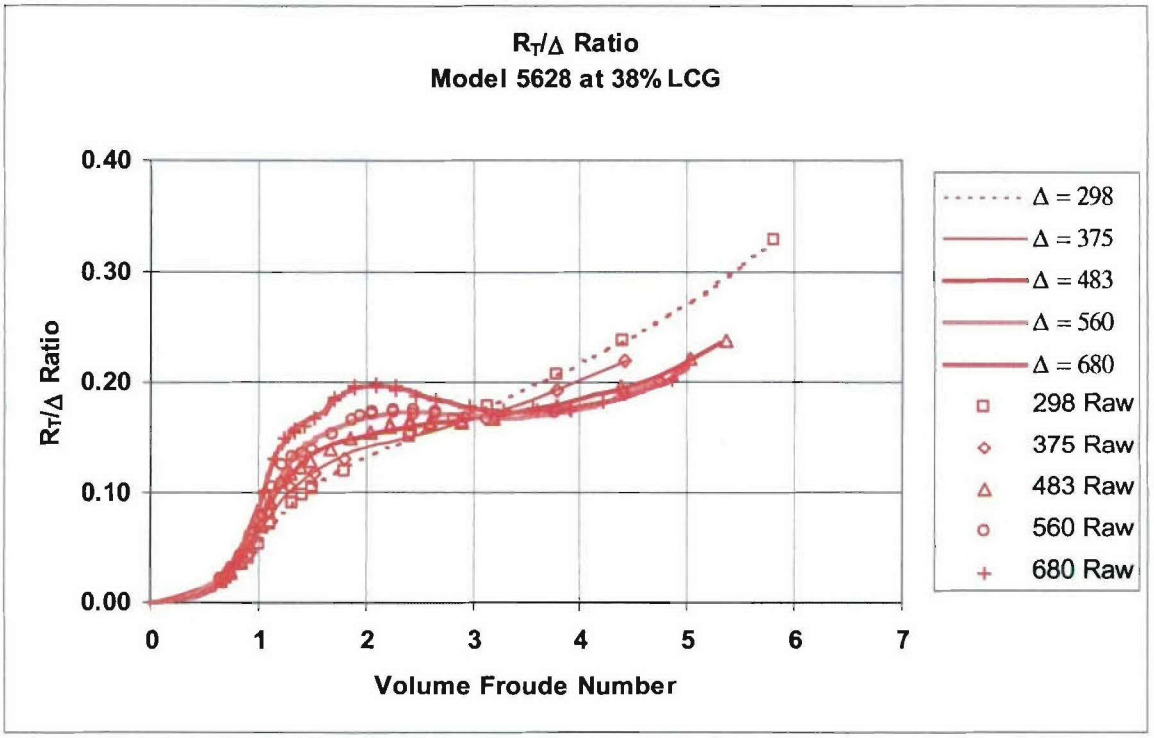

Figure 17. Model-Scale R_T/Displ for Model 5628 at 38% LCG

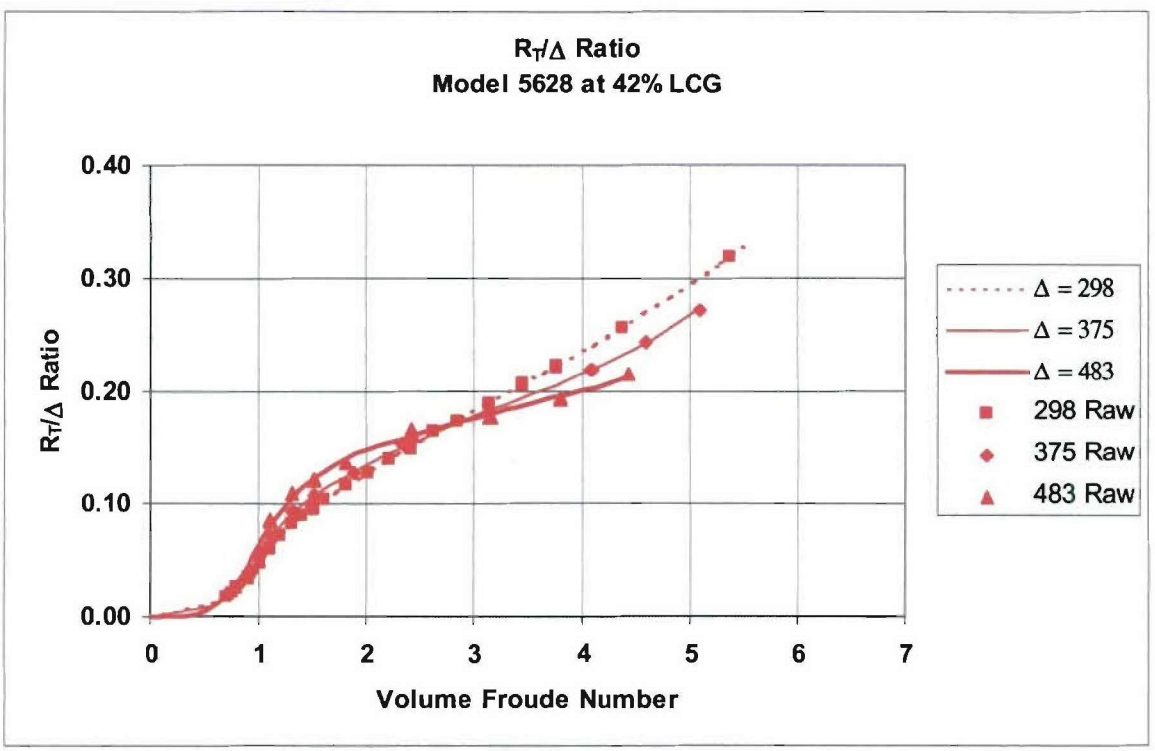

Figure 18. Model-Scale R_T/Displ for Model 5628 at 42% LCG

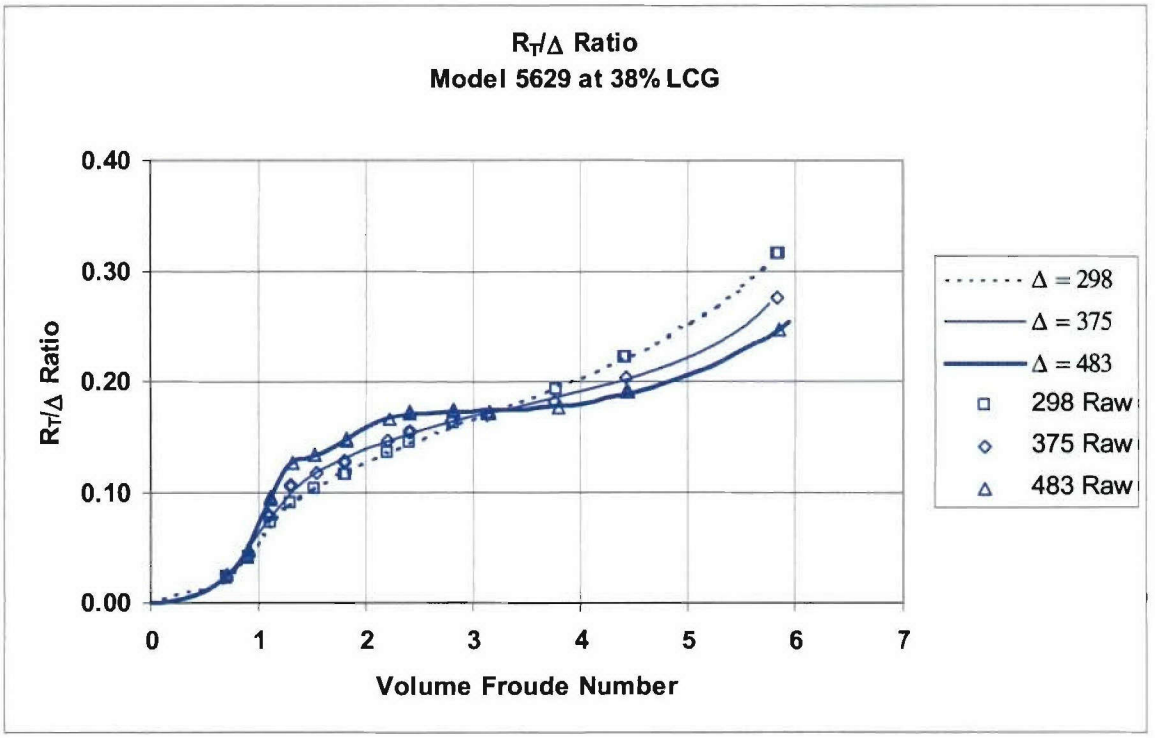

Figure 19. Model-Scale R_T/Displ for Model 5629 at 38% LCG

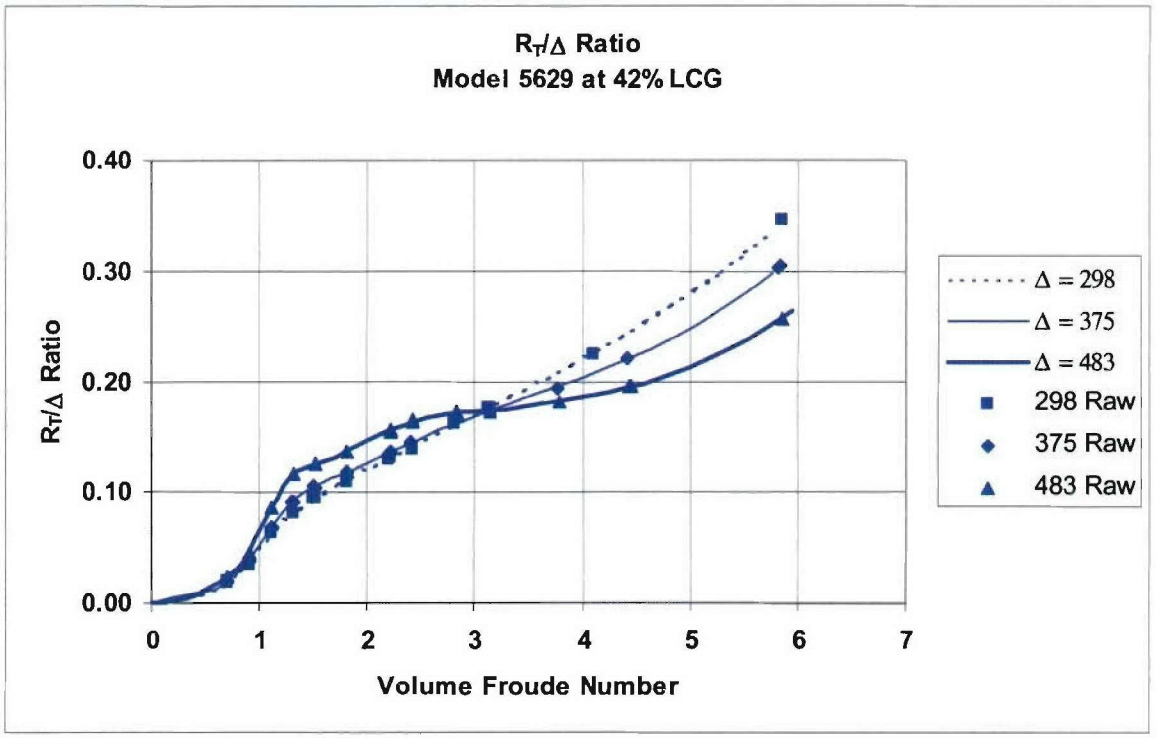

Figure 20. Model-Scale R_T/Displ for Model 5629 at 42% LCG

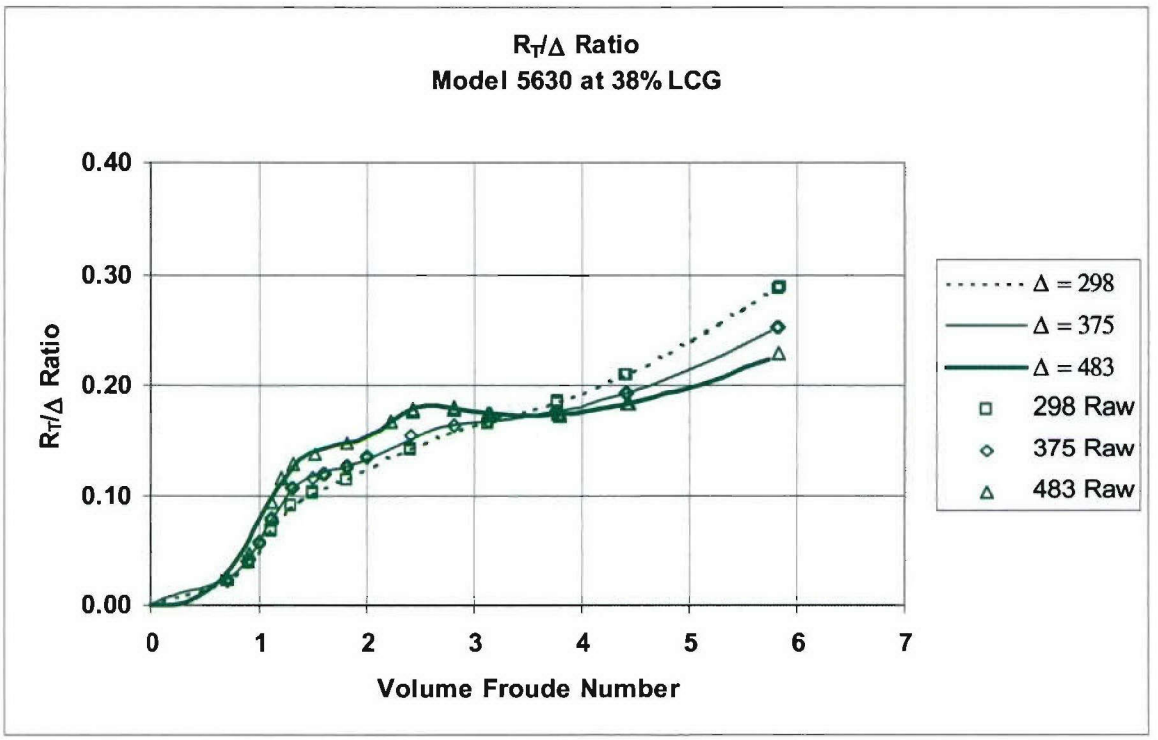

Figure 21. Model-Scale R_T/Displ for Model 5630 at 38% LCG

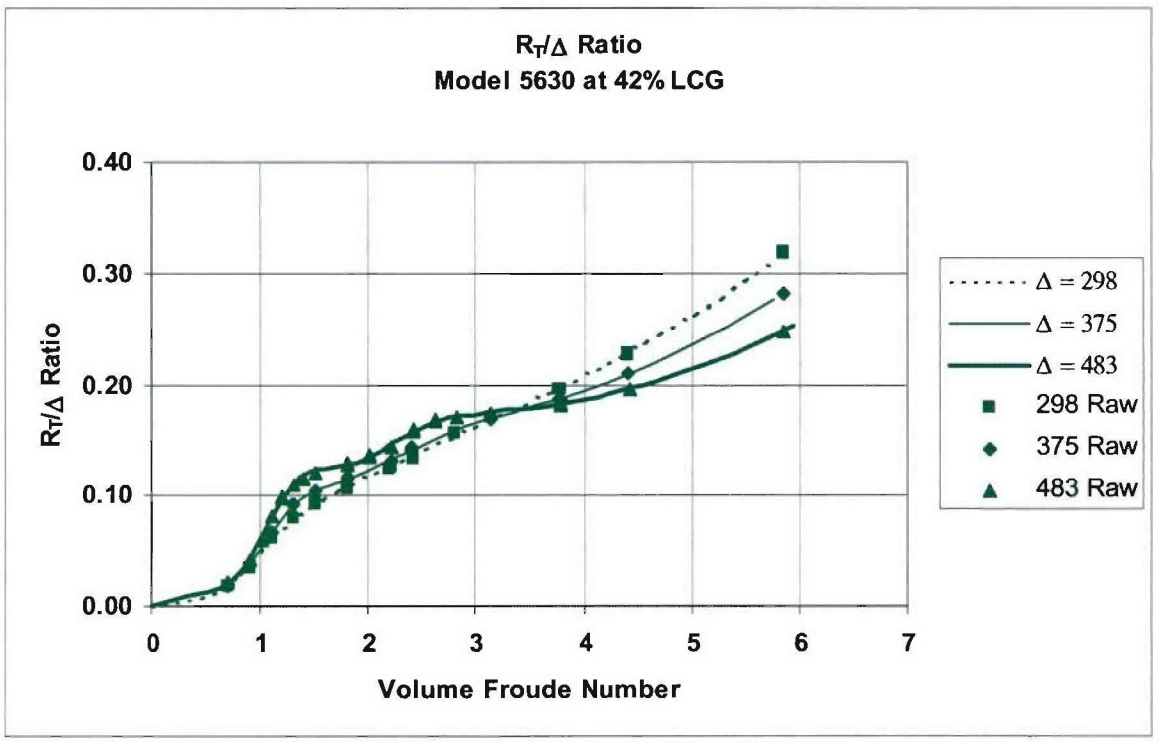

Figure 22. Model-Scale R_T/Displ for Model 5630 at 42% LCG

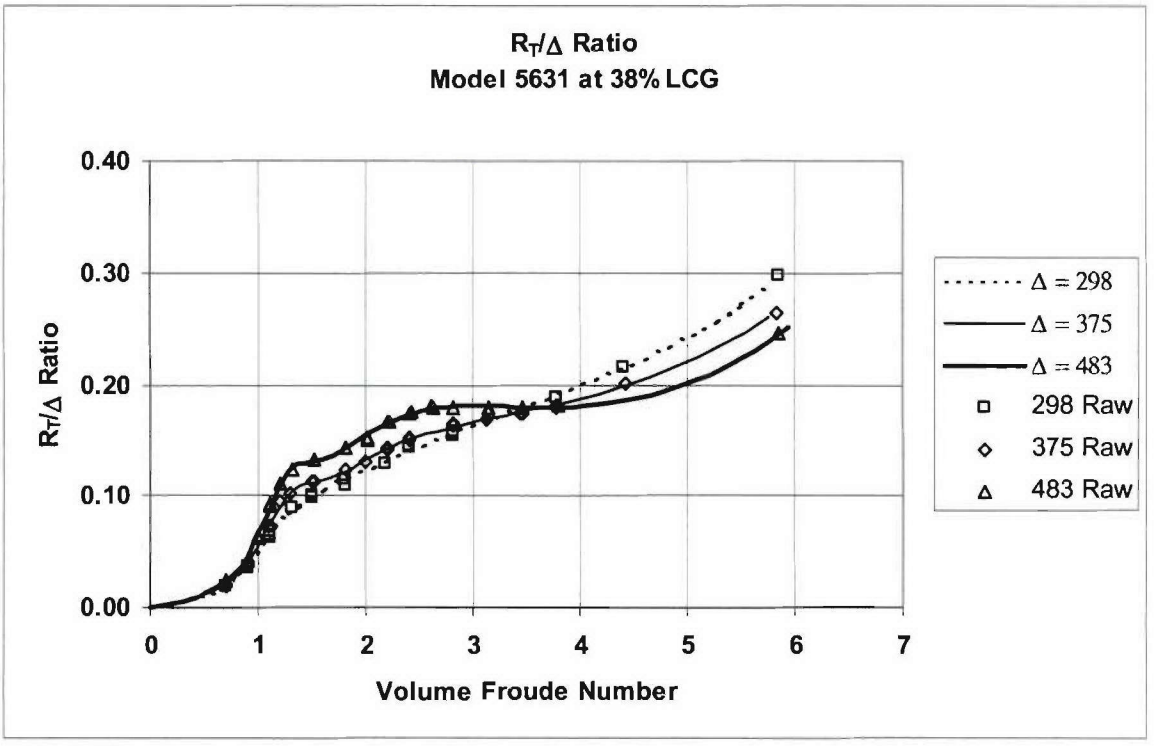

Figure 23. Model-Scale R_T/Displ for Model 5631 at 38% LCG

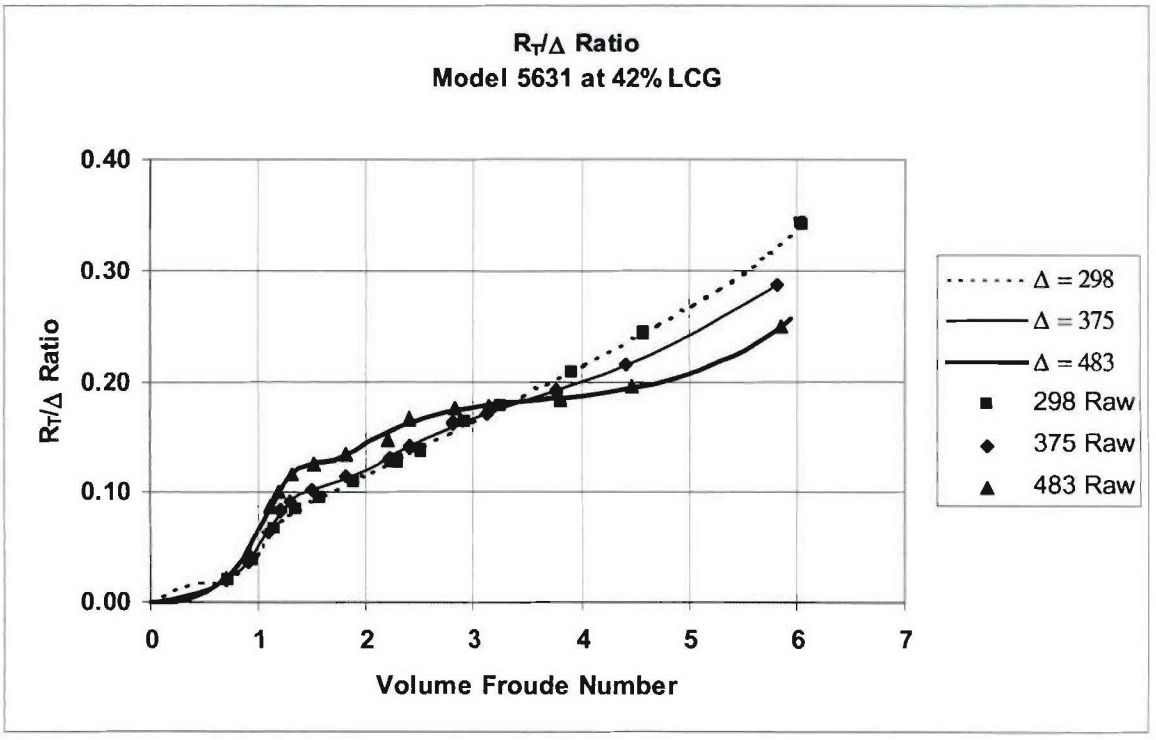

Figure 24. Model-Scale R_T/Displ for Model 5631 at 42% LCG

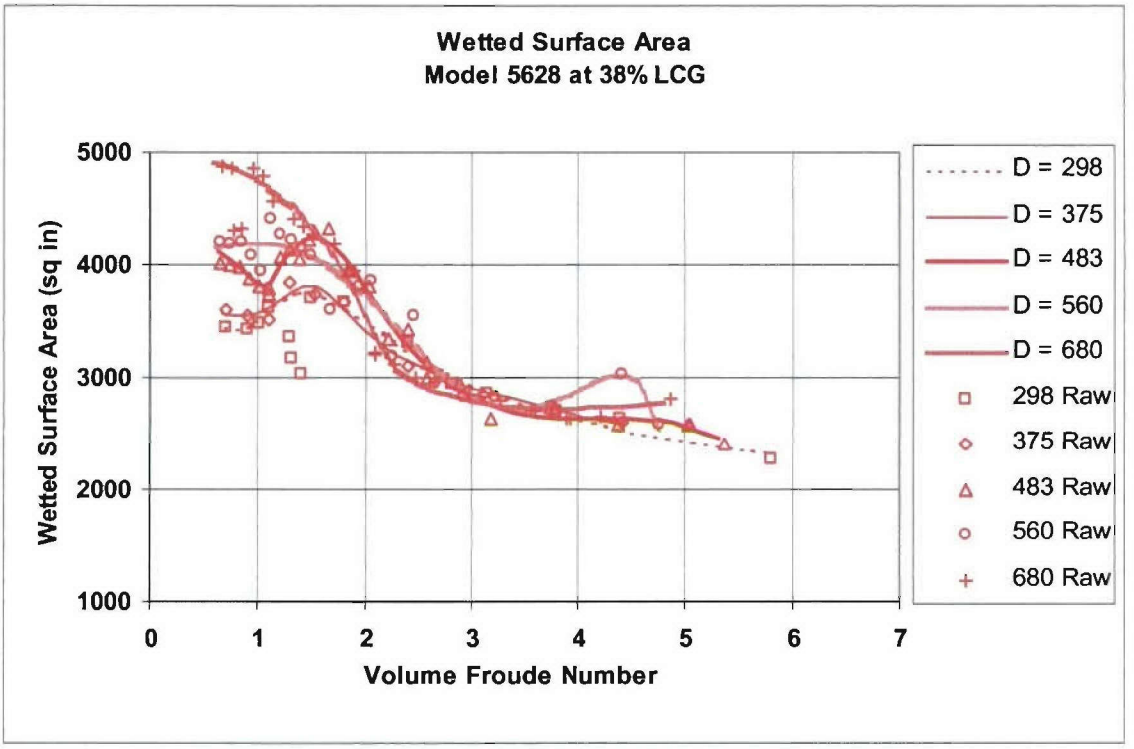

Figure 25. Model-Scale Dynamic Wetted Surface Area for Model 5628 at 38% LCG

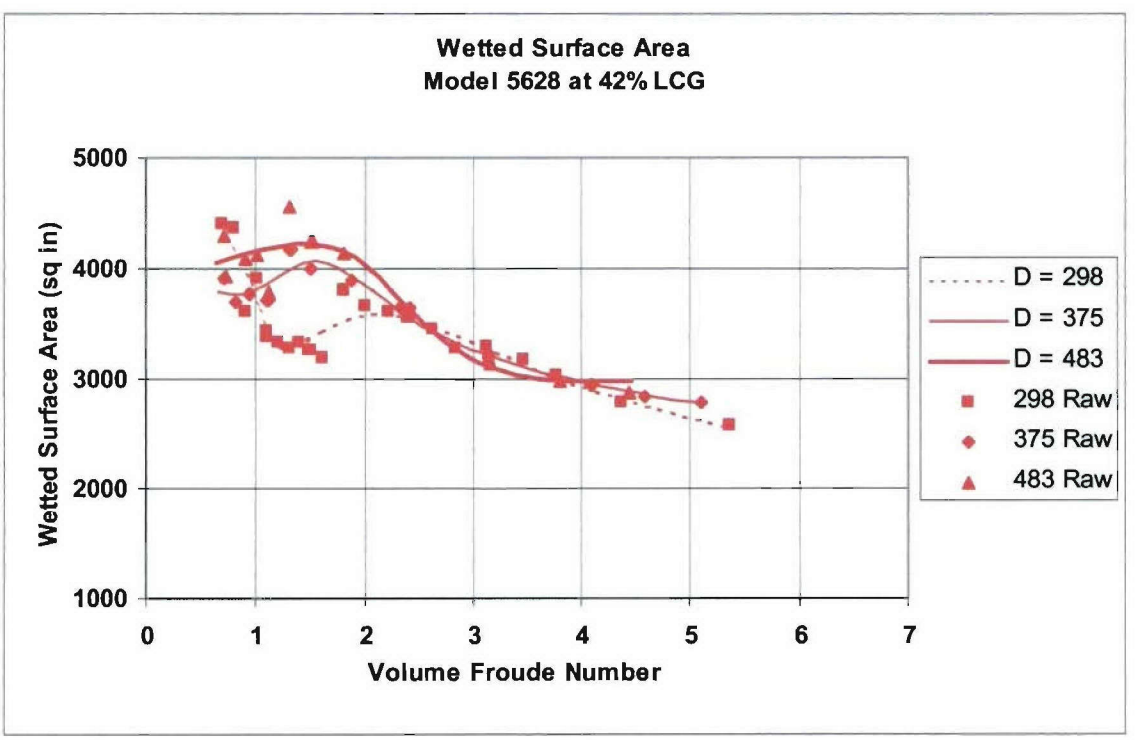

Figure 26. Model-Scale Dynamic Wetted Surface Area for Model 5628 at 42% LCG

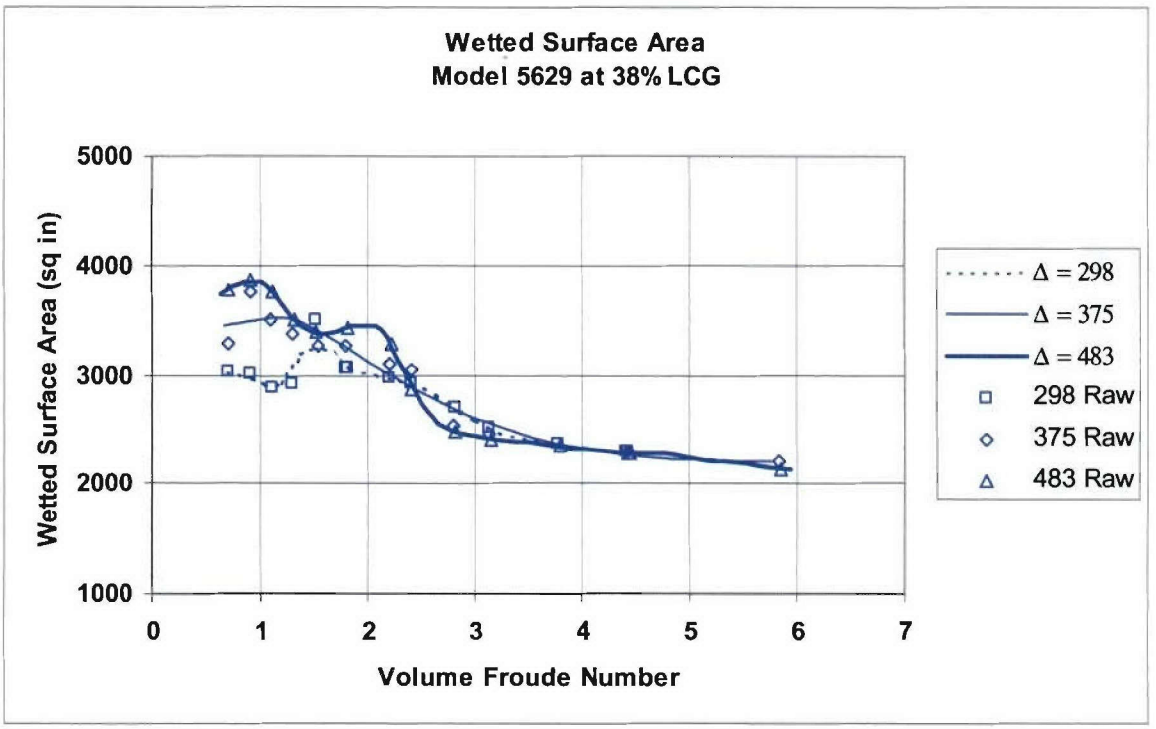

Figure 27. Model-Scale Dynamic Wetted Surface Area for Model 5629 at 38% LCG

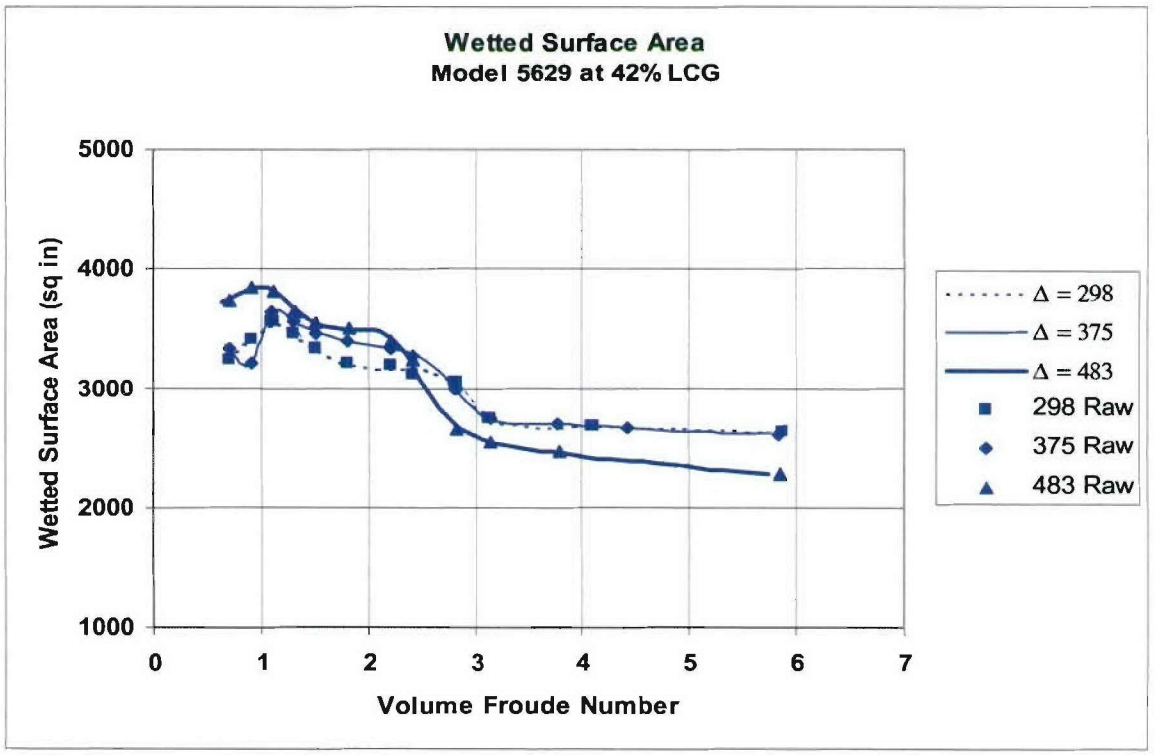

Figure 28. Model-Scale Dynamic Wetted Surface Area for Model 5629 at 42% LCG

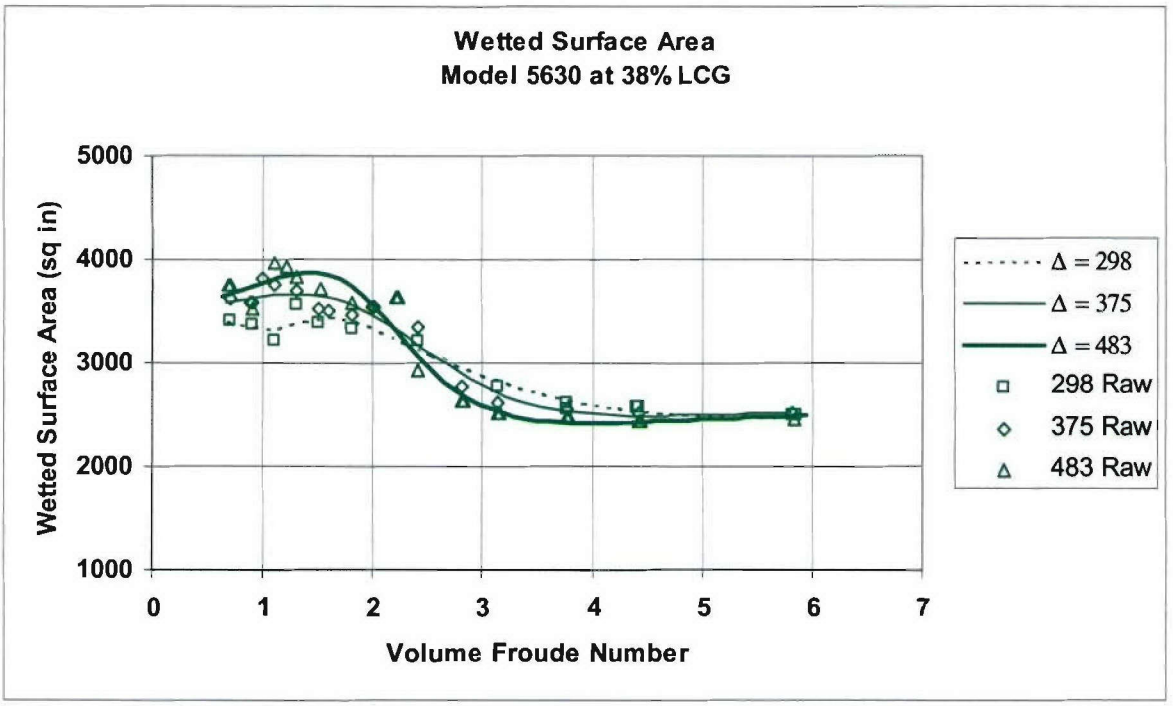

Figure 29. Model-Scale Dynamic Wetted Surface Area for Model 5630 at 38% LCG

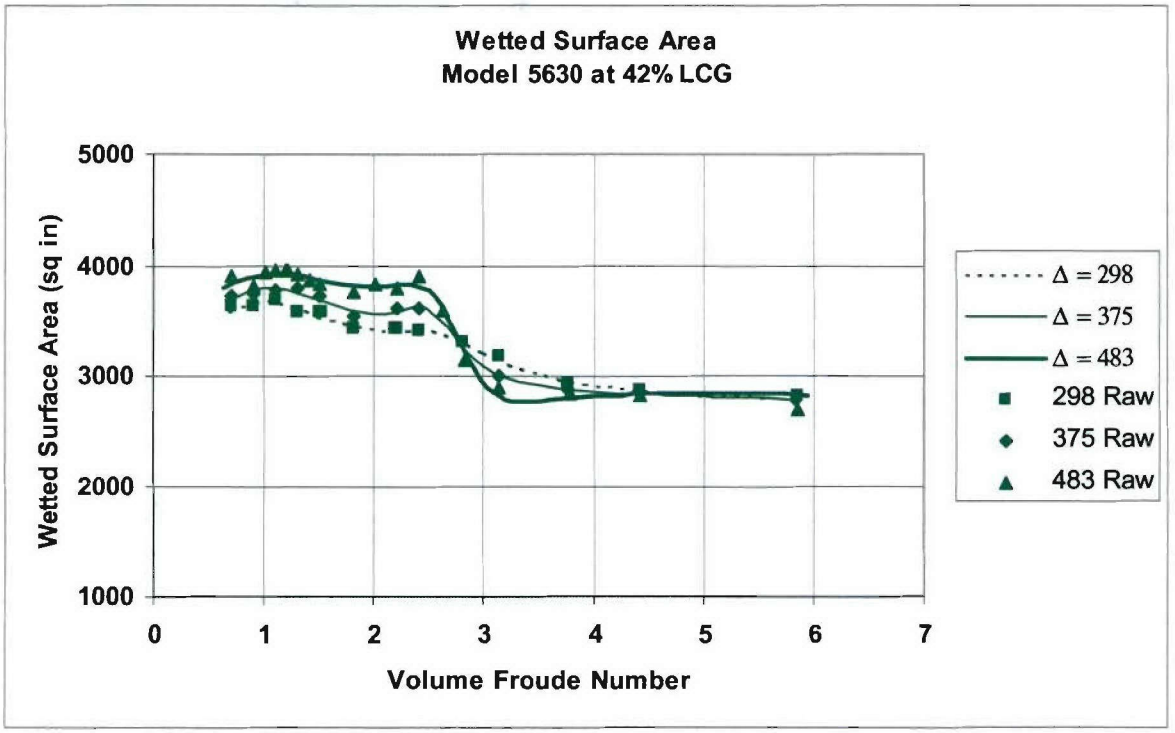

Figure 30. Model-Scale Dynamic Wetted Surface Area for Model 5630 at 42% LCG

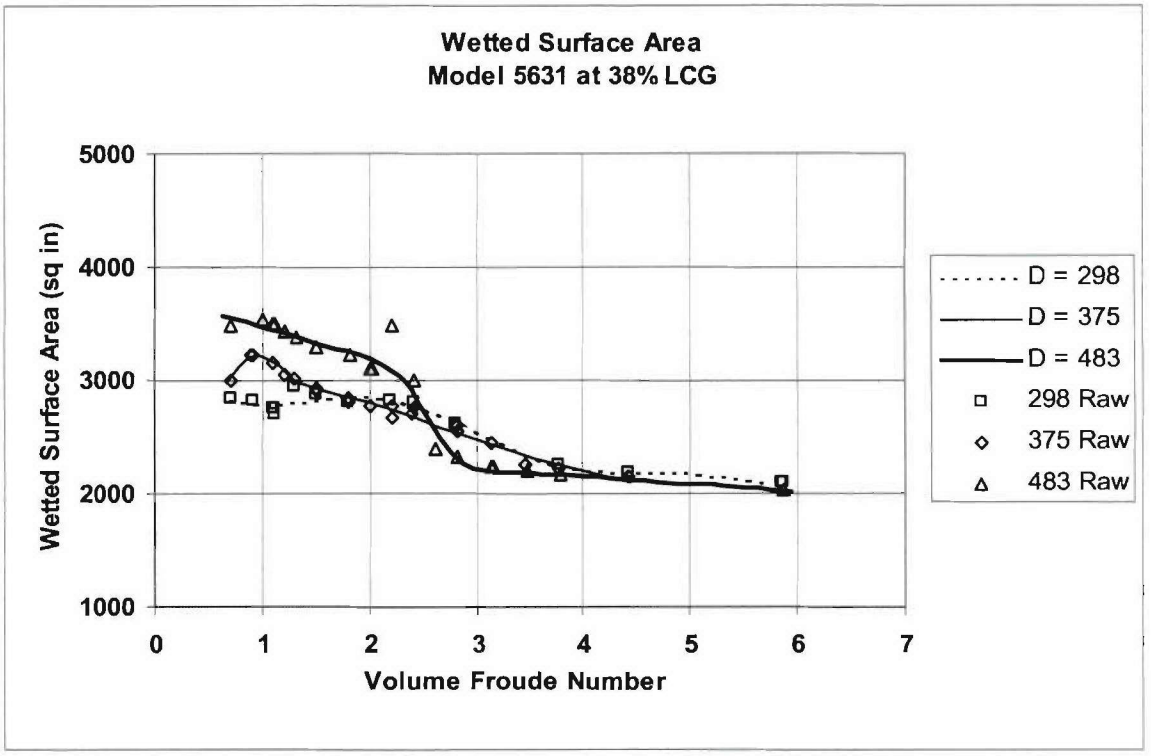

Figure 31. Model-Scale Dynamic Wetted Surface Area for Model 5631 at 38% LCG

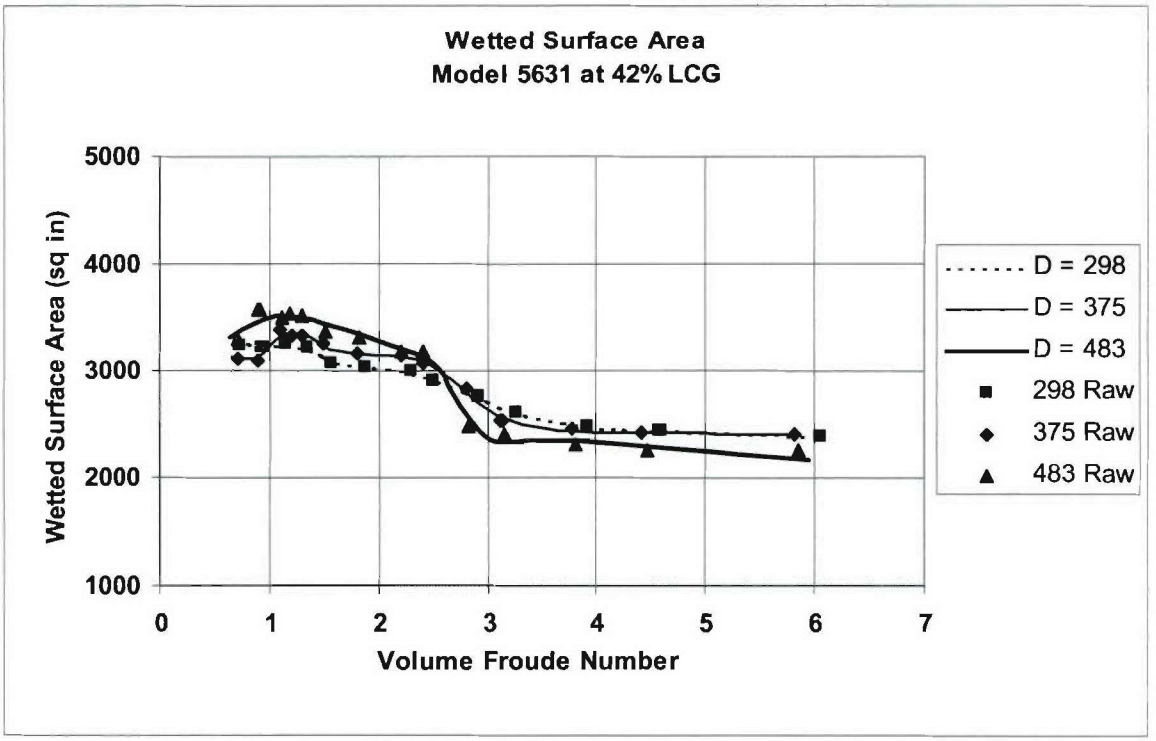

Figure 32. Model-Scale Dynamic Wetted Surface Area for Model 5631 at 42% LCG

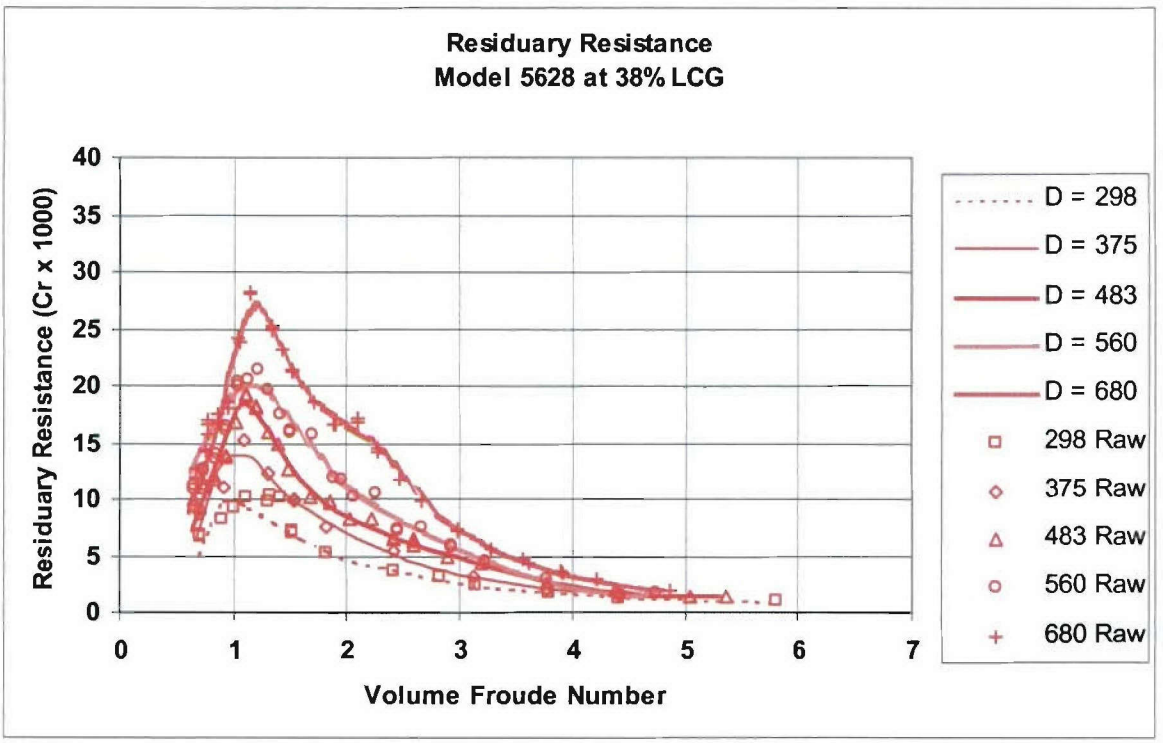

Figure 33. Residuary Resistance Coefficient for Model 5628 at 38% LCG

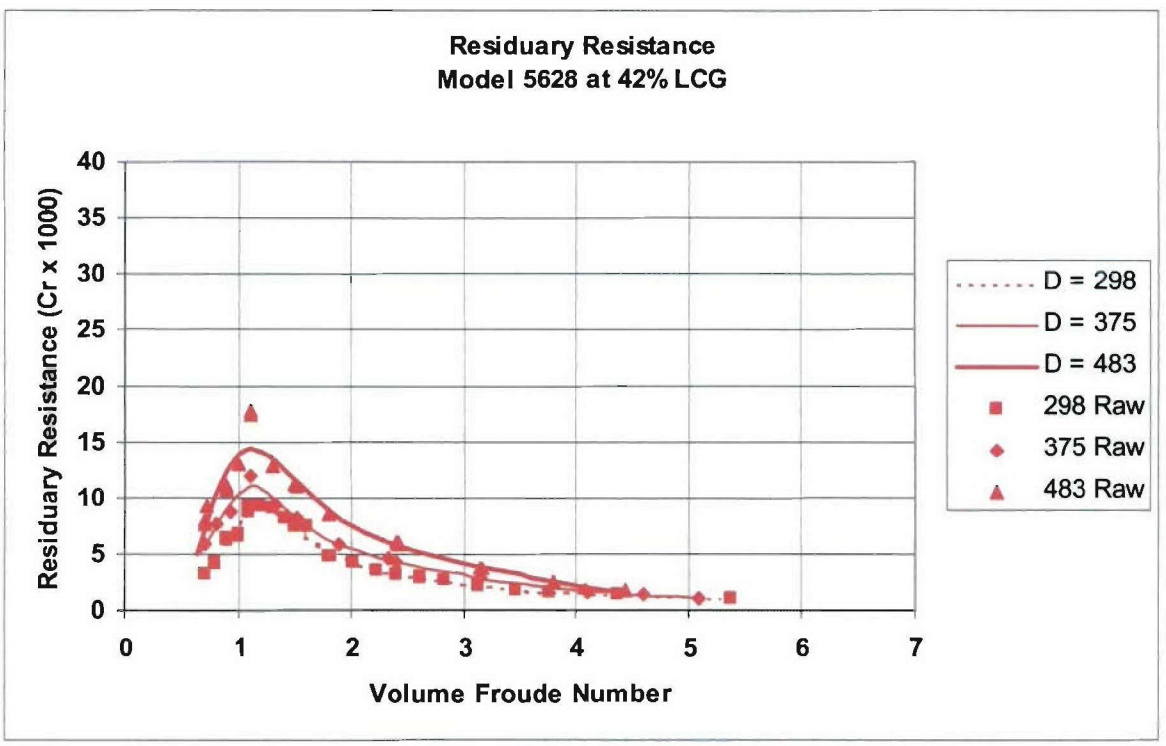

Figure 34. Residuary Resistance Coefficient for Model 5628 at 42% LCG

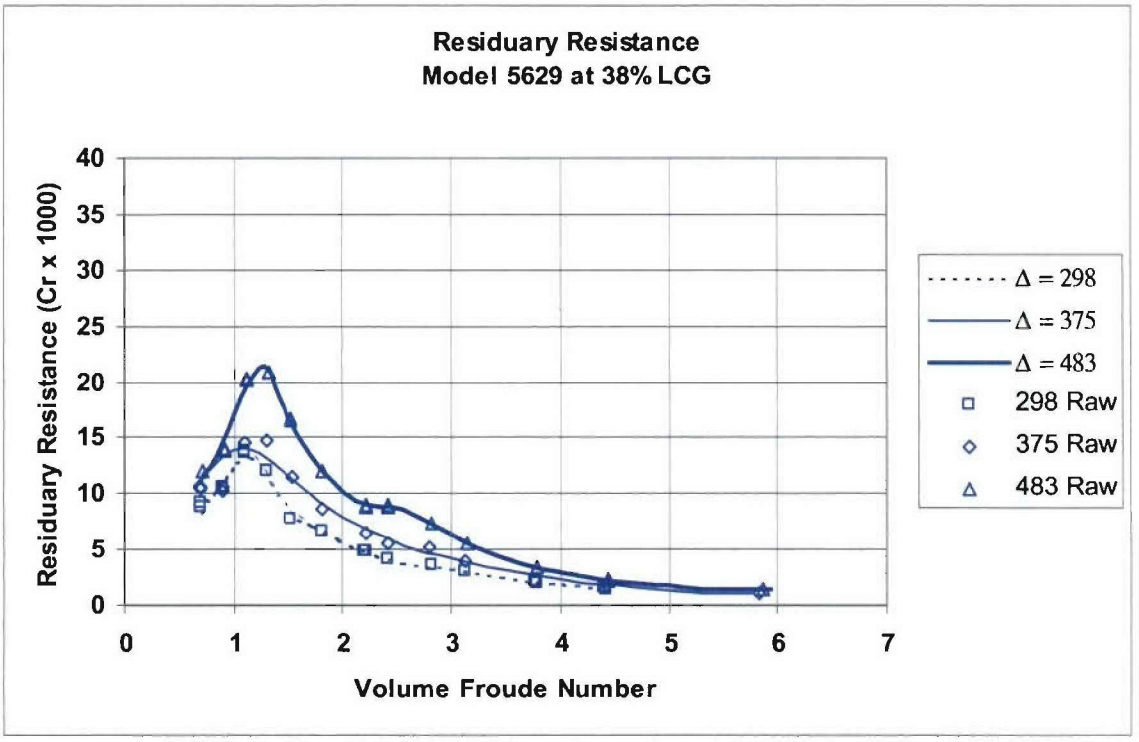

Figure 35. Residuary Resistance Coefficient for Model 5629 at 38% LCG

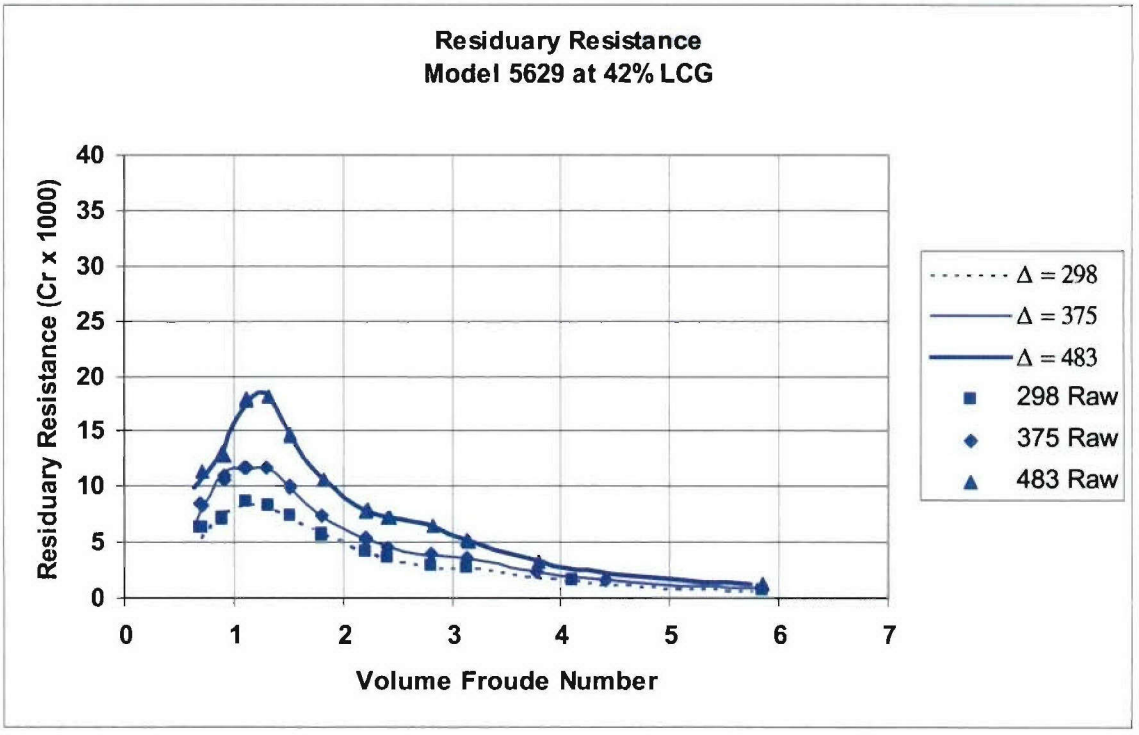

Figure 36. Residuary Resistance Coefficient for Model 5629 at 42% LCG

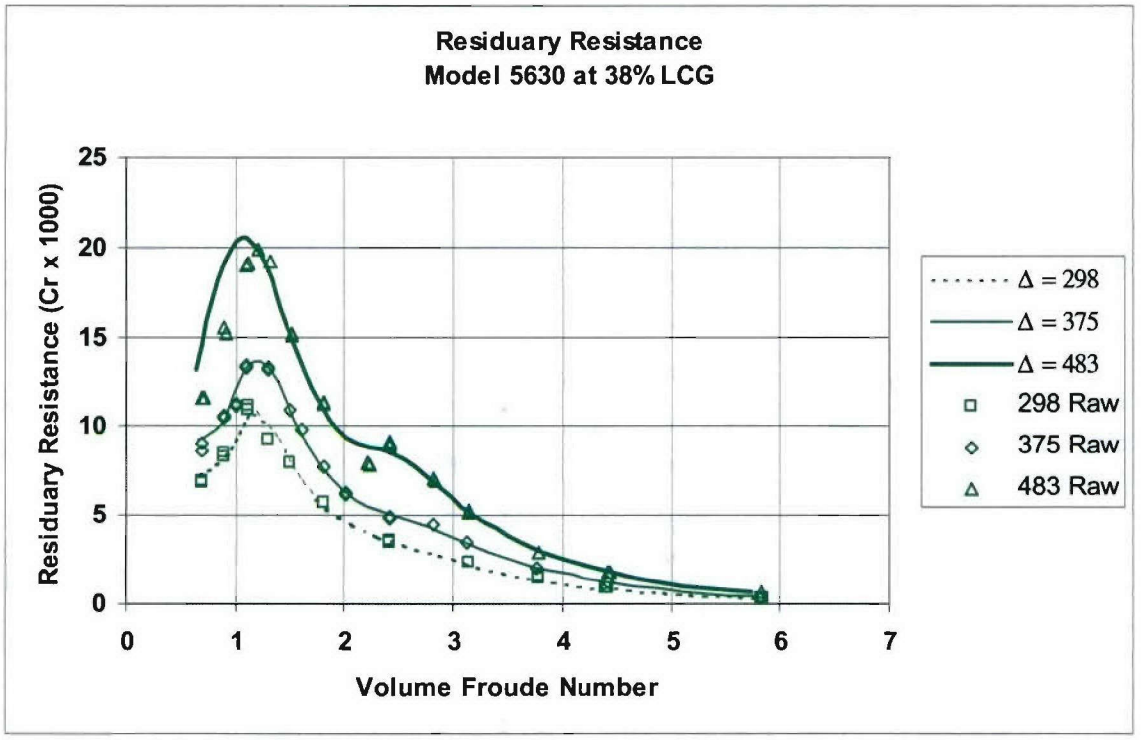

Figure 37. Residuary Resistance Coefficient for Model 5630 at 38% LCG

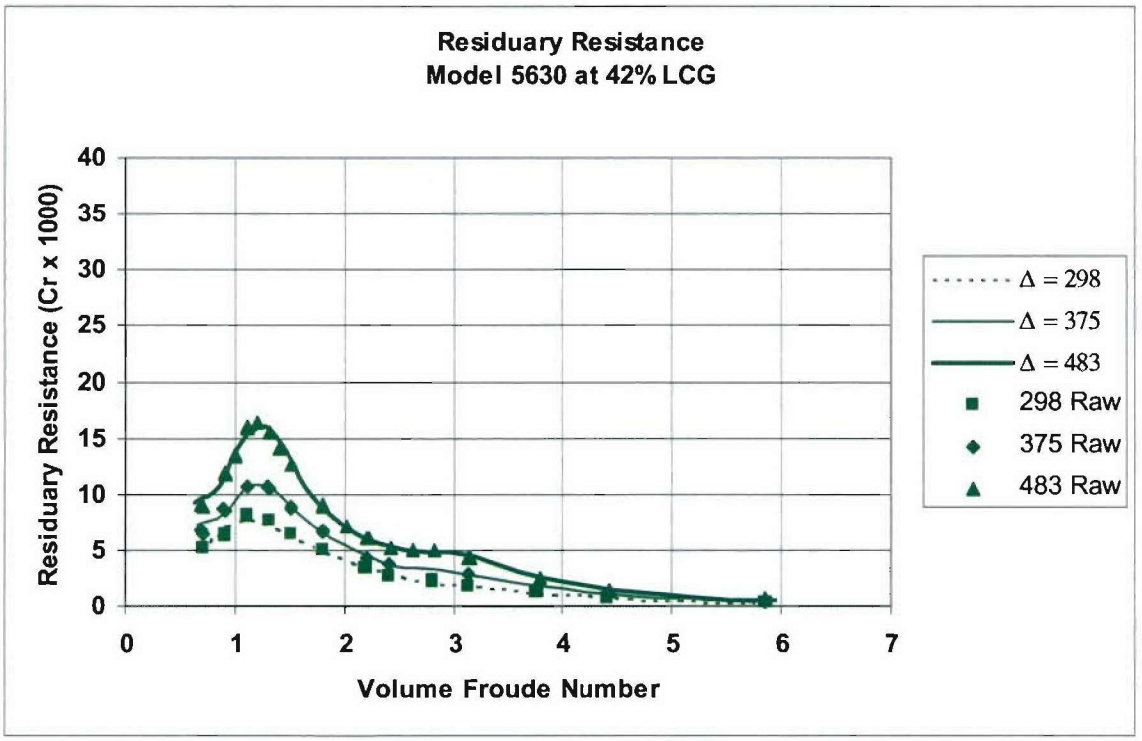

Figure 38. Residuary Resistance Coefficient for Model 5630 at 42% LCG

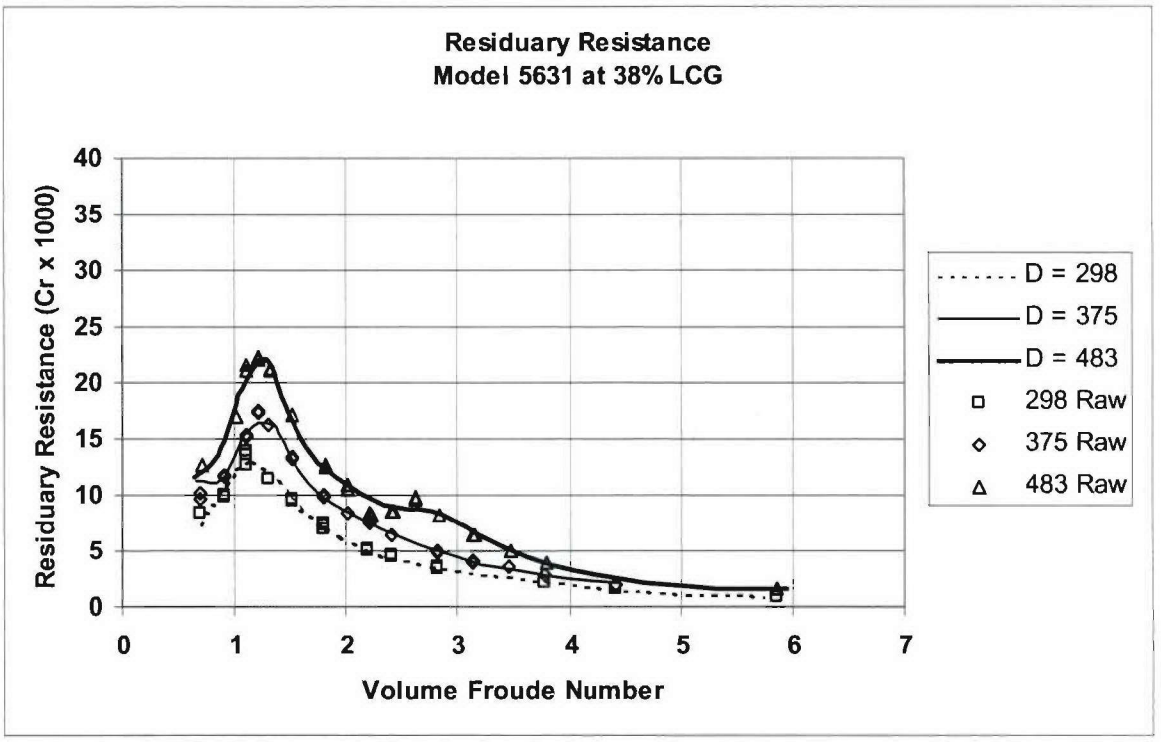

Figure 39. Residuary Resistance Coefficient for Model 5631 at 38% LCG

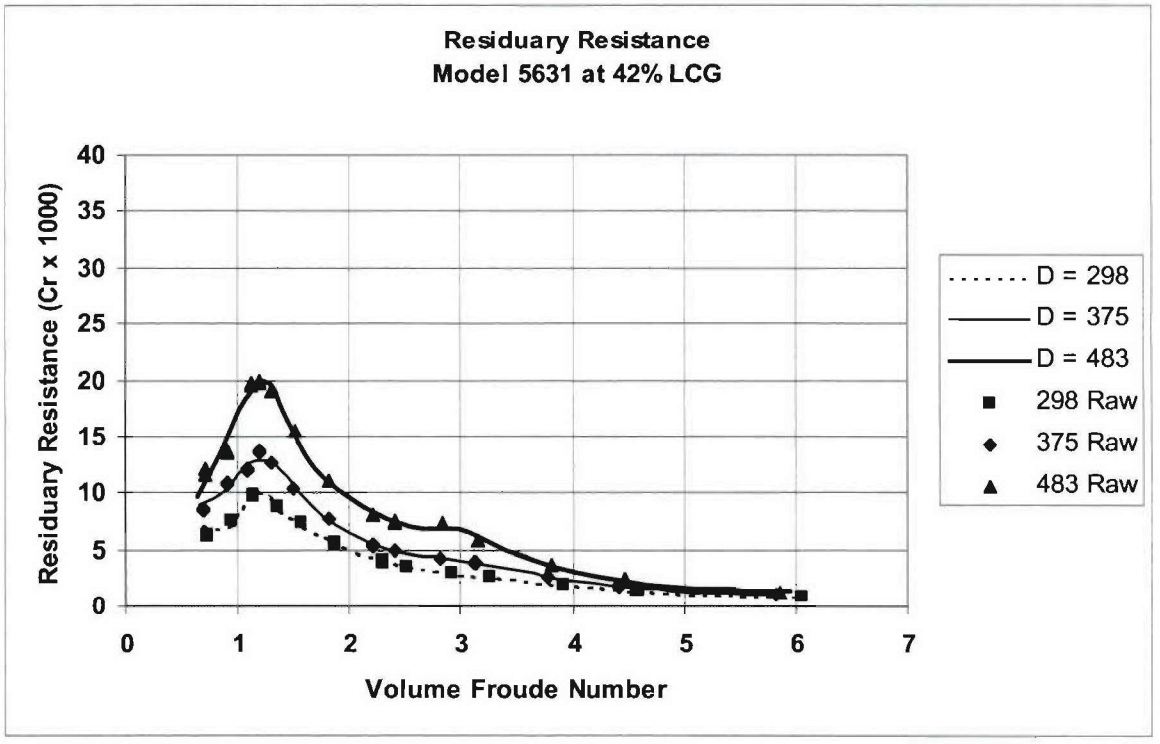

Figure 40. Residuary Resistance Coefficient for Model 5631 at 42% LCG

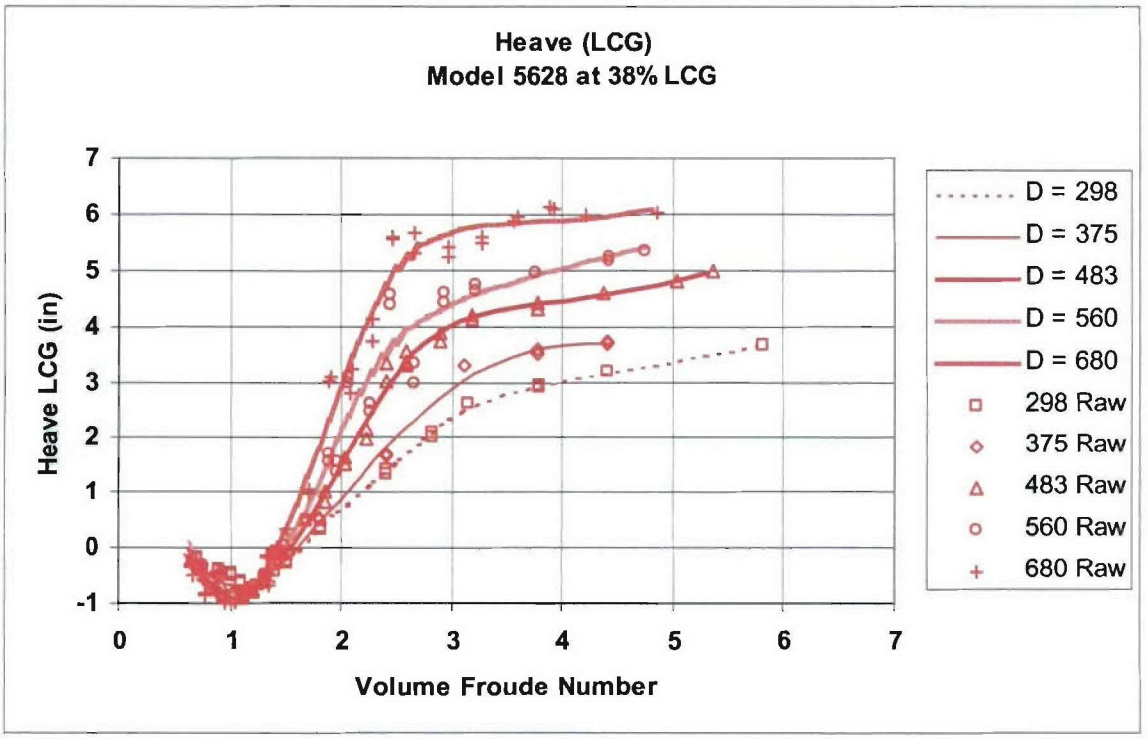

Figure 41. Model-Scale Center of Gravity Heave for Model 5628 at 38% LCG

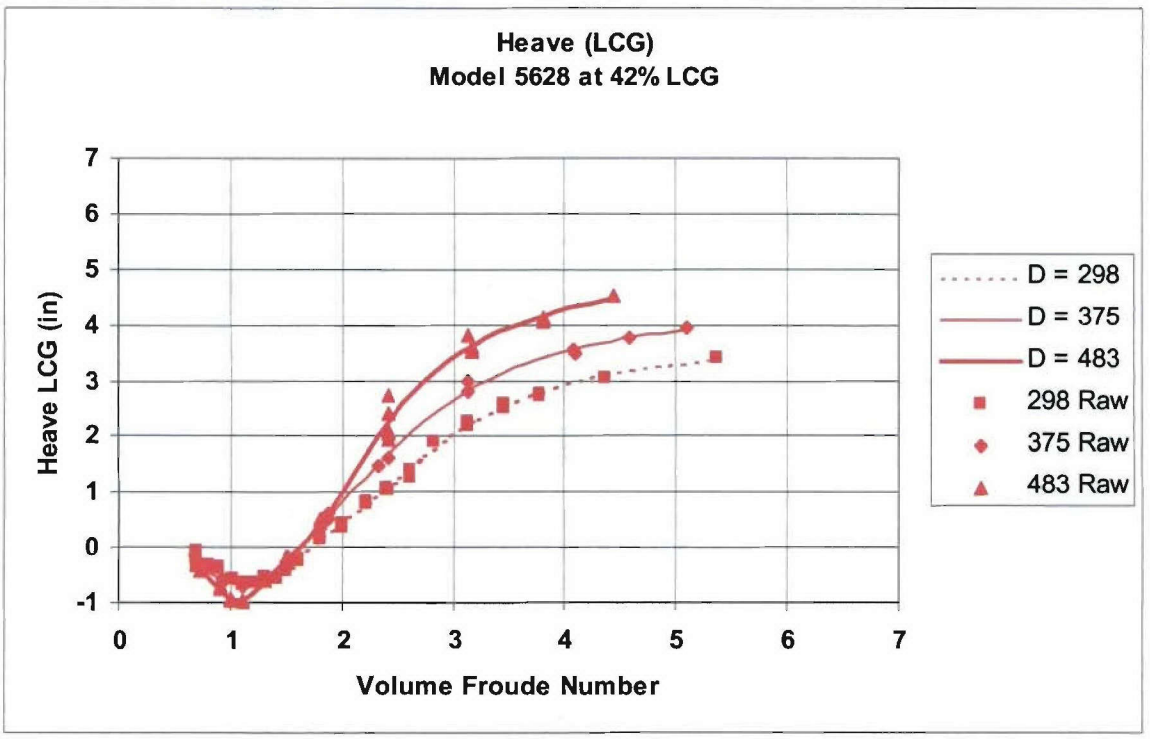

Figure 42. Model-Scale Center of Gravity Heave for Model 5628 at 42% LCG

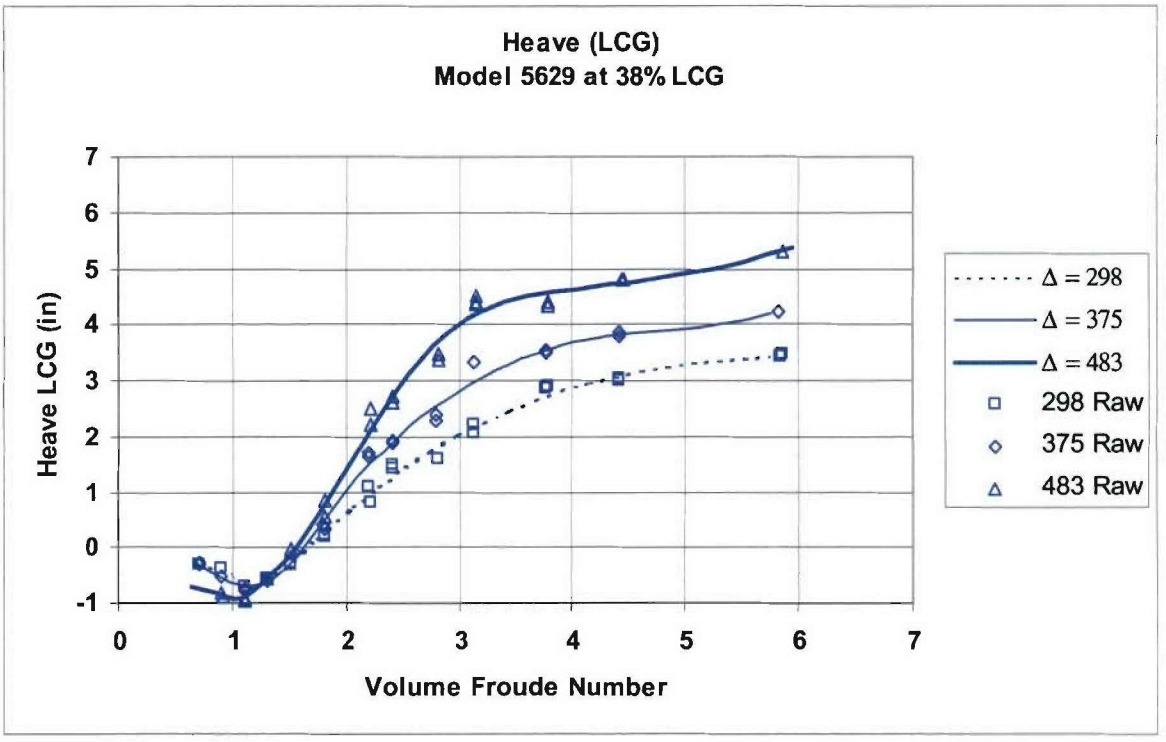

Figure 43. Model-Scale Center of Gravity Heave for Model 5629 at 38% LCG

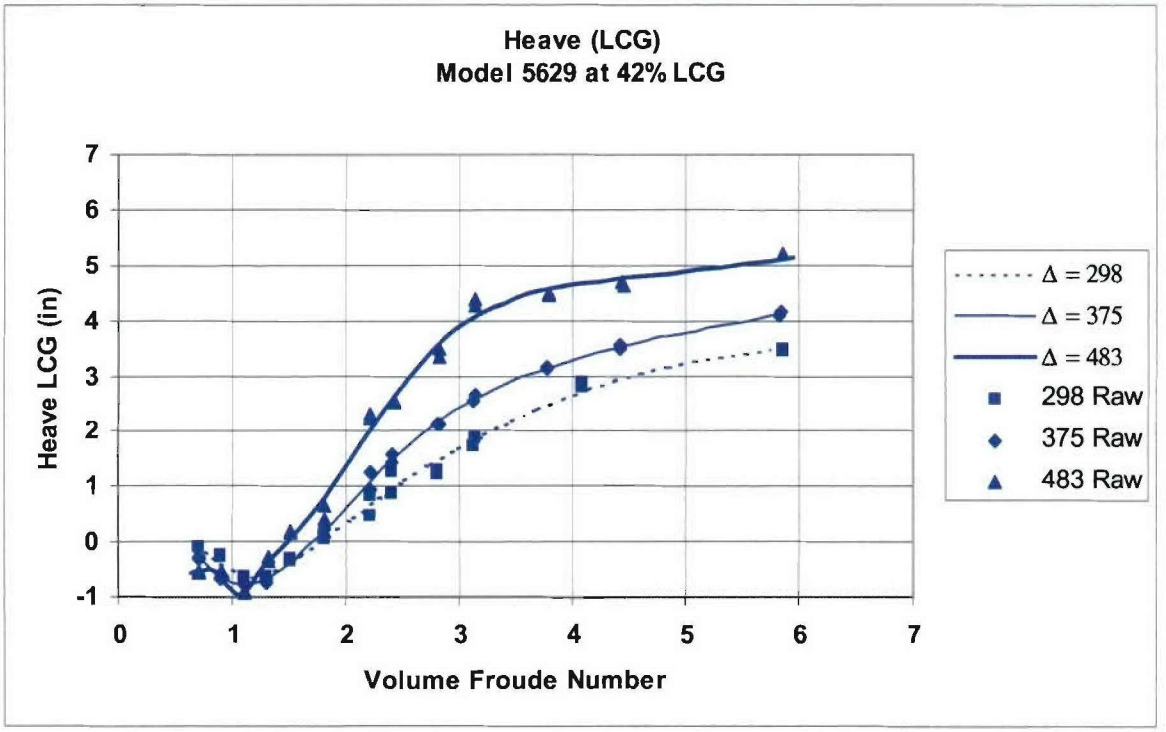

Figure 44. Model-Scale Center of Gravity Heave for Model 5629 at 42% LCG

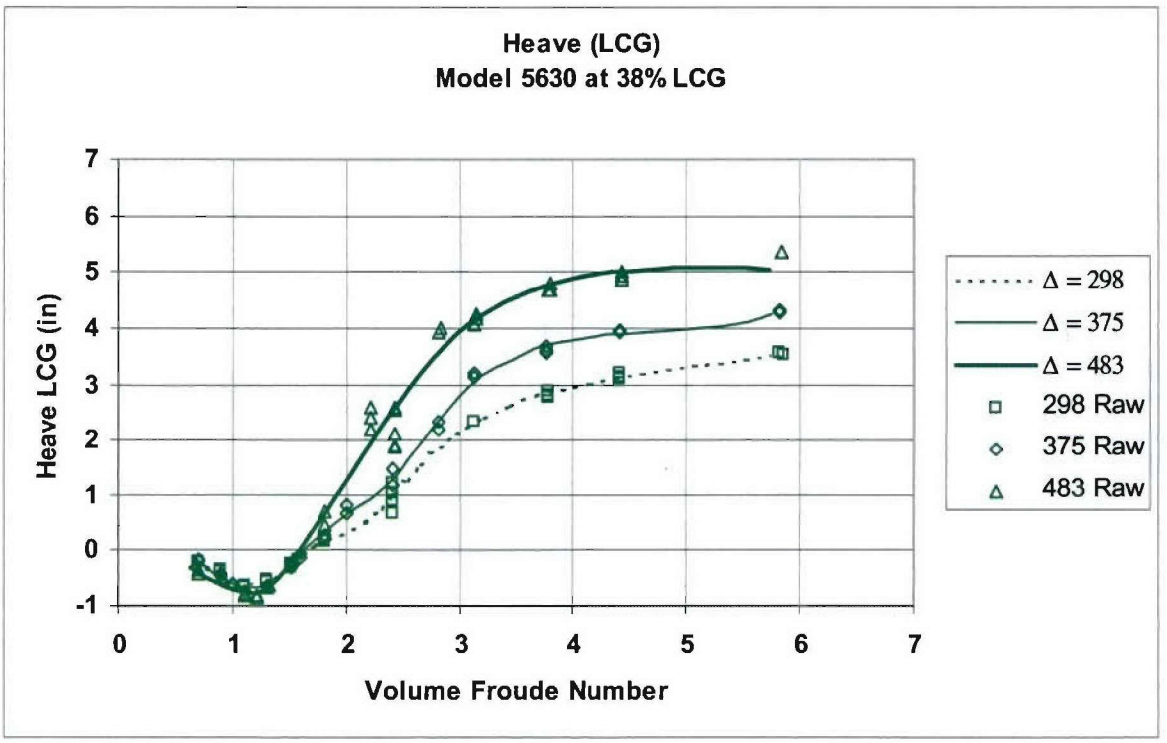

Figure 45. Model-Scale Center of Gravity Heave for Model 5630 at 38% LCG

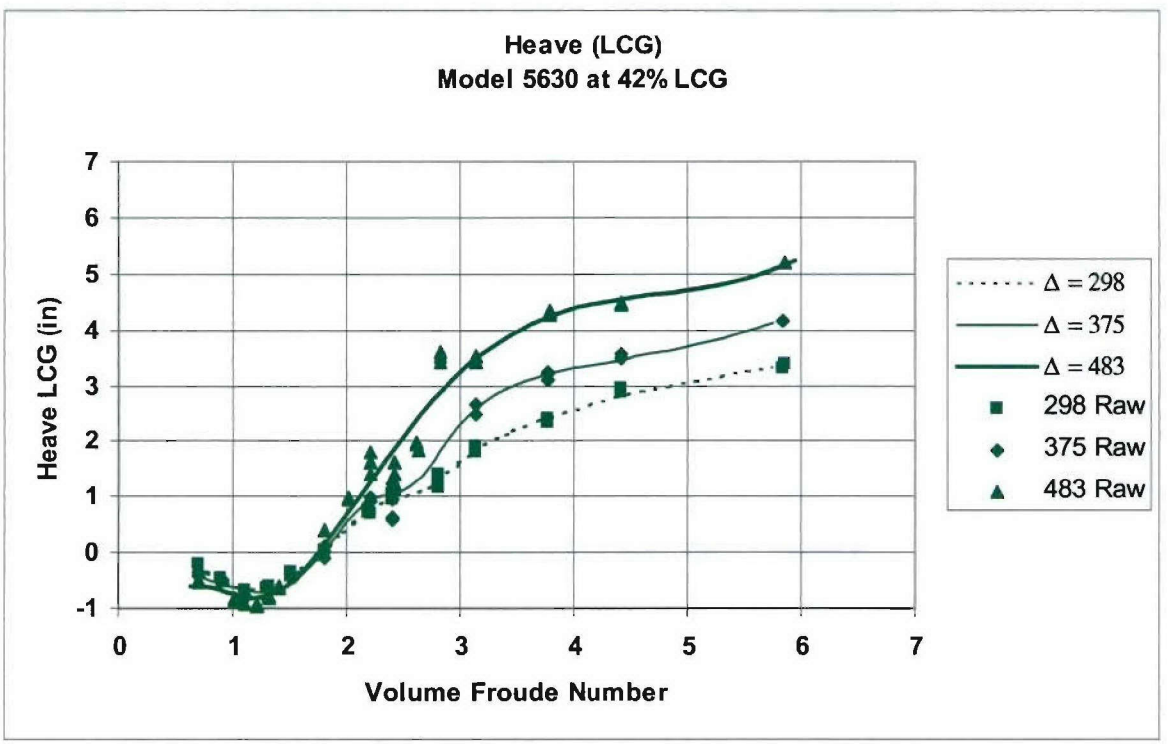

Figure 46. Model-Scale Center of Gravity Heave for Model 5630 at 42% LCG

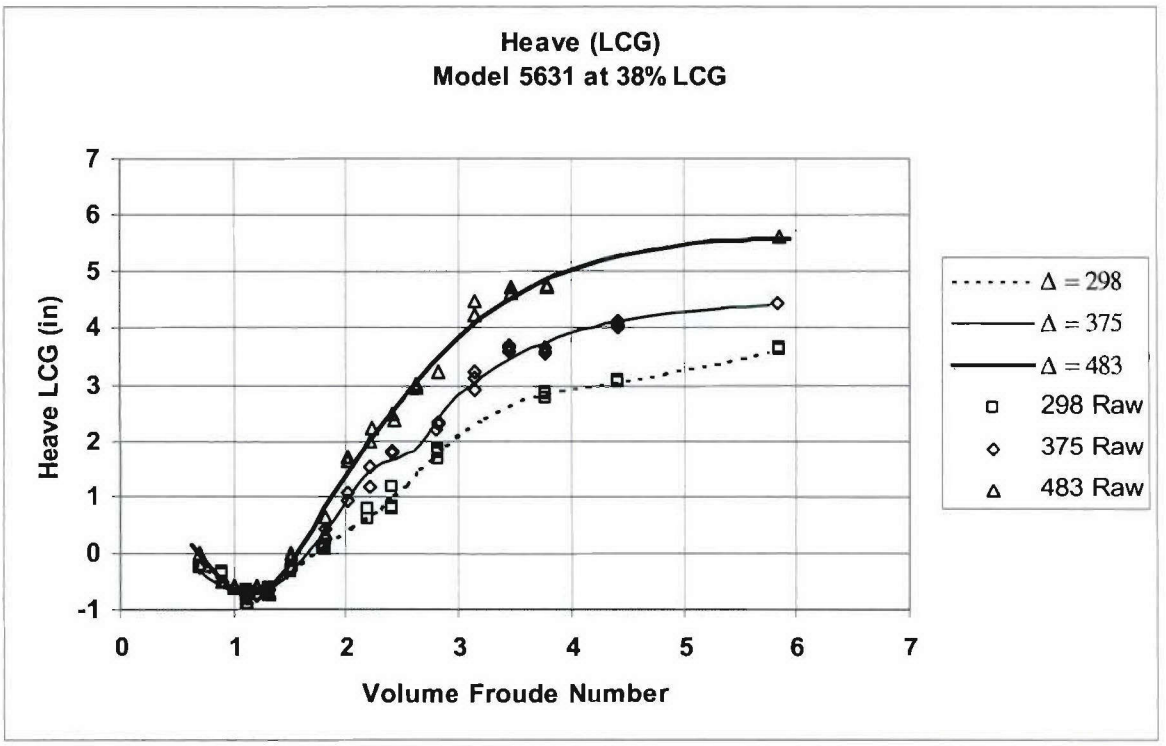

Figure 47. Model-Scale Center of Gravity Heave for Model 5631 at 38% LCG

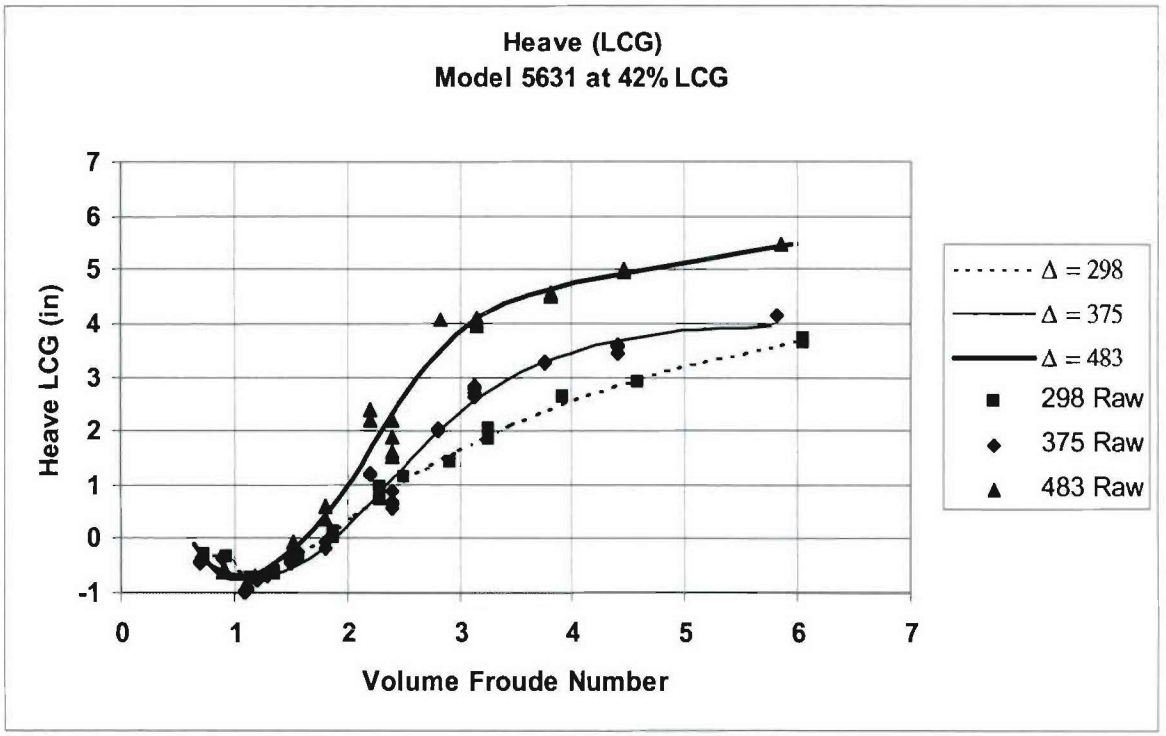

Figure 48. Model-Scale Center of Gravity Heave for Model 5631 at 42% LCG

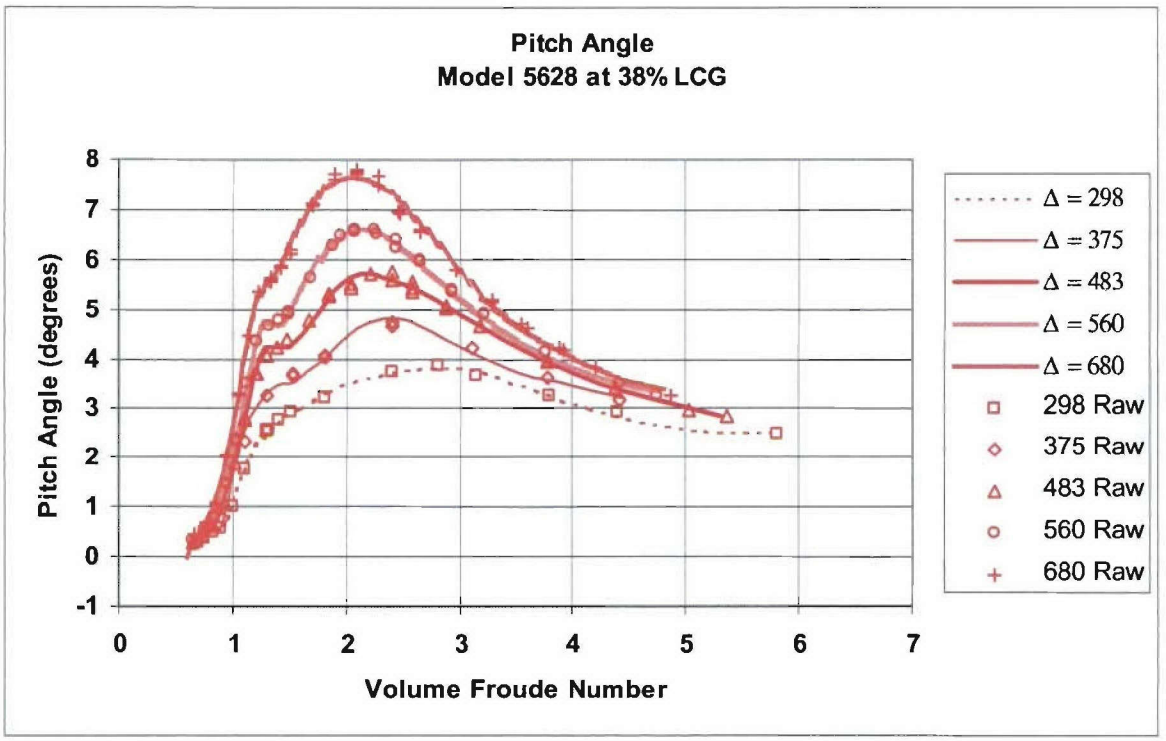

Figure 49. Pitch Angle for Model 5628 at 38% LCG

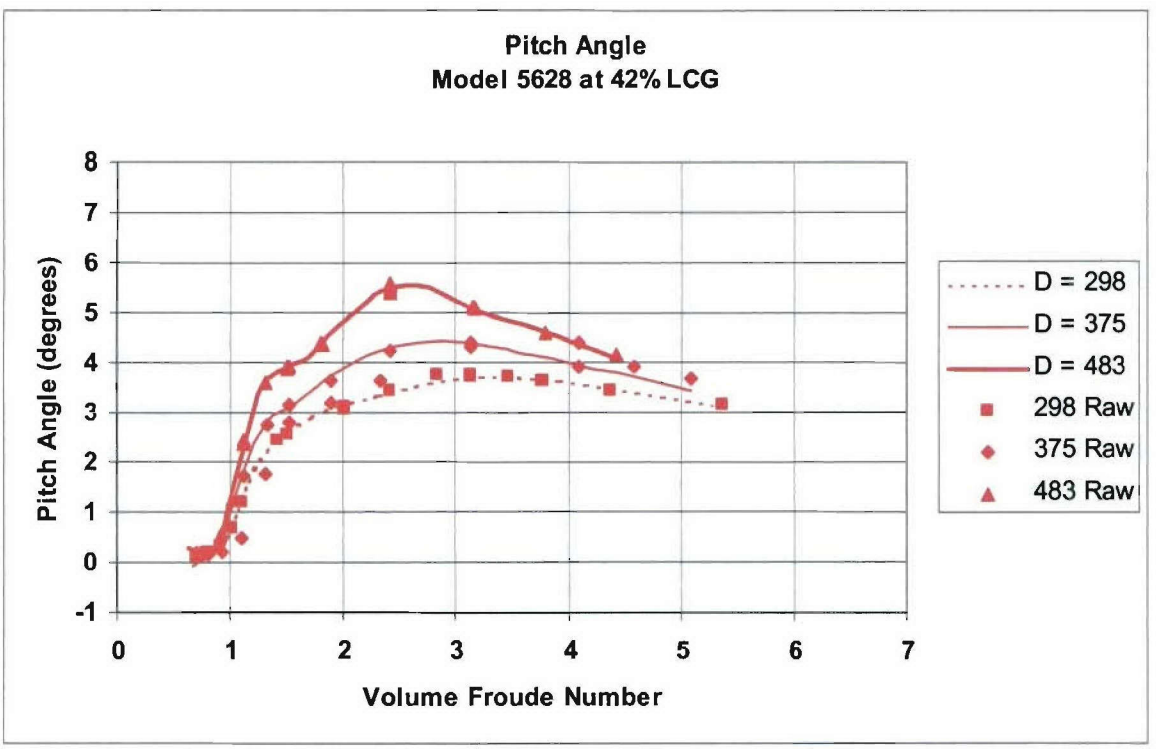

Figure 50. Pitch Angle for Model 5628 at 42% LCG

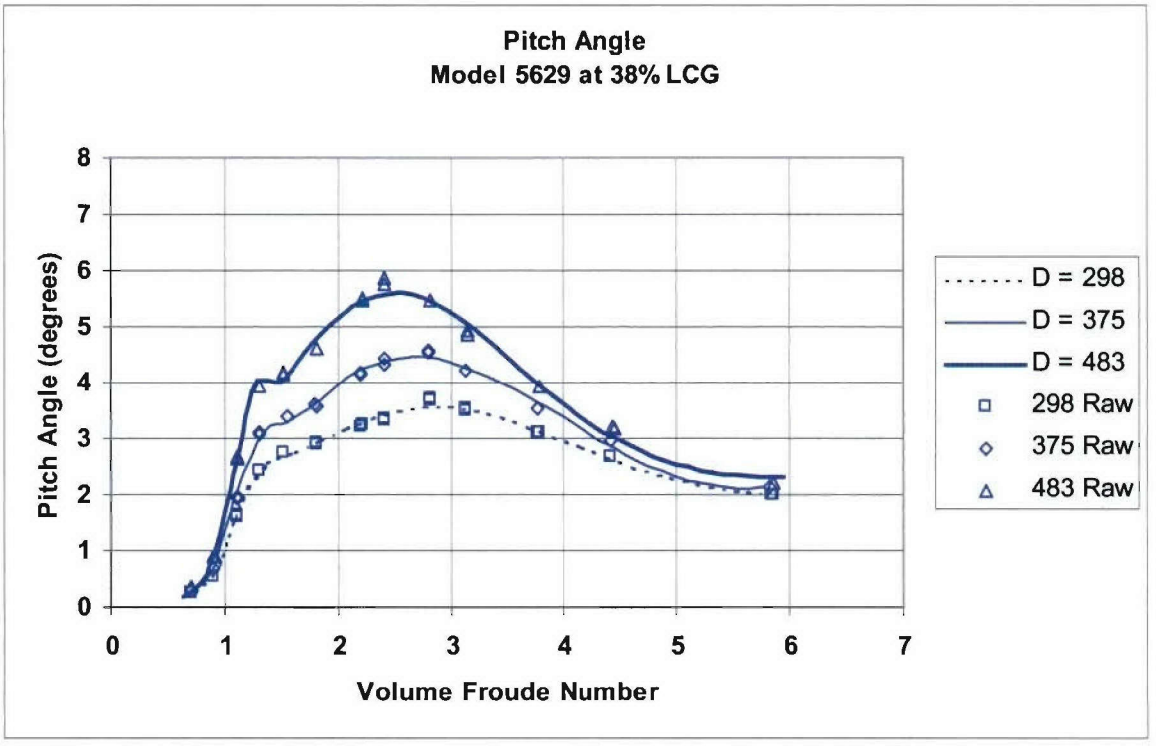

Figure 51. Pitch Angle for Model 5629 at 38% LCG

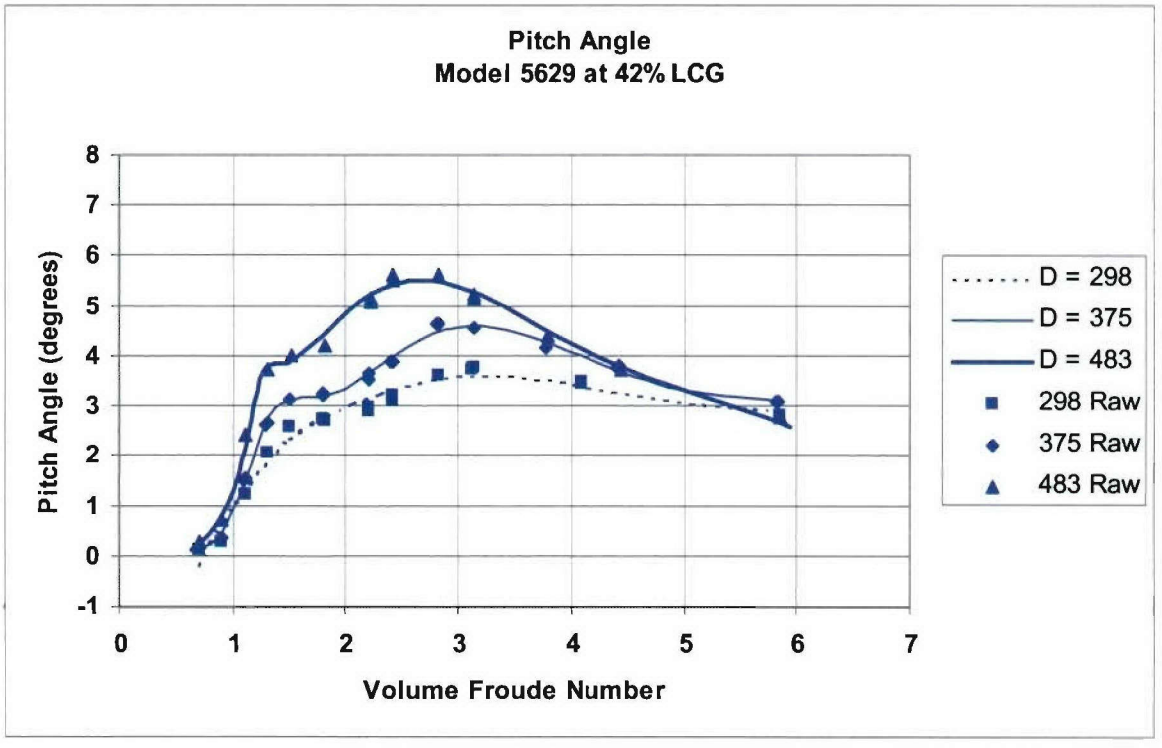

Figure 52. Pitch Angle for Model 5629 at 42% LCG

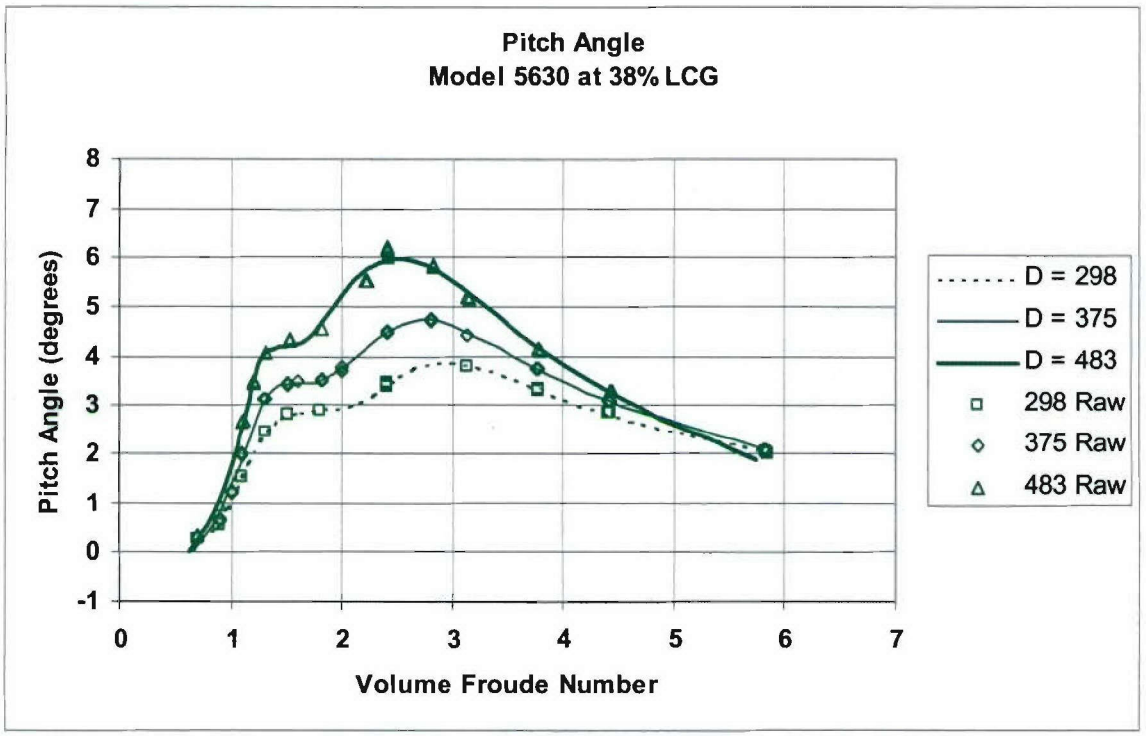

Figure 53. Pitch Angle for Model 5630 at 38% LCG

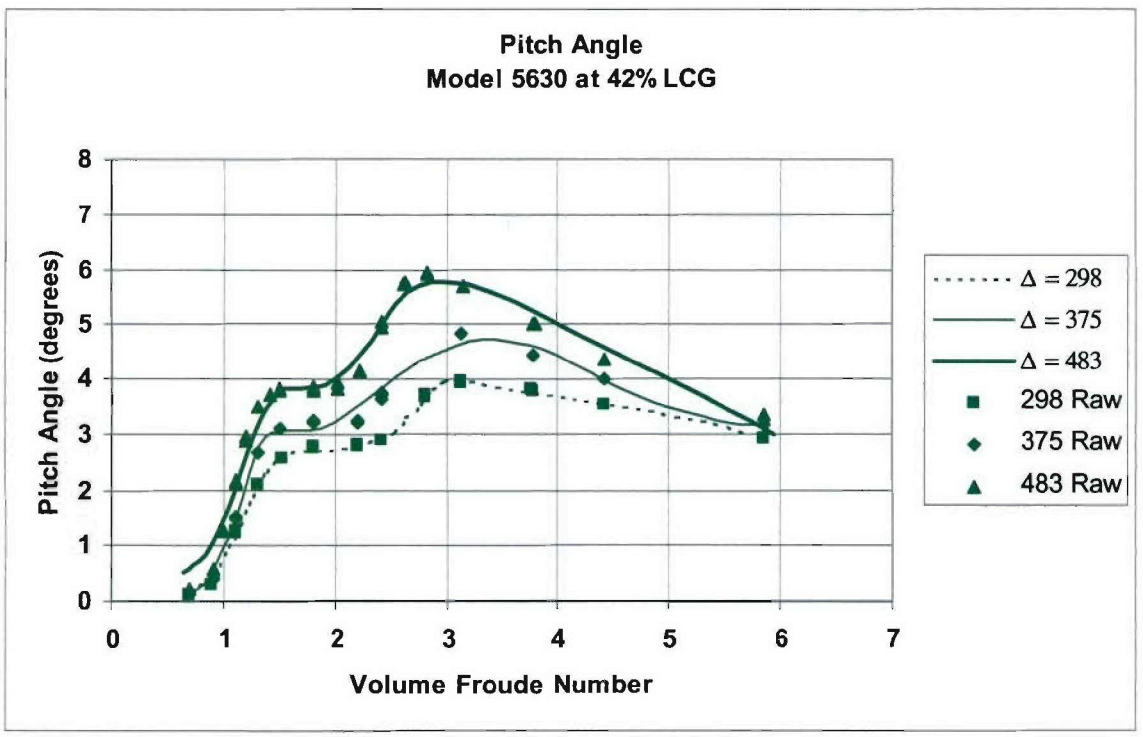

Figure 54. Pitch Angle for Model 5630 at 42% LCG

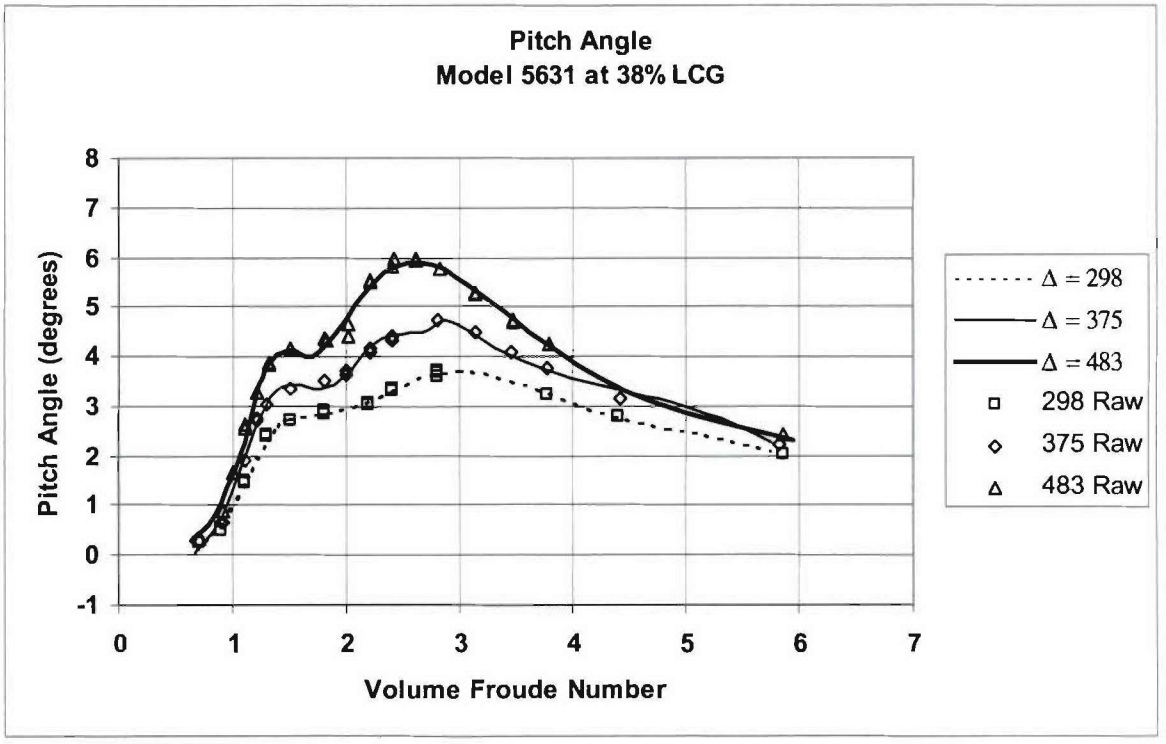

Figure 55. Pitch Angle for Model 5631 at 38% LCG

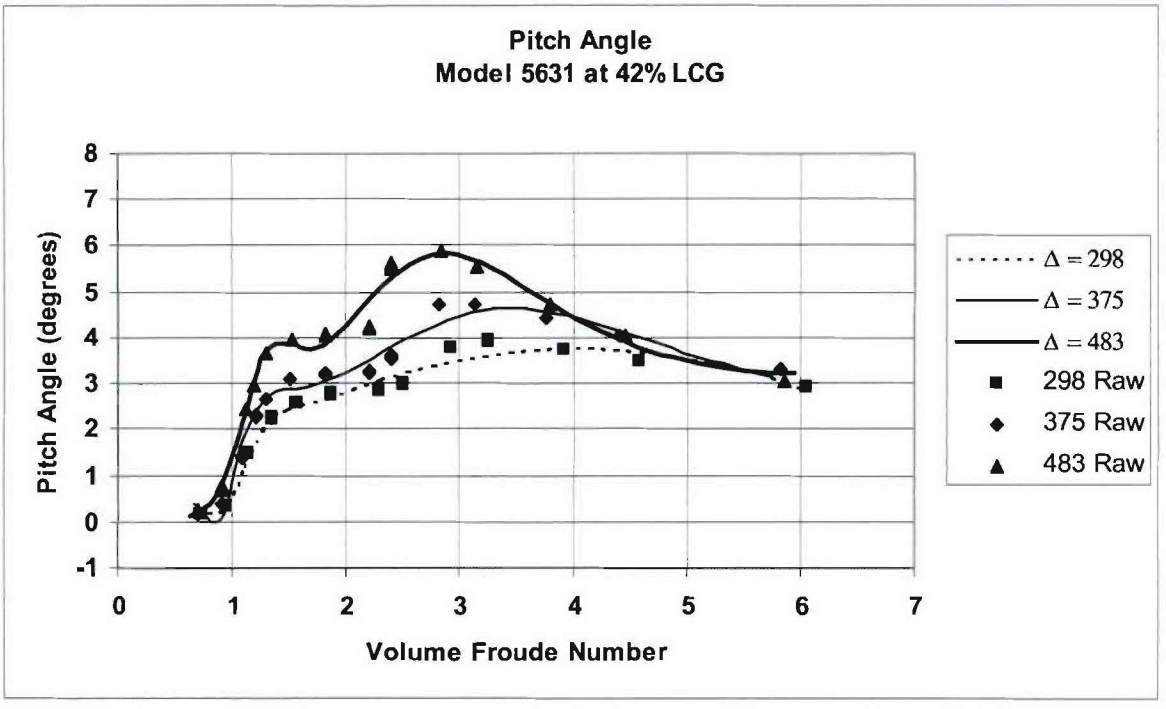

Figure 56. Pitch Angle for Model 5631 at 42% LCG

Table 5. Model-Scale RT/Displ at 298 Lbs of Displacement

Test #	8	5	22	25	10	13	16	19
Model #	**5628**	**5628**	**5629**	**5629**	**5630**	**5630**	**5631**	**5631**
Δ =	298	298	298	298	298	298	298	298
LCG	**38%**	**42%**	**38%**	**42%**	**38%**	**42%**	**38%**	**42%**

V_m (knots)	R_T/Δ Lbs/Lbs	R_T/Δ Lbs/Lbs	R_T/Δ Lbs/Lbs	R_T/Δ Lbs/Lbs	R_T/Δ Lbs/Lbs	R_T/Δ Lbs/Lbs	R_T/Δ Lbs/Lbs	R_T/Δ Lbs/Lbs
0	0.0000	0.0000	0.0000	0.0000	0.0000	0.0000	0.0000	0.0000
1	0.0039	0.0052	0.0066	0.0027	0.0063	0.0028	0.0054	0.0106
2	0.0099	0.0098	0.0123	0.0069	0.0127	0.0070	0.0102	0.0176
3	0.0169	0.0172	0.0205	0.0167	0.0210	0.0170	0.0176	0.0199
4	0.0461	0.0368	0.0446	0.0388	0.0394	0.0390	0.0405	0.0342
5	0.0727	0.0663	0.0763	0.0661	0.0735	0.0638	0.0721	0.0680
6	0.0945	0.0883	0.0959	0.0861	0.0957	0.0828	0.0922	0.0848
7	0.1111	0.1034	0.1087	0.1004	0.1063	0.0972	0.1053	0.0968
8	0.1240	0.1167	0.1194	0.1125	0.1155	0.1094	0.1162	0.1080
9	0.1349	0.1302	0.1292	0.1239	0.1257	0.1206	0.1262	0.1191
10	0.1447	0.1441	0.1387	0.1352	0.1366	0.1311	0.1358	0.1302
11	0.1542	0.1576	0.1478	0.1463	0.1473	0.1414	0.1450	0.1413
12	0.1635	0.1702	0.1567	0.1575	0.1569	0.1515	0.1539	0.1524
13	0.1729	0.1819	0.1654	0.1687	0.1647	0.1616	0.1625	0.1636
14	0.1824	0.1933	0.1740	0.1800	0.1708	0.1717	0.1708	0.1747
15	0.1921	0.2048	0.1825	0.1915	0.1762	0.1820	0.1791	0.1860
16	0.2022	0.2166	0.1912	0.2033	0.1820	0.1924	0.1873	0.1972
17	0.2127	0.2290	0.2000	0.2153	0.1890	0.2032	0.1956	0.2086
18	0.2237	0.2418	0.2093	0.2278	0.1974	0.2142	0.2041	0.2201
19	0.2353	0.2553	0.2190	0.2408	0.2071	0.2258	0.2131	0.2318
20	0.2476	0.2692	0.2296	0.2544	0.2179	0.2378	0.2226	0.2438
21	0.2607	0.2837	0.2412	0.2687	0.2296	0.2505	0.2329	0.2562
22	0.2747	0.2986	0.2541	0.2838	0.2420	0.2639	0.2444	0.2691
23	0.2898	0.3142	0.2688	0.3000	0.2550	0.2781	0.2573	0.2829
24	0.3062	0.3302	0.2860	0.3174	0.2684	0.2934	0.2721	0.2979
25	0.3239		0.3064	0.3362	0.2822	0.3097	0.2894	0.3149
26								0.3353
27								
28								

Table 6. Model-Scale RT/Displ at 375 Lbs of Displacement

Test #	9	6	23	26	11	14	17	20
Model #	**5628**	**5628**	**5629**	**5629**	**5630**	**5630**	**5631**	**5631**
Δ =	375	375	375	375	375	375	375	375
LCG	**38%**	**42%**	**38%**	**42%**	**38%**	**42%**	**38%**	**42%**

V_m (knots)	R_T/Δ Lbs/Lbs	R_T/Δ Lbs/Lbs	R_T/Δ Lbs/Lbs	R_T/Δ Lbs/Lbs	R_T/Δ Lbs/Lbs	R_T/Δ Lbs/Lbs	R_T/Δ Lbs/Lbs	R_T/Δ Lbs/Lbs
0	0.0000	0.0000	0.0000	0.0000	0.0000	0.0000	0.0000	0.0000
1	0.0054	0.0029	0.0025	0.0061	0.0094	0.0048	0.0043	0.0044
2	0.0119	0.0065	0.0087	0.0091	0.0138	0.0100	0.0104	0.0097
3	0.0159	0.0149	0.0222	0.0159	0.0208	0.0179	0.0200	0.0177
4	0.0467	0.0367	0.0464	0.0375	0.0396	0.0352	0.0383	0.0346
5	0.0785	0.0693	0.0768	0.0680	0.0769	0.0667	0.0751	0.0676
6	0.1038	0.0943	0.1023	0.0945	0.1079	0.0931	0.1061	0.0948
7	0.1209	0.1101	0.1192	0.1074	0.1195	0.1056	0.1127	0.1045
8	0.1320	0.1224	0.1305	0.1168	0.1247	0.1136	0.1210	0.1117
9	0.1397	0.1335	0.1391	0.1264	0.1315	0.1221	0.1322	0.1211
10	0.1459	0.1441	0.1466	0.1363	0.1416	0.1319	0.1430	0.1319
11	0.1517	0.1541	0.1533	0.1460	0.1530	0.1424	0.1518	0.1430
12	0.1574	0.1635	0.1595	0.1553	0.1618	0.1527	0.1587	0.1531
13	0.1635	0.1723	0.1652	0.1641	0.1662	0.1616	0.1639	0.1621
14	0.1700	0.1806	0.1705	0.1723	0.1682	0.1688	0.1684	0.1700
15	0.1769	0.1888	0.1756	0.1801	0.1699	0.1748	0.1725	0.1772
16	0.1844	0.1969	0.1805	0.1877	0.1725	0.1806	0.1768	0.1842
17	0.1924	0.2053	0.1854	0.1953	0.1762	0.1867	0.1815	0.1913
18	0.2010	0.2141	0.1905	0.2030	0.1810	0.1936	0.1867	0.1988
19	0.2101	0.2237	0.1959	0.2113	0.1867	0.2013	0.1926	0.2069
20	0.2197	0.2342	0.2018	0.2202	0.1934	0.2098	0.1993	0.2155
21		0.2457	0.2085	0.2301	0.2008	0.2192	0.2069	0.2249
22		0.2584	0.2163	0.2410	0.2091	0.2293	0.2153	0.2350
23		0.2724	0.2255	0.2532	0.2180	0.2400	0.2247	0.2460
24			0.2369	0.2667	0.2277	0.2515	0.2351	0.2577
25			0.2511	0.2817	0.2382	0.2636	0.2466	0.2703
26			0.2694	0.2982	0.2494	0.2763	0.2593	0.2838
27								
28								

Table 7. Model-Scale RT/Displ at 483 Lbs of Displacement

Test #	2	7	24	27	12	15	18	21
Model #	**5628**	**5628**	**5629**	**5629**	**5630**	**5630**	**5631**	**5631**
Δ =	483	483	483	483	483	483	483	483
LCG	**38%**	**42%**	**38%**	**42%**	**38%**	**42%**	**38%**	**42%**

V_m (knots)	R_T/Δ Lbs/Lbs	R_T/Δ Lbs/Lbs	R_T/Δ Lbs/Lbs	R_T/Δ Lbs/Lbs	R_T/Δ Lbs/Lbs	R_T/Δ Lbs/Lbs	R_T/Δ Lbs/Lbs	R_T/Δ Lbs/Lbs
0	0.0000	0.0000	0.0000	0.0000	0.0000	0.0000	0.0000	0.0000
1	0.0022	0.0000	0.0023	0.0022	0.0009	0.0062	0.0039	0.0006
2	0.0060	0.0010	0.0076	0.0072	0.0064	0.0099	0.0096	0.0048
3	0.0156	0.0121	0.0186	0.0176	0.0214	0.0170	0.0191	0.0155
4	0.0408	0.0376	0.0405	0.0381	0.0505	0.0344	0.0375	0.0372
5	0.0808	0.0714	0.0820	0.0756	0.0887	0.0691	0.0775	0.0744
6	0.1142	0.1005	0.1235	0.1134	0.1208	0.1065	0.1216	0.1139
7	0.1332	0.1205	0.1317	0.1240	0.1381	0.1223	0.1308	0.1251
8	0.1435	0.1340	0.1410	0.1313	0.1452	0.1250	0.1372	0.1288
9	0.1499	0.1437	0.1535	0.1421	0.1504	0.1291	0.1487	0.1385
10	0.1545	0.1512	0.1633	0.1525	0.1603	0.1394	0.1610	0.1501
11	0.1581	0.1575	0.1692	0.1605	0.1742	0.1527	0.1710	0.1600
12	0.1613	0.1633	0.1720	0.1660	0.1816	0.1636	0.1773	0.1674
13	0.1643	0.1687	0.1732	0.1696	0.1804	0.1699	0.1803	0.1726
14	0.1672	0.1739	0.1736	0.1722	0.1768	0.1730	0.1810	0.1762
15	0.1702	0.1791	0.1740	0.1744	0.1741	0.1750	0.1806	0.1788
16	0.1734	0.1843	0.1748	0.1767	0.1729	0.1770	0.1799	0.1808
17	0.1770	0.1896	0.1761	0.1792	0.1731	0.1795	0.1795	0.1828
18	0.1810	0.1952	0.1782	0.1822	0.1745	0.1827	0.1798	0.1848
19	0.1855	0.2009	0.1810	0.1858	0.1769	0.1866	0.1809	0.1872
20	0.1908	0.2068	0.1847	0.1902	0.1802	0.1912	0.1831	0.1900
21	0.1970	0.2131	0.1893	0.1953	0.1843	0.1966	0.1865	0.1936
22	0.2042		0.1948	0.2013	0.1891	0.2025	0.1910	0.1980
23	0.2129		0.2013	0.2083	0.1947	0.2092	0.1969	0.2034
24	0.2234		0.2090	0.2164	0.2009	0.2165	0.2042	0.2100
25	0.2362		0.2178	0.2257	0.2078	0.2244	0.2131	0.2182
26			0.2281	0.2364	0.2154	0.2331	0.2238	0.2284
27			0.2400	0.2487	0.2238	0.2424	0.2365	0.2411
28			0.2538	0.2628		0.2525	0.2517	0.2572

Table 8. Model-Scale RT/Displ at 560 Lbs of Displacement

Test #	3
Model #	**5628**
Δ =	560
LCG	**38%**

V_m (knots)	R_T/Δ Lbs/Lbs
0	0.0000
1	0.0014
2	0.0068
3	0.0200
4	0.0452
5	0.0812
6	0.1171
7	0.1418
8	0.1555
9	0.1639
10	0.1697
11	0.1728
12	0.1733
13	0.1721
14	0.1703
15	0.1689
16	0.1684
17	0.1691
18	0.1710
19	0.1743
20	0.1791
21	0.1856
22	0.1939
23	0.2045
24	
25	
26	
27	
28	

Table 9. Model-Scale RT/Displ at 680 Lbs of Displacement

Test #	4
Model #	**5628**
Δ =	680
LCG	**38%**

V_m (knots)	R_T/Δ Lbs/Lbs
0	0.0000
1	0.0011
2	0.0050
3	0.0151
4	0.0388
5	0.0861
6	0.1404
7	0.1617
8	0.1739
9	0.1884
10	0.1964
11	0.1964
12	0.1919
13	0.1863
14	0.1813
15	0.1774
16	0.1750
17	0.1738
18	0.1740
19	0.1754
20	0.1780
21	0.1816
22	0.1865
23	0.1924
24	0.1997
25	
26	
27	
28	

Table 10. Model-Scale Dynamic Wetted Surface Area at 298 Lbs of Displacement

Test #	8	5	22	25	10	13	16	19
Model #	**5628**	**5628**	**5629**	**5629**	**5630**	**5630**	**5631**	**5631**
Δ =	298	298	298	298	298	298	298	298
LCG	**38%**	**42%**	**38%**	**42%**	**38%**	**42%**	**38%**	**42%**

V_m (knots)	S_{DYN} in^2	S_{DYN} in^2	S_{DYN} in^2	S_{DYN} in^2	S_{DYN} in^2	S_{DYN} in^2	S_{DYN} in^2	S_{DYN} in^2
0								
1								
2								
3	3454.1	4370.4	3026.5	3240.0	3410.4	3575.3	2834.3	3257.3
4	3441.2	3926.3	2968.3	3423.3	3338.7	3666.5	2791.5	3234.7
5	3644.1	3333.5	2900.1	3558.4	3318.2	3658.3	2791.5	3235.3
6	3763.9	3309.6	3199.4	3418.5	3403.1	3589.8	2815.7	3208.2
7	3724.3	3432.1	3242.4	3269.0	3441.4	3508.1	2844.5	3065.7
8	3605.2	3538.7	3062.2	3193.5	3400.2	3444.1	2860.5	3037.9
9	3459.7	3590.6	3002.0	3164.2	3309.7	3413.4	2851.3	3015.9
10	3313.8	3583.7	2956.1	3161.2	3198.4	3415.3	2811.1	2975.4
11	3179.0	3530.2	2874.0	3159.1	3084.5	3412.3	2741.0	2908.9
12	3059.0	3447.3	2731.3	3077.0	2977.5	3342.2	2648.1	2818.5
13	2953.7	3350.3	2584.3	2859.1	2881.9	3221.2	2543.6	2719.2
14	2862.0	3249.5	2484.3	2712.2	2798.9	3110.9	2439.9	2630.7
15	2782.0	3151.1	2423.2	2675.1	2728.5	3030.3	2348.6	2563.4
16	2712.0	3058.2	2381.5	2671.9	2669.8	2973.4	2277.4	2517.2
17	2650.6	2972.1	2348.3	2673.9	2621.4	2932.2	2229.7	2486.5
18	2596.2	2893.0	2318.7	2674.5	2582.3	2901.0	2203.6	2465.6
19	2547.9	2820.6	2290.9	2672.7	2551.3	2876.7	2193.0	2450.7
20	2504.8	2754.4		2669.0	2527.3	2857.0	2189.6	2439.2
21	2465.9	2693.8		2663.7	2509.5	2840.8	2184.9	2429.4
22	2430.9	2638.2		2657.3	2497.2	2827.1	2172.9	2420.6
23	2399.0	2587.1		2649.9	2489.5	2815.3	2152.2	2412.4
24	2369.9			2641.8	2486.2	2805.1	2127.0	2404.3
25	2343.3			2633.2	2486.6	2796.2	2107.2	2396.4
26								2388.5
27								
28								

Table 11. Model-Scale Dynamic Wetted Surface Area at 375 Lbs of Displacement

Test #	9	6	23	26	11	14	17	20
Model #	**5628**	**5628**	**5629**	**5629**	**5630**	**5630**	**5631**	**5631**
Δ =	375	375	375	375	375	375	375	375
LCG	**38%**	**42%**	**38%**	**42%**	**38%**	**42%**	**38%**	**42%**

V_m (knots)	S_{DYN} in^2	S_{DYN} in^2	S_{DYN} in^2	S_{DYN} in^2	S_{DYN} in^2	S_{DYN} in^2	S_{DYN} in^2	S_{DYN} in^2
0								
1								
2								
3	3566.1	3794.4	3447.4	3361.8	3568.5	3663.2	2977.2	3131.3
4	3556.7	3775.8	3481.2	3192.5	3613.6	3769.8	3198.7	3123.3
5	3617.2	3858.0	3526.1	3644.2	3644.5	3796.8	3149.6	3333.0
6	3752.7	3995.7	3495.6	3542.1	3653.6	3747.5	2982.3	3328.9
7	3807.3	4065.2	3397.6	3458.5	3631.8	3664.2	2909.9	3212.8
8	3645.7	4000.3	3266.6	3403.0	3570.4	3591.2	2858.1	3162.4
9	3430.1	3854.8	3127.2	3363.0	3466.3	3559.1	2801.9	3146.0
10	3259.8	3694.8	2992.0	3329.6	3325.3	3585.1	2736.9	3131.2
11	3133.1	3549.6	2866.5	3280.3	3163.1	3622.3	2665.5	3071.7
12	3034.8	3425.2	2753.1	3153.0	3000.0	3455.6	2591.1	2924.6
13	2954.2	3320.0	2652.4	2918.0	2853.6	3172.7	2517.0	2731.0
14	2885.2	3230.5	2564.4	2750.5	2733.9	3013.9	2445.3	2582.0
15	2824.4	3153.6	2488.6	2701.8	2643.3	2940.3	2377.4	2499.7
16	2769.5	3086.8	2424.3	2693.0	2579.0	2901.3	2313.8	2460.2
17	2719.2	3028.0	2370.6	2689.1	2536.2	2877.1	2254.8	2441.8
18	2672.7	2975.8	2326.7	2682.8	2509.8	2859.9	2200.2	2432.6
19	2629.2	2929.1	2291.6	2674.0	2495.3	2846.6	2149.8	2427.5
20	2588.3	2886.9	2264.4	2663.5	2489.4	2835.6	2103.3	2423.9
21		2848.6	2243.9	2652.5	2489.4	2826.3		2421.0
22		2813.7	2229.3	2641.6	2493.4	2818.1		2418.1
23		2781.6	2219.5	2631.5	2500.1	2810.8		2415.1
24			2213.6	2622.8	2508.5	2804.1		2412.0
25			2210.6	2616.0	2517.9	2797.9		2408.8
26			2209.9	2611.5	2527.9	2792.2		2405.4
27								
28								

Table 12. Model-Scale Dynamic Wetted Surface Area at 483 Lbs of Displacement

Test #	2	7	24	27	12	15	18	21
Model #	**5628**	**5628**	**5629**	**5629**	**5630**	**5630**	**5631**	**5631**
Δ =	483	483	483	483	483	483	483	483
LCG	**38%**	**42%**	**38%**	**42%**	**38%**	**42%**	**38%**	**42%**

V_m (knots)	S_{DYN} in^2	S_{DYN} in^2	S_{DYN} in^2	S_{DYN} in^2	S_{DYN} in^2	S_{DYN} in^2	S_{DYN} in^2	S_{DYN} in^2
0								
1								
2								
3	4118.5	4057.0	3742.2	3725.4	3625.5	3790.6	3566.1	3323.0
4	3964.7	4116.6	3852.7	3810.6	3708.8	3877.5	3513.0	3452.9
5	3812.1	4172.9	3819.5	3847.9	3789.2	3926.7	3453.2	3516.4
6	4065.8	4216.4	3539.4	3687.6	3851.5	3918.8	3391.0	3504.6
7	4248.5	4231.7	3397.2	3553.1	3870.1	3873.3	3330.6	3450.2
8	4178.5	4198.4	3394.6	3499.6	3812.7	3827.3	3274.1	3381.1
9	3937.5	4098.9	3448.1	3497.4	3658.1	3805.0	3218.4	3311.9
10	3642.0	3931.9	3405.2	3480.1	3421.0	3811.9	3142.8	3246.1
11	3365.5	3721.9	3037.0	3306.7	3153.6	3822.9	2983.6	3168.6
12	3138.4	3509.4	2656.4	2978.4	2912.0	3727.7	2672.4	3011.0
13	2964.9	3327.8	2495.5	2725.6	2726.1	3360.0	2364.1	2669.8
14	2838.7	3191.4	2437.2	2596.7	2597.9	2955.4	2229.3	2386.3
15	2751.0	3098.2	2408.5	2532.3	2516.2	2792.5	2194.8	2334.0
16	2693.7	3039.2	2386.4	2494.2	2467.4	2766.3	2185.7	2344.7
17	2660.2	3004.8	2364.0	2466.8	2440.7	2778.3	2178.1	2351.5
18	2644.4	2986.9	2339.1	2443.9	2428.2	2796.0	2167.7	2347.8
19	2640.3	2979.9	2311.4	2423.0	2424.6	2811.1	2154.7	2336.5
20	2641.0	2979.9	2289.0	2403.2	2426.6	2822.5	2140.0	2320.6
21	2639.1	2984.1	2286.4	2384.0	2432.0	2830.2	2124.4	2302.1
22	2626.7		2275.6	2365.3	2439.3	2835.0	2108.7	2282.4
23	2596.5		2253.8	2347.1	2447.7	2837.5	2093.1	2262.1
24	2542.8		2229.3	2329.2	2456.6	2838.2	2078.0	2241.8
25	2462.4		2204.4	2311.7	2465.7	2837.3	2063.4	2221.7
26			2179.7	2294.6	2474.7	2835.3	2049.6	2202.1
27			2155.3	2277.8	2483.5	2832.4	2036.5	2183.0
28			2131.3	2261.5	2491.9	2828.7	2024.2	2164.6

Table 13. Model-Scale Dynamic Wetted Surface Area at 560 Lbs of Displacement

Test #	3
Model #	**5628**
Δ =	560
LCG	**38%**

V_m (knots)	S_{DYN} in^2
0	
1	
2	
3	4161.0
4	4187.3
5	4195.0
6	4171.2
7	4106.5
8	3996.9
9	3844.9
10	3659.6
11	3455.6
12	3250.6
13	3062.9
14	2908.6
15	2799.0
16	2739.8
17	2731.3
18	2769.7
19	2846.7
20	2944.9
21	3020.9
22	2966.1
23	2528.1
24	
25	
26	
27	
28	

Table 14. Model-Scale Dynamic Wetted Surface Area at 680 Lbs of Displacement

Test #	4
Model #	**5628**
Δ =	680
LCG	**38%**

V_m (knots)	S_{DYN} in^2
0	
1	
2	
3	4912.8
4	4854.4
5	4754.4
6	4610.5
7	4424.8
8	4199.7
9	3923.0
10	3556.7
11	3184.2
12	2992.7
13	2904.3
14	2843.3
15	2796.5
16	2762.8
17	2741.0
18	2729.3
19	2725.8
20	2728.6
21	2736.0
22	2746.7
23	2759.8
24	2774.4
25	
26	
27	
28	

Table 15. Residuary Resistance Coefficient at 280 Lbs of Displacement

Test #	8	5	22	25	10	13	16	19
Model #	**5628**	**5628**	**5629**	**5629**	**5630**	**5630**	**5631**	**5631**
Δ =	298	298	298	298	298	298	298	298
LCG	**38%**	**42%**	**38%**	**42%**	**38%**	**42%**	**38%**	**42%**

V_m (knots)	C_R x1000	C_R x1000	C_R x1000	C_R x1000	C_R x1000	C_R x1000	C_R x1000	C_R x1000
0								
1								
2								
3	5.044	3.396	8.313	5.470	7.214	4.818	7.306	7.138
4	9.783	5.880	11.374	7.794	8.256	7.109	10.874	7.056
5	9.297	9.270	13.255	8.457	10.659	7.756	12.968	9.973
6	7.826	8.518	9.930	7.874	9.124	6.963	11.120	8.405
7	6.517	6.621	7.690	6.811	6.849	5.866	8.794	7.087
8	5.464	5.127	6.578	5.686	5.363	4.849	6.977	5.770
9	4.634	4.125	5.420	4.697	4.447	3.962	5.661	4.765
10	3.967	3.457	4.491	3.872	3.835	3.201	4.717	4.029
11	3.443	2.979	3.841	3.216	3.364	2.592	4.034	3.502
12	3.014	2.604	3.458	2.824	2.944	2.189	3.535	3.130
13	2.656	2.299	3.179	2.753	2.535	1.936	3.160	2.852
14	2.354	2.050	2.872	2.611	2.140	1.726	2.864	2.613
15	2.096	1.848	2.547	2.314	1.783	1.522	2.606	2.381
16	1.876	1.683	2.241	2.011	1.483	1.326	2.359	2.151
17	1.686	1.548	1.971	1.748	1.244	1.144	2.109	1.928
18	1.524	1.435	1.741	1.527	1.056	0.982	1.860	1.720
19	1.385	1.340	1.548	1.341	0.906	0.837	1.622	1.530
20	1.267	1.260		1.187	0.783	0.712	1.410	1.360
21	1.168	1.191		1.058	0.677	0.603	1.237	1.210
22	1.086	1.131		0.951	0.583	0.510	1.110	1.080
23	1.020	1.079		0.865	0.497	0.432	1.028	0.970
24	0.970			0.797	0.417	0.367	0.984	0.884
25	0.935			0.745	0.343	0.316	0.964	0.825
26								0.804
27								
28								

Table 16. Residuary Resistance Coefficient at 375 Lbs of Displacement

Test #	9	6	23	26	11	14	17	20
Model #	**5628**	**5628**	**5629**	**5629**	**5630**	**5630**	**5631**	**5631**
Δ =	375	375	375	375	375	375	375	375
LCG	**38%**	**42%**	**38%**	**42%**	**38%**	**42%**	**38%**	**42%**

V_m (knots)	C_R x1000	C_R x1000	C_R x1000	C_R x1000	C_R x1000	C_R x1000	C_R x1000	C_R x1000
0								
1								
2								
3	6.258	5.134	10.618	6.865	9.256	7.227	11.244	8.902
4	12.829	8.658	13.065	11.134	10.176	8.193	11.411	10.306
5	13.873	10.950	13.944	11.503	13.402	10.656	15.554	12.772
6	12.007	9.815	12.899	11.498	13.044	10.511	16.320	12.476
7	9.719	7.880	11.067	9.470	10.197	8.576	12.521	10.060
8	8.163	6.472	9.327	7.621	7.794	6.802	10.055	7.931
9	6.979	5.533	7.909	6.260	6.321	5.468	8.557	6.481
10	5.932	4.837	6.780	5.231	5.520	4.421	7.419	5.478
11	5.023	4.261	5.866	4.456	5.038	3.617	6.433	4.792
12	4.268	3.756	5.111	3.983	4.565	3.291	5.562	4.406
13	3.655	3.307	4.473	3.827	4.001	3.209	4.807	4.189
14	3.160	2.908	3.926	3.596	3.418	2.929	4.167	3.914
15	2.757	2.557	3.450	3.164	2.889	2.534	3.631	3.531
16	2.424	2.253	3.032	2.718	2.436	2.143	3.187	3.112
17	2.151	1.991	2.663	2.333	2.054	1.802	2.822	2.716
18	1.929	1.769	2.337	2.013	1.731	1.517	2.522	2.368
19	1.741	1.583	2.050	1.750	1.458	1.282	2.277	2.071
20	1.575	1.430	1.799	1.534	1.226	1.089	2.077	1.822
21		1.306	1.583	1.359	1.027	0.929		1.613
22		1.208	1.403	1.217	0.858	0.795		1.439
23		1.134	1.258	1.103	0.712	0.683		1.294
24			1.152	1.014	0.588	0.588		1.174
25			1.089	0.944	0.482	0.506		1.074
26			1.079	0.890	0.391	0.436		0.992
27								
28								

Table 17. Residuary Resistance Coefficient at 483 Lbs of Displacement

Test #	2	7	24	27	12	15	18	21
Model #	**5628**	**5628**	**5629**	**5629**	**5630**	**5630**	**5631**	**5631**
Δ =	483	483	483	483	483	483	483	483
LCG	**38%**	**42%**	**38%**	**42%**	**38%**	**42%**	**38%**	**42%**

V_m (knots)	C_R x1000	C_R x1000	C_R x1000	C_R x1000	C_R x1000	C_R x1000	C_R x1000	C_R x1000
0								
1								
2								
3	7.223	4.974	10.502	9.805	13.162	9.179	11.570	9.690
4	12.980	11.184	13.336	12.548	18.216	10.743	13.600	13.746
5	18.263	14.166	18.553	16.723	20.510	14.650	19.518	18.252
6	16.648	13.681	21.407	18.522	18.943	16.028	22.093	19.749
7	13.176	11.721	16.989	15.025	15.419	13.324	17.255	15.727
8	10.642	9.695	13.476	11.895	12.118	10.004	13.614	12.129
9	8.993	8.074	11.018	9.810	9.946	7.749	11.537	10.197
10	7.850	6.894	9.277	8.251	8.986	6.449	10.105	8.877
11	6.971	6.050	8.804	7.344	8.701	5.596	9.139	7.764
12	6.207	5.403	8.551	7.010	8.123	4.963	8.831	6.993
13	5.501	4.845	7.588	6.558	7.094	4.831	8.617	6.926
14	4.839	4.321	6.426	5.829	5.997	4.854	7.712	6.802
15	4.222	3.818	5.389	5.040	5.020	4.377	6.512	5.912
16	3.655	3.340	4.536	4.323	4.195	3.682	5.421	4.949
17	3.143	2.898	3.851	3.709	3.508	3.041	4.526	4.159
18	2.687	2.497	3.306	3.198	2.940	2.510	3.812	3.528
19	2.291	2.140	2.875	2.775	2.467	2.081	3.244	3.021
20	1.957	1.825	2.515	2.428	2.074	1.734	2.794	2.611
21	1.689	1.548	2.183	2.145	1.745	1.450	2.437	2.277
22	1.490		1.927	1.914	1.470	1.217	2.157	2.007
23	1.365		1.741	1.728	1.239	1.024	1.940	1.791
24	1.318		1.602	1.581	1.047	0.864	1.775	1.624
25	1.358		1.501	1.468	0.887	0.729	1.656	1.501
26			1.432	1.387	0.755	0.617	1.579	1.421
27			1.394	1.334	0.646	0.523	1.539	1.385
28			1.385			0.445	1.535	1.399

Table 18. Residuary Resistance Coefficient at 560 Lbs of Displacement

Test #	3
Model #	**5628**
Δ =	560
LCG	**38%**

V_m (knots)	C_R x1000
0	
1	
2	
3	12.226
4	16.478
5	19.544
6	19.782
7	17.630
8	14.864
9	12.506
10	10.685
11	9.238
12	8.009
13	6.934
14	5.981
15	5.118
16	4.325
17	3.593
18	2.927
19	2.339
20	1.848
21	1.496
22	1.392
23	1.933
24	
25	
26	
27	
28	

Table 19. Residuary Resistance Coefficient at 680 Lbs of Displacement

Test #	4
Model #	**5628**
Δ =	680
LCG	**38%**

V_m (knots)	C_R x1000
0	
1	
2	
3	8.689
4	14.498
5	22.607
6	27.013
7	23.515
8	20.046
9	18.159
10	16.729
11	15.236
12	12.979
13	10.676
14	8.779
15	7.270
16	6.064
17	5.091
18	4.305
19	3.671
20	3.163
21	2.758
22	2.432
23	2.166
24	1.949
25	
26	
27	
28	

Table 20. Model-Scale Center of Gravity Heave at 298 Lbs of Displacement

Test #	8	5	22	25	10	13	16	19
Model #	**5628**	**5628**	**5629**	**5629**	**5630**	**5630**	**5631**	**5631**
Δ =	298	298	298	298	298	298	298	298
LCG	**38%**	**42%**	**38%**	**42%**	**38%**	**42%**	**38%**	**42%**

V_m (knots)	CG Heave In	CG Heave in	CG Heave in	CG Heave in	CG Heave in	CG Heave in	CG Heave in	CG Heave in
0								
1								
2								
3	-0.152	-0.113	-0.326	-0.062	-0.164	-0.217	-0.189	-0.284
4	-0.444	-0.475	-0.428	-0.382	-0.444	-0.502	-0.435	-0.356
5	-0.599	-0.647	-0.715	-0.642	-0.616	-0.647	-0.702	-0.746
6	-0.460	-0.553	-0.504	-0.530	-0.484	-0.579	-0.541	-0.583
7	-0.054	-0.203	-0.102	-0.232	-0.073	-0.299	-0.131	-0.274
8	0.410	0.193	0.322	0.101	0.195	0.110	0.180	0.079
9	0.809	0.530	0.727	0.442	0.360	0.536	0.454	0.437
10	1.182	0.888	1.102	0.779	0.732	0.874	0.785	0.780
11	1.586	1.275	1.441	1.102	1.249	1.018	1.204	1.099
12	1.991	1.654	1.746	1.406	1.736	1.192	1.667	1.392
13	2.330	1.996	2.017	1.689	2.121	1.608	2.090	1.660
14	2.581	2.289	2.256	1.948	2.409	1.944	2.416	1.903
15	2.759	2.533	2.467	2.185	2.623	2.188	2.640	2.125
16	2.890	2.732	2.650	2.398	2.786	2.377	2.790	2.327
17	2.992	2.892	2.810	2.589	2.914	2.534	2.896	2.512
18	3.079	3.021	2.947	2.759	3.020	2.668	2.980	2.682
19	3.158	3.123	3.064	2.909	3.110	2.787	3.056	2.839
20	3.234	3.205	3.163	3.042	3.189	2.895	3.131	2.984
21	3.310	3.271	3.246	3.158	3.262	2.995	3.209	3.118
22	3.389	3.323	3.314	3.259	3.331	3.089	3.294	3.243
23	3.471	3.364	3.369	3.346	3.397	3.178	3.385	3.359
24	3.558		3.411	3.422	3.461	3.265	3.485	3.467
25	3.650		3.443	3.488	3.524	3.349	3.592	3.569
26								3.664
27								
28								

Table 21. Model-Scale Center of Gravity Heave at 375 Lbs of Displacement

Test #	9	6	23	26	11	14	17	20
Model #	**5628**	**5628**	**5629**	**5629**	**5630**	**5630**	**5631**	**5631**
Δ =	375	375	375	375	375	375	375	375
LCG	**38%**	**42%**	**38%**	**42%**	**38%**	**42%**	**38%**	**42%**

V_m (knots)	CG Heave in	CG Heave in	CG Heave In	CG Heave in	CG Heave in	CG Heave in	CG Heave in	CG Heave in
0								
1								
2								
3	-0.2269	-0.3269	-0.2681	-0.1931	-0.1408	-0.4034	-0.2356	-0.3513
4	-0.6080	-0.5233	-0.5357	-0.6445	-0.4828	-0.5556	-0.5644	-0.5895
5	-0.6718	-0.7009	-0.6954	-0.7775	-0.6887	-0.6831	-0.7074	-0.6978
6	-0.4849	-0.5253	-0.6005	-0.6390	-0.6075	-0.7161	-0.6035	-0.6730
7	-0.1220	-0.1691	-0.1985	-0.3125	-0.2119	-0.5381	-0.2508	-0.5079
8	0.3467	0.2865	0.3898	0.1268	0.2728	-0.0657	0.2853	-0.2083
9	0.8623	0.7819	0.9945	0.6137	0.6250	0.5444	0.9011	0.2013
10	1.3802	1.2720	1.5249	1.0965	0.9156	0.9240	1.4664	0.6803
11	1.8693	1.7268	1.9675	1.5416	1.3435	1.0516	1.6762	1.1829
12	2.3100	2.1308	2.3387	1.9325	1.9252	1.3850	1.9018	1.6689
13	2.6914	2.4786	2.6573	2.2657	2.5089	1.9815	2.5481	2.1107
14	3.0089	2.7719	2.9354	2.5454	2.9791	2.5068	2.9952	2.4940
15	3.2622	3.0159	3.1774	2.7792	3.3142	2.8506	3.3147	2.8154
16	3.4534	3.2171	3.3824	2.9756	3.5397	3.0611	3.5565	3.0784
17	3.5864	3.3821	3.5479	3.1422	3.6882	3.1967	3.7450	3.2896
18	3.6656	3.5170	3.6730	3.2859	3.7858	3.2949	3.8942	3.4572
19	3.6959	3.6272	3.7613	3.4122	3.8513	3.3775	4.0137	3.5886
20	3.6821	3.7171	3.8210	3.5257	3.8973	3.4565	4.1100	3.6909
21		3.7905	3.8632	3.6298	3.9329	3.5392	4.1881	3.7699
22		3.8504	3.9001	3.7273	3.9653	3.6301	4.2515	3.8302
23		3.8992	3.9427	3.8206	4.0011	3.7326	4.3027	3.8759
24			3.9998	3.9113	4.0487	3.8492	4.3434	3.9098
25			4.0786	4.0010	4.1219	3.9826	4.3742	3.9346
26			4.1847	4.0908	4.2515	4.1355	4.3939	3.9520
27								
28								

Table 22. Model-Scale Center of Gravity Heave at 483 Lbs of Displacement

Test #	2	7	24	27	12	15	18	21
Model #	**5628**	**5628**	**5629**	**5629**	**5630**	**5630**	**5631**	**5631**
Δ =	483	483	483	483	483	483	483	483
LCG	**38%**	**42%**	**38%**	**42%**	**38%**	**42%**	**38%**	**42%**

V_m (knots)	CG Heave in	CG Heave in	CG Heave in	CG Heave in	CG Heave in	CG Heave in	CG Heave In	CG Heave in
0								
1								
2								
3	-0.0141	-0.1313	-0.7234	-0.5565	-0.2987	-0.6165	0.1524	-0.1100
4	-0.6623	-0.6412	-0.8234	-0.5498	-0.5521	-0.6234	-0.3620	-0.6272
5	-0.8253	-0.9808	-0.9201	-0.9629	-0.7524	-0.7915	-0.6994	-0.7186
6	-0.5815	-0.7214	-0.6344	-0.4365	-0.7353	-0.7891	-0.6476	-0.5759
7	-0.1351	-0.2481	-0.1560	0.0057	-0.2900	-0.5545	-0.2101	-0.2696
8	0.4501	0.1549	0.4433	0.5069	0.3306	-0.1283	0.4135	0.1731
9	1.1588	0.7355	1.1197	1.0991	0.9820	0.4192	1.0804	0.7357
10	1.9347	1.3973	1.8267	1.7447	1.6560	1.0215	1.7312	1.3912
11	2.6721	2.0281	2.5096	2.3841	2.3173	1.6271	2.3398	2.0899
12	3.2750	2.5716	3.1153	2.9626	2.9228	2.1997	2.8916	2.7636
13	3.7075	3.0152	3.6071	3.4466	3.4440	2.7168	3.3789	3.3483
14	3.9902	3.3676	3.9739	3.8273	3.8709	3.1660	3.7996	3.8087
15	4.1659	3.6452	4.2279	4.1133	4.2078	3.5432	4.1561	4.1447
16	4.2754	3.8641	4.3943	4.3219	4.4660	3.8494	4.4536	4.3797
17	4.3489	4.0383	4.5011	4.4717	4.6594	4.0901	4.6990	4.5436
18	4.4060	4.1787	4.5725	4.5794	4.8012	4.2731	4.8993	4.6632
19	4.4591	4.2937	4.6270	4.6588	4.9030	4.4080	5.0613	4.7578
20	4.5156	4.3898	4.6767	4.7200	4.9741	4.5054	5.1915	4.8400
21	4.5802	4.4717	4.7297	4.7706	5.0219	4.5765	5.2951	4.9173
22	4.6558		4.7904	4.8162	5.0520	4.6325	5.3769	4.9940
23	4.7446		4.8611	4.8607	5.0690	4.6845	5.4409	5.0720
24	4.8484		4.9428	4.9069	5.0760	4.7434	5.4902	5.1524
25	4.9688		5.0358	4.9570	5.0756	4.8195	5.5275	5.2351
26			5.1397	5.0126	5.0697	4.9229	5.5551	5.3201
27			5.2541	5.0750	5.0598	5.0629	5.5747	5.4070
28			5.3783	5.1450	5.0469	5.2484	5.5879	5.4954

Table 23. Model-Scale Center of Gravity Heave at 560 Lbs of Displacement

Test #	3
Model #	**5628**
Δ =	560
LCG	**38%**

V_m (knots)	CG Heave in
0	
1	
2	
3	0.0481
4	-0.6728
5	-0.8129
6	-0.5965
7	-0.1555
8	0.5362
9	1.4568
10	2.4057
11	3.1686
12	3.6958
13	4.0465
14	4.2901
15	4.4736
16	4.6238
17	4.7553
18	4.8756
19	4.9889
20	5.0974
21	5.2023
22	5.3042
23	5.4036
24	
25	
26	
27	
28	

Table 24. Model-Scale Center of Gravity Heave at 680 Lbs of Displacement

Test #	4
Model #	**5628**
Δ =	680
LCG	**38%**

V_m (knots)	CG Heave in
0	
1	
2	
3	-0.2114
4	-0.7297
5	-0.9862
6	-0.7827
7	-0.1301
8	0.7602
9	1.7649
10	2.8746
11	3.9367
12	4.7381
13	5.2412
14	5.5287
15	5.6873
16	5.7746
17	5.8243
18	5.8558
19	5.8803
20	5.9052
21	5.9359
22	5.9770
23	6.0337
24	6.1126
25	
26	
27	
28	

Table 25. Pitch Angle at 298 Lbs of Displacement

Test #	8	5	22	25	10	13	16	19
Model #	**5628**	**5628**	**5629**	**5629**	**5630**	**5630**	**5631**	**5631**
Δ =	298	298	298	298	298	298	298	298
LCG	**38%**	**42%**	**38%**	**42%**	**38%**	**42%**	**38%**	**42%**

V_m (knots)	Trim Deg	Trim Deg	Trim Deg	Trim Deg	Trim Deg	Trim Deg	Trim Deg	Trim Deg
0								
1								
2								
3	0.316	0.139	0.212	-0.189	0.207	0.208	0.115	0.294
4	0.590	0.300	0.620	0.648	0.609	0.467	0.642	0.234
5	2.012	1.594	1.901	1.412	1.785	1.355	1.703	1.511
6	2.710	2.414	2.585	2.067	2.627	2.319	2.587	2.313
7	3.036	2.772	2.756	2.503	2.856	2.674	2.793	2.535
8	3.351	3.059	2.950	2.799	2.950	2.707	2.862	2.708
9	3.548	3.216	3.165	3.044	2.980	2.746	3.002	2.896
10	3.659	3.350	3.355	3.250	3.234	2.847	3.211	3.083
11	3.762	3.490	3.492	3.411	3.584	3.032	3.447	3.256
12	3.838	3.609	3.563	3.523	3.814	3.538	3.642	3.406
13	3.829	3.689	3.563	3.587	3.863	3.964	3.726	3.530
14	3.725	3.726	3.499	3.606	3.774	3.958	3.677	3.627
15	3.559	3.725	3.381	3.585	3.606	3.860	3.532	3.697
16	3.370	3.692	3.223	3.534	3.407	3.771	3.341	3.742
17	3.183	3.637	3.041	3.461	3.205	3.696	3.146	3.763
18	3.013	3.566	2.853	3.375	3.017	3.627	2.966	3.760
19	2.868	3.487	2.672	3.284	2.847	3.558	2.809	3.735
20	2.749	3.401	2.507	3.196	2.696	3.486	2.675	3.687
21	2.656	3.314	2.365	3.116	2.562	3.408	2.558	3.617
22	2.589	3.227	2.248	3.048	2.439	3.322	2.451	3.526
23	2.547	3.141	2.155	2.994	2.324	3.226	2.347	3.413
24	2.527		2.086	2.955	2.208	3.118	2.236	3.278
25	2.529		2.035	2.929	2.085	2.997	2.103	3.121
26								2.939
27								
28								

Table 26. Pitch Angle at 375 Lbs of Displacement

Test #	9	6	23	26	11	14	17	20
Model #	**5628**	**5628**	**5629**	**5629**	**5630**	**5630**	**5631**	**5631**
Δ =	375	375	375	375	375	375	375	375
LCG	**38%**	**42%**	**38%**	**42%**	**38%**	**42%**	**38%**	**42%**

V_m (knots)	Trim Deg	Trim Deg	Trim Deg	Trim Deg	Trim Deg	Trim Deg	Trim Deg	Trim Deg
0								
1								
2								
3	0.444	-0.087	0.230	0.096	0.007	0.082	0.064	0.366
4	0.475	0.322	0.615	0.370	0.693	0.426	0.723	0.026
5	2.559	1.705	2.066	1.512	1.958	1.479	1.996	1.848
6	3.387	2.844	3.125	2.797	3.204	2.827	3.186	2.742
7	3.529	3.150	3.290	3.132	3.465	3.064	3.450	2.870
8	3.954	3.504	3.564	3.144	3.476	3.058	3.368	2.988
9	4.425	3.861	3.932	3.334	3.758	3.224	3.626	3.214
10	4.741	4.142	4.234	3.662	4.152	3.516	4.190	3.518
11	4.811	4.322	4.409	4.013	4.513	3.854	4.444	3.846
12	4.663	4.408	4.461	4.305	4.719	4.177	4.508	4.145
13	4.400	4.421	4.412	4.498	4.709	4.444	4.727	4.383
14	4.125	4.381	4.287	4.577	4.529	4.627	4.502	4.543
15	3.893	4.309	4.107	4.550	4.268	4.713	4.180	4.621
16	3.715	4.216	3.889	4.438	3.989	4.699	3.912	4.623
17	3.578	4.113	3.644	4.270	3.725	4.596	3.715	4.562
18	3.462	4.004	3.382	4.072	3.486	4.423	3.564	4.451
19	3.350	3.895	3.116	3.871	3.273	4.209	3.439	4.304
20	3.230	3.785	2.858	3.682	3.083	3.981	3.323	4.133
21		3.676	2.623	3.517	2.910	3.763	3.204	3.950
22		3.565	2.422	3.380	2.751	3.572	3.073	3.765
23		3.447	2.268	3.273	2.599	3.417	2.922	3.584
24			2.165	3.196	2.449	3.299	2.744	3.415
25			2.121	3.146	2.296	3.215	2.527	3.262
26			2.136	3.121	2.137	3.161	2.258	3.126
27								
28								

Table 27. Pitch Angle at 483 Lbs of Displacement

Test #	2	7	24	27	12	15	18	21
Model #	**5628**	**5628**	**5629**	**5629**	**5630**	**5630**	**5631**	**5631**
Δ =	483	483	483	483	483	483	483	483
LCG	**38%**	**42%**	**38%**	**42%**	**38%**	**42%**	**38%**	**42%**

V_m (knots)	Trim Deg	Trim Deg	Trim Deg	Trim Deg	Trim Deg	Trim Deg	Trim Deg	Trim Deg
0								
1								
2								
3	0.327	0.286	0.187	0.110	0.010	0.498	0.309	0.141
4	0.593	0.282	0.566	0.566	0.781	0.839	0.833	0.537
5	2.323	1.838	2.138	1.638	2.168	1.742	2.055	1.937
6	4.125	3.500	3.978	3.678	3.992	3.008	3.755	3.650
7	4.209	3.870	4.006	3.827	4.196	3.752	4.130	3.862
8	4.775	4.138	4.531	4.197	4.365	3.805	4.011	3.718
9	5.439	4.637	5.011	4.644	4.973	3.888	4.503	4.051
10	5.700	5.041	5.349	5.048	5.553	4.210	5.179	4.608
11	5.648	5.458	5.541	5.340	5.899	4.674	5.690	5.161
12	5.461	5.553	5.590	5.491	5.976	5.358	5.915	5.576
13	5.214	5.504	5.500	5.502	5.833	5.689	5.869	5.788
14	4.939	5.265	5.289	5.396	5.550	5.772	5.625	5.793
15	4.657	5.041	4.986	5.207	5.196	5.712	5.274	5.630
16	4.384	4.868	4.630	4.968	4.820	5.573	4.884	5.360
17	4.131	4.745	4.257	4.708	4.452	5.391	4.502	5.039
18	3.902	4.601	3.892	4.445	4.105	5.188	4.151	4.712
19	3.697	4.411	3.556	4.193	3.784	4.976	3.839	4.404
20	3.516	4.239	3.257	3.958	3.490	4.760	3.567	4.130
21	3.356	4.027	3.002	3.745	3.221	4.544	3.331	3.897
22	3.213		2.791	3.553	2.973	4.328	3.128	3.703
23	3.085		2.623	3.382	2.741	4.113	2.951	3.548
24	2.970		2.496	3.227	2.521	3.897	2.797	3.427
25	2.865		2.406	3.085	2.307	3.680	2.661	3.335
26			2.350	2.944	2.091	3.460	2.542	3.271
27			2.325	2.786	1.865	3.237	2.436	3.228
28			2.328	2.563		3.009	2.329	3.204

Table 28. Pitch Angle at 560 Lbs of Displacement

Test #	3
Model #	**5628**
Δ =	560
LCG	**38%**

V_m (knots)	Trim Deg
0	0.000
1	0.000
2	0.000
3	0.195
4	0.762
5	2.464
6	4.643
7	4.695
8	5.624
9	6.279
10	6.590
11	6.561
12	6.278
13	5.874
14	5.445
15	5.043
16	4.686
17	4.378
18	4.118
19	3.898
20	3.713
21	3.558
22	3.428
23	3.320
24	
25	
26	
27	
28	

Table 29. Pitch Angle at 680 Lbs of Displacement

Test #	4
Model #	**5628**
Δ =	680
LCG	**38%**

V_m (knots)	Trim Deg
0	
1	
2	
3	-0.011
4	0.833
5	2.586
6	5.077
7	5.774
8	6.702
9	7.397
10	7.648
11	7.605
12	7.298
13	6.810
14	6.262
15	5.738
16	5.271
17	4.871
18	4.532
19	4.247
20	4.008
21	3.808
22	3.639
23	3.496
24	3.373
25	
26	
27	
28	

REFERENCES

[1] Zseleczky, John, "Effective Horsepower Model Tests of the U.S. Coast Guard 47' Motor Lifeboat (MLB)", United States Naval Academy, Division of Engineering and Weapons, Annapolis, 1988.

THIS PAGE IS INTENTIONALLY LEFT BLANK

DISTRIBUTION

Number of Copies	Office	Individual	Total Copies
5	United States Coast Guard Engineering and Logistics Center Code 046		5
1	DTIC		6
1	3442 (Library) 5010 (w/o enclosure)		7
4	5060	Walden	11
2	5200	5200 Office Files	13
3	5200	Metcalf, Day, Karafiath	16